

Pål Wagner

# Analysis and Testing of Ground Fault Protection Function Performance in Compensated Distribution Grids

Master's thesis in Electric Power Engineering

Supervisor: Hans Kristian Høidalen

Co-supervisor: Thomas Treider

June 2022



Pål Wagner

# **Analysis and Testing of Ground Fault Protection Function Performance in Compensated Distribution Grids**

Master's thesis in Electric Power Engineering  
Supervisor: Hans Kristian Høidalen  
Co-supervisor: Thomas Treider  
June 2022

Norwegian University of Science and Technology  
Faculty of Information Technology and Electrical Engineering  
Department of Electric Power Engineering



---

## Preface

This thesis was written at the Norwegian University of Science and Technology (NTNU), Department of Electric Power Engineering on the subject of Power System Protection and Control. The work presented in this thesis was carried out during the Spring semester of 2022 and is the final work of the 2 year MSc program in Electric Power Engineering.

In ever-growing electric power systems, electrical grid companies have started replacing overhead lines with underground cables. The replacement of overhead lines with underground cables introduces challenges for ground fault protection schemes that still use Wattmetric-based ground fault protection function. Consequently, the objective of this master thesis is to perform practical testing and analysis of three ground fault protection functions - Wattmetric, Admittance, and Transient based ground fault protection functions, such that their performance and limits due to increasing cable length and fault resistance can be established. The work presented in this thesis is based upon a Simulink model of an electric distribution grid and an existing Norwegian distribution grid. The latter was carried out in cooperation with a Norwegian electrical grid company, which name will remain undisclosed due to confidential information shared in later sections of this thesis.

Contents of theoretical background, ground fault protection practice, and ground fault protection functionality in Siemens SIPROTEC 7UM85 relay, which was used for practical testing of ground fault protection functions, were partly developed in my specialization project with the title "Fault Handling in Resonance Grounding", which was carried out in Autumn semester of 2021. It is assumed that readers of this thesis have basic knowledge within Power System Protection and Control.

I want to express my gratitude to my supervisor Hans Kristian Høidalen and my co-supervisor, Thomas Treider, for their guidance throughout the final year of my master's program. In addition, I would like to thank Ruben Hodnebrug, protection systems manager at Agder Energi, who has been a great discussion partner on the subject of power system protection in distribution systems, Einar Lamo, technical supervisor for protection relays in Siemens, Norway, who has assisted with DIGSI, as well as his thoughts on ground fault protection function performance, and Ari Wahlroos, an electrical engineer at ABB, who has shared his experience with electrical grids containing large amounts of cables.

Trondheim, June 2022

Pål Wagner



---

## Abstract

In recent years, the worldwide trend in medium voltage distribution systems grounded through an arc suppression coil has been to replace overhead lines with underground cables. In doing so, many long-term economic as well as technical advantages can be achieved. Increasing cable length in an electrical power system results in a significant increase in the total capacitance of that network. Distribution systems in Norway have been utilizing traditional, Wattmetric-based ground fault protection functions to ensure safety and achieve optimal protection against single line to ground faults. As the capacitance in the electrical transmission system increases, the residual current of transformer neutral becomes increasingly reactive, resulting in a small resistive current which is not sufficient for Wattmetric-based ground fault detection and disconnection.

This master thesis uses Matlab combined with Simulink to establish a two-feeder, 22 kV distribution system grounded through an arc suppression coil. Siemens SIPROTEC 7UM85 relay is used to analyze and test the performance of Wattmetric, Admittance, and Transient-based protection functions. Simulink is used to investigate three different cases - a small Simulink model where lengths of both feeders are relatively short is used to analyze how varying sensitivity of ground fault protection functions affect their performance. A large Simulink model, where the cable length of the protected feeder is varied between 20 km - 100 km, is used to investigate ground fault protection function performance limits with respect to increasing capacitance. Lastly, a large Simulink model is used to investigate the performance of Wattmetric, Admittance, and Transient-based protection functions during an intermittent ground fault. COMTRADE files were made for all of the abovementioned cases and were tested in a laboratory using the mentioned relay. Performance of Wattmetric, Admittance, and Transient-based ground fault protection functions were also tested on a real Norwegian distribution grid. This was done by acquiring COMTRADE files from a Norwegian electrical grid company and testing these files in a laboratory.

Analysis and testing of Wattmetric, Admittance and Transient based ground fault protection functions presented in this thesis have demonstrated that using a simulated distribution system, cable lengths above 50 km contribute with sufficient ground-fault current contribution for decreasing Wattmetric based ground fault protection function performance. It was found that at a cable length of 70 km, the Wattmetric-based protection function is no longer able to neither detect nor disconnect ground fault with fault resistance above  $3k\Omega$ . Furthermore, when using a single, long cable, Transient based protection function performance is both poor and inconsistent. This was found to be due to the significant damping that the series connection of zero sequence resistance introduces. Lastly, using the simulated system demonstrates that the Admittance-based ground fault protection function has superior performance compared to both Wattmetric and Transient-based ground fault protection functions. It is demonstrated that the Admittance-based ground fault protection function has excellent performance for cable lengths 20 km - 100 km, and for fault resistances  $0\Omega - 4.5k\Omega$ . The above findings were further strengthened by testing 38 COMTRADE files from a real Norwegian distribution system. It was demonstrated that of a total of 38 files, Wattmetric, Admittance, and Transient based ground fault protection functions were able to detect 68.42%, 94.32%, and 81.57% of ground faults, respectively.





---

## Sammendrag

De siste årene har den globale trenden i medium-spennings distribusjonsnett jordet via resonansspole vært å erstatte luftlinjer med underjordiske kabler. Ved å gjøre dette, langsiktige økonomiske og tekniske fordeler kan oppnås. Økende kabellengde i et elektrisk distribusjonsnett medfører en stor økning i kapasitans i det elektriske distribusjonsnettet. Distribusjonsnett i Norge har brukt tradisjonelt, Wattmetriskbasert jordfeilsvern, for å sikre en trygg drift, og oppnå optimal beskyttelse mot enfase jordfeil. Når kapasitansen i et elektrisk distribusjonsnett øker, vil nullsekvensstrømmen i nøytralpunktet av transformatoren bli mer reaktiv, noe som fører til en liten resistiv strøm, som ikke er stor nok for Wattmetriskbasert jordfeildeteksjon og utkobling.

Denne masteravhandlingen tar i bruk Matlab i kombinasjon med Simulink til å etablere et 22 kV, spolejordet distribusjonsnett med to avganger. Relé av typen Siemens SIPROTEC 7UM85 blir brukt til å analysere og teste ytelsen av Wattmetrisk-, Admittans- og Transientbasert jordfeilsfunksjoner. Simulink blir brukt til å undersøke tre ulike tilfeller - en liten Simulink-modell der lengden av begge avgangene er relativt korte blir brukt til å undersøke hvordan variasjon av sensitiviteten til jordfeilsfunksjoner påvirker funksjonenes ytelse. Stor Simulink-modell, der kabellengden av beskyttet avgang blir variert mellom 20 km og 100 km, blir brukt til å undersøke begrensningene av jordfeilsfunksjoner, med tanke på økende kapasitans. Til slutt, blir stor Simulink-modell brukt til å undersøke ytelsen av Wattmetrisk-, Admittans- og Transientbasert jordfeilsfunksjoner når intermitterende jordfeil inntreffer. Det ble opprettet COMTRADE-filer for hver av de ovenfor nevnte tilfellene, og disse ble testet i laboratoriet på det nevnte reléet. Ytelsen av Wattmetrisk-, Admittans-, og Transientbasert jordfeilsfunksjon ble også testet i et eksisterende, norsk distribusjonsnett. Dette ble gjort ved å få tilgang til COMTRADE-filer fra et Norsk nettselskap, og teste disse i laboratoriet.

Analysen og testing av Wattmetrisk-, Admittans- og Transientbasert jordfeilsfunksjonytelse i denne masteravhandlingen har presentert at ved bruk av et simulert distribusjonssystem, kabellengde over 50 km bidrar med nok jordfeilstrøm for å minke ytelsen av Wattmetriskbasert jordfeilsfunksjon. Videre ble det funnet at ved kabellengde 70 km, Wattmetriskbasert jordfeilsfunksjon er ikke lenger i stand til å verken detektere eller koble ut jordfeil med feilresistans over  $3k\Omega$ . Videre blir det vist at ved bruk av en enkel, lang kabel, ytelsen av Transientbasert jordfeilsfunksjon blir både dårlig og inkonsistent. Årsaken til dette ble funnet til å være stor demping grunnet stor nullsekvensresistans. Til slutt, ved bruk av et simulert system, ble det demonstrert at Admittansbasert jordfeilsfunksjon er overlegen sammenlignet med Wattmetrisk- og Transientbasert jordfeilsfunksjon. Det ble demonstrert at for kabellengdene mellom 20 km - 100 km, og for feilresistansene  $0\Omega - 4.5k\Omega$ , Admittansbasert jordfeilsfunksjon har utmerket ytelse. Funnene beskrevet ovenfor ble forsterket ved å teste 38 COMTRADE-filer tilhørende ekte, norsk distribusjonsnett. Det ble demonstrert at ved å teste totalt 38 COMTRADE-filer tilhørende ekte distribusjonsnett, Wattmetrisk-, Admittans- og Transientbasert jordfeilsfunksjon var i stand til å detektere hhv. 68.42%, 94.32% og 81.57% av jordfeilene.



---

# Table of Contents

<b>1</b>	<b>Introduction</b>	<b>1</b>
1.1	Background for Research . . . . .	1
1.2	Approach for Research . . . . .	1
1.3	Objective of Research . . . . .	2
1.4	Limitations of Research . . . . .	2
<b>2</b>	<b>Theoretical Background</b>	<b>3</b>
2.1	Sequence Networks . . . . .	3
2.2	Single Line to Ground Fault . . . . .	4
2.3	Increasing Cabling in Electrical Supply Systems . . . . .	7
2.4	System Neutral Grounding Through Arc Suppression Coil . . . . .	8
2.5	Ground Fault Protection Practice . . . . .	10
2.5.1	Wattmetric Based Protection Function . . . . .	10
2.5.2	Wischer Principle . . . . .	11
2.5.3	Zero Sequence Energy Method . . . . .	12
2.5.4	Admittance Based Protection Function . . . . .	12
<b>3</b>	<b>Siemens SIPROTEC 7UM85 Ground Fault Protection Functionality</b>	<b>14</b>
3.1	Wattmetric Based Ground Fault Protection . . . . .	14
3.2	Transient Based Ground Fault Protection . . . . .	15
3.3	Admittance Based Ground Fault Protection With $G_0$ or $B_0$ Measurement . . . . .	16
<b>4</b>	<b>Methodology</b>	<b>17</b>
4.1	Modeling Using Matlab and Simulink . . . . .	17
4.2	Application of Ground Fault . . . . .	18
4.3	Generation of COMTRADE-files . . . . .	19
4.4	Processing Data From Norwegian Distribution Network . . . . .	20
4.4.1	Company A . . . . .	20
4.5	Configuration of Siemens 7UM85 and Protection Functions . . . . .	21
4.5.1	Configuration of DIGSI . . . . .	21
4.5.2	Configuration of Protection Functions for Simulink Model . . . . .	24
4.5.3	Configuration of Protection Functions for Company A . . . . .	25
4.6	Connection Between Power Source and Relay . . . . .	25
<b>5</b>	<b>Ground Fault Protection Function Performance</b>	<b>27</b>

---

5.1	Ground Fault Protection Performance due to Parameter Sensitivity . . . . .	27
5.2	Ground Fault Protection Performance due to Increasing Cable Length . . . . .	30
5.3	Ground Fault Protection Performance During Intermittent Ground Fault . . . . .	32
5.4	Ground Fault Protection Performance in Norwegian Distribution Grid . . . . .	33
<b>6</b>	<b>Analysis of Ground Fault Protection Performance</b>	<b>36</b>
6.1	Effect of Varying Settings Sensitivity . . . . .	36
6.2	Effect of Increasing Cable Length . . . . .	37
6.3	Ground Fault Protection Function Performance in Norwegian Distribution Grid . .	42
<b>7</b>	<b>Discussion</b>	<b>45</b>
7.1	Design of Simulink Model . . . . .	45
7.2	Ground Fault Protection Function Configuration . . . . .	46
7.3	Ground Fault Protection Performance in Small Simulink Model . . . . .	47
7.4	Ground Fault Protection Performance in Large Simulink Model . . . . .	48
7.5	Ground fault Protection Performance in Real Distribution Grid . . . . .	50
<b>8</b>	<b>Conclusion</b>	<b>51</b>
<b>9</b>	<b>Recommendations for Further Work</b>	<b>52</b>

---

# 1 Introduction

## 1.1 Background for Research

Traditionally, overhead lines have been used to build the electrical distribution grid due to long distances and low costs. High voltage levels with low current have been used to transfer the electrical power across long distances such that electrical losses could be reduced, as well as the quality of power increased. To maintain a secure delivery of power, the distribution grid has to be secured against electrical faults, the most common being single line to ground fault, which is responsible for 70%-80% of electrical faults in the distribution system[1]. Today, the most common ground fault protection function in arc suppression coil grounded electrical grids in Norway is the Wattmetric-based function, which utilizes three different vectors to identify and disconnect a ground fault. Fault direction is made by measuring the active component of zero sequence current compared to zero-sequence voltage, which has also to exceed a pre-determined threshold. If the direction is determined, both zero-sequence voltage and current have to exceed their threshold values for the ground fault to be disconnected.

In recent years, the trend in electrical supply systems around the world has been to replace traditional overhead lines with underground cables, partly due to the expansion of the renewable energy arsenal[2]. There are many advantages of such a decision, such as increased public support for electrical grid expansion[3], as well as technical and economic advantages, such as lower voltage drop, lower maintenance cost as well as longer lifetime[4]. Even though increasing cabling in the distribution grid provides many advantages, it also introduces a large disadvantage for today's ground fault protection scheme. On average, cables contribute 40 times more capacitance per length than overhead lines. The increased capacitance of a protected feeder will have a large impact on the angle between the zero-sequence voltage and current. Too much capacitance on a protected feeder can compromise the Wattmetric-based protection function, due to large capacitive current, and relatively small resistive current. In addition, increasing amounts of cable result in fault current that does not extinguish by itself. This means that in today's ground fault protection scheme, the Wattmetric-based ground fault protection function is one of the limiting factors in grid expansion using cables.

Modern commercially available relays contain both Wattmetric-based ground fault protection function, as well as alternative protection functions, such as Admittance based and Transient based. The functionality for ground fault detection of modern ground fault protection functions is different from Wattmetric based, enabling the possibility for these ground fault protection functions to perform better in highly cabled networks.

## 1.2 Approach for Research

Simulink was used to perform simulations on a 22 kV distribution grid grounded through an arc suppression coil, containing two feeders - one containing both cable and overhead line and one containing a pure overhead line. To prepare simulation results for laboratory testing, a script was written to convert Simulink results to COMTRADE formatted files. The testing of COMTRADE formatted files was performed in the laboratory, on the actual Siemens SIPROTEC 7UM85 relay in combination with Advanced Transplay in OMICRON. The base case in this thesis is a single line to ground faults.

For investigation of ground fault protection function performance in real distribution networks, a Norwegian electrical grid company was contacted, and COMTRADE files, as well as protection function parameters from one of their electrical facilities, were provided.

All of the COMTRADE files mentioned above were tested with Wattmetric based, Admittance based, and Transient based ground fault protection functions. To enable a direct comparison of ground fault protection performance, all protection functions were tested with the same zero-sequence threshold values.

---

### 1.3 Objective of Research

The main objective of research in this thesis is to demonstrate that the traditional, i.e Wattmetric-based ground fault protection function is a sub-optimal protection scheme in a distribution grid containing large amounts of capacitance. The main objective is achieved through several sub-objectives in both simulated and real-life electrical distribution grids.

Objectives for the research in Simulink simulated distribution system are as follows:

- Perform single line to ground fault experiments on Wattmetric based, Admittance based, and Transient based ground fault protection functions in a physical laboratory using an actual relay.
- Investigate which ground fault protection function has optimal performance when cable length and fault resistance increase.
- Analyse the ground fault protection performance to establish how increasing cable length affects the protection performance and determine the cable length that leads to unacceptable performance.

The objective for research in a real-life distribution system is as follows:

- Use COMTRADE-files from real-life distribution grid to perform experiments on Wattmetric based, Admittance based, and Transient based ground fault protection functions using the same zero-sequence threshold values as used in today's distribution grid.
- Vary the direction determination parameter for Admittance-based ground fault protection and zero-sequence voltage threshold value for Transient-based ground fault protection function and investigate how different sensitivity affects protection performance.
- Analyze how a change in sensitivity of Admittance based and Transient based ground fault protection function affects protection performance.

All the objectives presented above were performed in a physical laboratory using an actual relay combined with Advanced Transplay in OMICRON.

### 1.4 Limitations of Research

The following limitations apply to this thesis:

- Only single line to ground faults are investigated.
- Transformer grounded through arc suppression coil in parallel with a resistor. Other types of grounding are not taken into consideration.
- Each ground fault is always applied at the end of fault affected feeder.
- Ground faults that are applied have a fixed value for fault resistance rather than a variable value, which might be more realistic.

---

## 2 Theoretical Background

This section is based upon the preparation work for this master thesis [5] and is included for the overall readability and understanding of the methodology, results, and analysis presented in later sections. The first two subsections present the basic theory of sequence networks and ground fault calculations. The third subsection presents both advantages and disadvantages of using cables instead of overhead lines and background theory on how intermittent ground faults can occur in cabled networks. The fourth subsection presents background theory on grounding through arc suppression coil. Lastly, the fifth subsection presents the theory on practice of ground fault protection functions that are used in this thesis.

### 2.1 Sequence Networks

Symmetrical faults affect all the phases of the power system, such that currents and voltages are in balance. Unsymmetrical faults, on the other hand, such as a single line to ground, result in unbalanced currents and voltages in the different phases, meaning that the conventional, per-phase equivalent circuits cannot be used to solve for fault currents and voltages. The solution to this problem is to introduce three balanced circuits representing positive, negative, and zero sequences, one circuit for each phase in the power system. This approach is called Fortescue's Theorem, or Symmetrical Component Theory. It explains how three unbalanced current or voltage vectors can be converted into three sets of balanced vectors, giving one set for each sequence diagram. The positive sequence can be illustrated as the original circuit, containing the voltage source and impedances, and its vectors are symmetrically displaced with respect to each other and have the same phase sequence as the original, unbalanced vectors. The negative sequence is identical to the positive sequence but without the voltage source. Its vectors, like positive sequence, are symmetrically displaced with respect to each other but have the opposite phase sequence. Lastly, vectors belonging to the zero sequence are in phase and with the same amplitude.

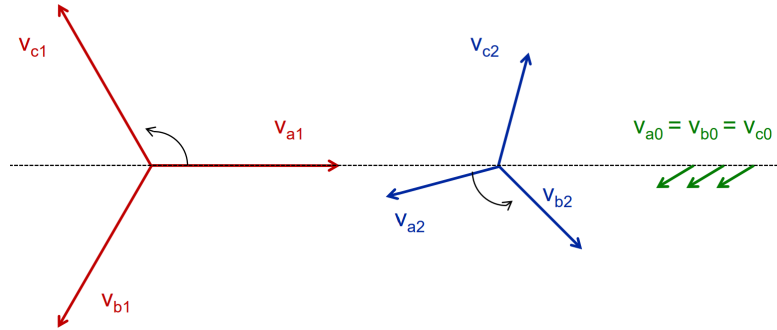


Figure 2.1: Illustration of voltage vector displacement in the different sequences [6]

The original, unbalanced phase voltages can be written as a sum of all the sequence voltages belonging to the respective phases. In addition, due to the same amplitude within the sequences, the phase-shift operator,  $h$ , is utilized to express all the voltages by a single-phase voltage:

$$V_a = V_a^{(0)} + V_a^{(+)} + V_a^{(-)} = V_a^{(0)} + V_a^{(+)} + V_a^{(-)} \quad (2.1.1)$$

$$V_b = V_b^{(0)} + V_b^{(+)} + V_b^{(-)} = V_a^{(0)} + h^2 \times V_a^{(+)} + h \times V_a^{(-)} \quad (2.1.2)$$

$$V_c = V_c^{(0)} + V_c^{(+)} + V_c^{(-)} = V_a^{(0)} + h \times V_a^{(+)} + h^2 \times V_a^{(-)} \quad (2.1.3)$$

Equations for currents  $I_a$ ,  $I_b$  and  $I_c$  are equal to equations 2.1.1-2.1.3. By rewriting equations 2.1.1-2.1.3 into matrix form, sequence currents and voltages can simply be calculated:

$$\begin{bmatrix} V_a \\ V_b \\ V_c \end{bmatrix} = \begin{bmatrix} 1 & 1 & 1 \\ 1 & h^2 & h \\ 1 & h & h^2 \end{bmatrix} \begin{bmatrix} V_a^{(0)} \\ V_a^{(+)} \\ V_a^{(-)} \end{bmatrix} \quad \text{and} \quad \begin{bmatrix} I_a \\ I_b \\ I_c \end{bmatrix} = \begin{bmatrix} 1 & 1 & 1 \\ 1 & h^2 & h \\ 1 & h & h^2 \end{bmatrix} \begin{bmatrix} I_a^{(0)} \\ I_a^{(+)} \\ I_a^{(-)} \end{bmatrix} \quad (2.1.4)$$

Using equation 2.1.4, sequence network elements can simply be calculated:

$$[V_{(0),(+),(-)}] = [H]^{-1} [V_{abc}] \quad \text{and} \quad [I_{(0),(+),(-)}] = [H]^{-1} [I_{abc}] \quad (2.1.5)$$

The information and theory presented above are acquired from the preparation work for this thesis[5].

## 2.2 Single Line to Ground Fault

In the event of SLG, the fault current can be calculated by utilizing the sequence networks described in 2.1. To satisfy the boundaries, the positive, negative, and zero sequences have to be connected in series, as shown in figure 2.2. As a consequence of series connection, the voltages over respective sequence networks become:

$$V_{(0)} = -Z_f \times I_{(0)} \quad (2.2.1)$$

$$V_{(+)} = V_f - Z_{(+)} \times I_{(+)} \quad (2.2.2)$$

$$V_{(-)} = -Z_{(-)} \times I_{(-)} \quad (2.2.3)$$

Where  $V_f$  is the pre-fault voltage at the faulted bus.

Using equations 2.2.1-2.2.3, the zero-sequence current can be written as a sum of sequence voltage, divided by the fault impedance:

$$I_0 = \frac{V_f}{(Z_{(0)} + Z_{(+)} + Z_{(-)}) + 3Z_f} \quad (2.2.4)$$

Given equation 2.2.4, and given SLG fault at bus k, the fault current becomes:

$$I_k^{(0)} = I_k^{(+)} = I_k^{(-)} = \frac{V_f}{(Z_{kk}^{(0)} + Z_{kk}^{(+)} + Z_{kk}^{(-)}) + 3Z_f} \quad (2.2.5)$$

Where  $Z_{kk}^a$  is the diagonal element of the ZBus for sequence a.

The method presented above is an analytical approach to calculating SLG faults in power system analysis. In reality, the voltage in the neutral point, and the fault current will be slightly affected by the asymmetry ( $\Delta C$ ), conductive elements (G), and capacitance to ground, as illustrated in figure 2.3. The capacitance to ground of a given system is equal to the zero sequence capacitance of conductive elements in that system and can be expressed as demonstrated in equation 2.2.6

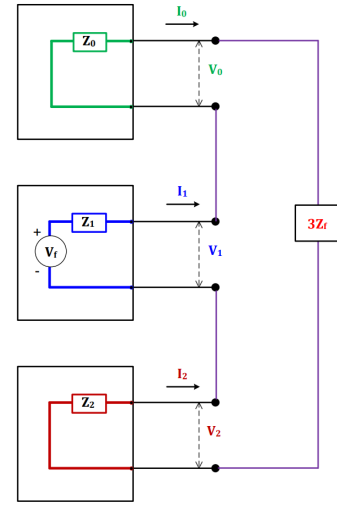


Figure 2.2: Positive, negative, and zero sequences connected in series [6] (2.2.4)

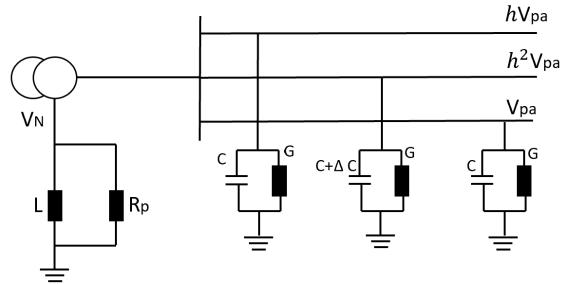


Figure 2.3: Illustration of a network containing asymmetry and conductive elements [7]



---


$$C_g = L_{OH}C_{OH,0} + L_{cable}C_{cable,0} \quad (2.2.6)$$

The asymmetry of a system,  $\Delta C$ , is not a physical capacitance observed in a power system but rather a theoretical capacitance that indicates the difference between the three phases of a given feeder. The asymmetry of a system is small when the system contains solely overhead lines but can vary from 1%-10% of total cable capacitance to ground when the system involves cables. The asymmetry can be expressed as a function of total capacitance to ground:

$$\Delta C = p_{asymmetry}C_g \quad (2.2.7)$$

Where  $p_{asymmetry}$  is the percentage of system asymmetry.

The conductance to ground,  $G$ , similarly to  $\Delta C$ , is not a physical resistor observed in a power system, rather than a theoretical quantity for representation of currents flowing to the ground. The conductance to the ground represents the leakage currents of insulators present in the power system and is, therefore, weather dependent. In warm and dry weather conditions, the conductance to the ground will be small and will increase with humidity in the air. The conductance to the ground for cables is negligible, whereas, for overhead lines, it can vary between 1%-10% of total overhead line capacitance to the ground. Consequently, conductance to the ground can be written as a function of overhead line length and zero sequence capacitance:

$$\Delta G = p_{conductance}L_{OH}C_{OH}\omega \quad (2.2.8)$$

Where  $p_{conductance}$  is the percentage of system conductance to ground.

By taking asymmetry, conductance to ground and capacitance to ground into consideration, and using figure 2.3 as reference, the currents in phases a, b and c can be written in the following form:

$$\begin{aligned} I_a &= (V_N + V_{pa}) \times (G + j\omega C) \\ I_b &= (V_N + h^2V_{pa}) \times (G + j\omega(C + \Delta C)) \\ I_c &= (V_N + hV_{pa}) \times (G + j\omega C) \end{aligned} \quad (2.2.9)$$

The zero sequence current is the current flowing through the transformer neutral admittance:

$$3I_0 = I_a + I_b + I_c = -V_n \left( \frac{1}{j\omega L} + \frac{1}{R_p} \right) \quad (2.2.10)$$

By summing phase currents presented in equation 2.2.9, and taking transformer neutral admittance in consideration, zero sequence current can be written as:

$$3I_0 = 3V_n(j\omega\Delta C + 3(j\omega C + G) + \frac{1}{j\omega L} + \frac{1}{R_p}) = (-h^2V_{pa})j\omega\Delta C \quad (2.2.11)$$

By using equation 2.2.11, the neutral voltage is expressed as:

$$V_N = V_0 = \frac{(-h^2V_{pa})j\omega\Delta C}{3G + \frac{1}{R_p} + j\omega\Delta C + j\omega 3C + \frac{1}{j\omega L}} = \frac{-h^2V_{pa}}{1 + \frac{s}{u} - j\frac{d}{u}} \quad (2.2.12)$$

Where s, u and d in equation 2.2.12 are expressed as:

$$\begin{aligned}
s &= 3\omega C - \frac{1}{\omega L} \\
u &= \omega \Delta C \\
d &= 3G + \frac{1}{R_p}
\end{aligned}
\tag{2.2.13}$$

Parameter  $s$  in equation 2.2.13 defines the compensation degree of the system and is  $0$ ,  $< 0$ , or  $> 0$  when the system is in resonance, over-compensation, and under-compensation, respectively. Parameter  $u$  is related to system asymmetry, and parameter  $d$  is related to system conductance to ground.

Given equation 2.2.12, the magnitude of neutral voltage can be written as:

$$|V_n| = \frac{V_{pa}}{\sqrt{1 + (\frac{s}{u})^2 + (\frac{d}{u})^2}} \tag{2.2.14}$$

The maximum voltage in system neutral is solely given by the compensation parameter,  $s$ . Consequently, the maximum neutral voltage occurs when parameter  $s$  is equal to zero, i.e when the system is in resonance:

$$|V_n|_{max|s \rightarrow 0} = V_{pa} \frac{u}{d} = \frac{V_{pa} \omega \Delta C}{3G + \frac{1}{R_p}} \tag{2.2.15}$$

When a ground fault occurs, the fault current will flow through the fault resistance and return to the transformer neutral through the ground. This means that the fault current has to pass through conductances to ground, capacitance to ground and the neutral admittance of the transformer neutral. Consequently, the system shown in figure 2.3 can be modeled as an equivalent circuit shown in figure 2.4.

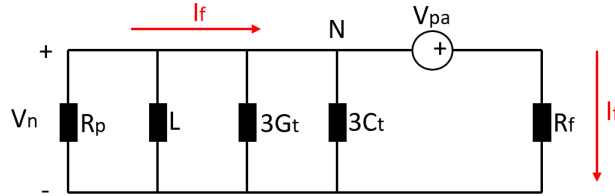


Figure 2.4: The equivalent circuit of the system is shown in figure 2.3 with a fault on phase A [7]

The zero sequence current in the faulty feeder can then be written as sum of feeders zero sequence current and the fault current:

$$3I_{0f} = V_n(3G_f + j\omega 3C_f) + I_f \tag{2.2.16}$$

Where  $G_f$  and  $C_f$  represent the conductance and capacitance to the ground of the fault-affected feeder. The fault current,  $I_f$ , can be derived from the circuit in figure 2.4:

$$I_f = -V_n \left( 3G_t + \frac{1}{R_p} + j\omega C_t + \frac{1}{j\omega L} \right) \tag{2.2.17}$$

---

Combining equations 2.2.16 and 2.2.17 equals to total zero sequence current of the faulty feeder:

$$3I_{0f} = V_n(3G_f + j\omega 3C_f - 3G_t - \frac{1}{R_p} - j\omega C_t - \frac{1}{j\omega L}) \quad (2.2.18)$$

The information and theory presented above, in subsections 2.1 and 2.2, is based on this thesis's preparation work[5].

## 2.3 Increasing Cabling in Electrical Supply Systems

In recent years, electrical grid companies across the electrical power supply industry have shown interest in replacing overhead lines with underground cables. Some of the most important reasons for underground cables replacing overhead lines are as follows:

1. Underground cables are less affected by weather conditions such as lightning and storm, ensuring more secure power delivery.
2. Instances where the power supply is interrupted due to breakage of the overhead line are eliminated.
3. The lifetime of underground cables is longer than of overhead lines.
4. Overhead lines transmit power through bare conductors, making the possibility of exposure to a high voltage high compared to insulated underground cables.

As transmission lines tend to be lengthy, it is also essential to take voltage drop into consideration, which can be written as a function of the current the conductor is carrying, multiplied by the impedance of the conductor:

$$V_{drop} = IZ = I(\sqrt{R^2 + X^2}) = I(\sqrt{R^2 + (\omega L)^2}) \quad (2.3.1)$$

The impedance of overhead lines is mainly dominated by the inductance, such that the resistive part of the equation 2.3.1 can be neglected, resulting in voltage drop being proportional to the inductance:

$$V_{drop} \propto L \quad (2.3.2)$$

Due to  $L_{cable} \ll L_{OH}$ , replacement of overhead lines with underground cables also results in less voltage drop in the transmission system.

The compelling arguments presented above of underground cables replacing overhead lines might not be as persuasive for engineers responsible for the safety of the transmission system. Cables, unlike overhead lines, contribute to large capacitances to the transmission system and, as presented in equations in subsection 2.2, as well as table 2.1, contribute to large ground fault currents.

Table 2.1: Relation between fault current produced by overhead line and cable [8]

Conductor type	$C_0$ [ $\mu F/km$ ]	Ground fault current [A/km]	Ratio $\frac{I_{f,cable}}{I_{f,OH}}$
Overhead line	0.0061	0.07	1.00
Cable 3x70mm <sup>2</sup>	0.18	1.96	29.50
Cable 3x120mm <sup>2</sup>	0.23	2.50	37.70
Cable 3x185mm <sup>2</sup>	0.26	2.83	42.60
Cable 3x240mm <sup>2</sup>	0.30	3.26	49.20

Due to increasing capacitive ground fault currents, the traditional ground fault protection functions, such as Wattmetric, might struggle with ground fault detection and disconnection due to capacitive currents affecting the angle between zero sequence current and voltage, as demonstrated in equation 2.2.18.

Underground cable insulation introduces other concerning issues, such as ground fault type. Information provided in section 2.2 provides a good understanding of single line to ground fault calculation methods during a permanent ground fault. A possible consequence of cable insulation breakdown might be an intermittent ground fault, which conventional ground fault protection functions have not been designed to protect against. Damages in cable insulation might lead to ignition of the ground fault (1), and as the voltage of the fault-affected phase is reduced, the system will try to stabilize by restoring the nominal voltage (2). As the phase voltages stabilize to their nominal values (3), the breakdown of the cable insulation won't be able to carry the full phase voltage, re-igniting the fault (4) [9]. This type of fault is called intermittent ground fault and is illustrated in figure 2.5

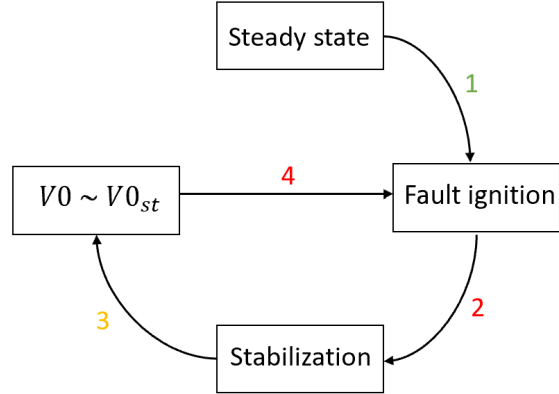


Figure 2.5: Intermittent ground fault

## 2.4 System Neutral Grounding Through Arc Suppression Coil

System neutral in distribution grid is usually grounded using arc suppression coil, meaning that a coil is present in transformer neutral, as illustrated in figure 2.6. In the event of a single-phase ground fault, the resulting ground current will mainly be capacitive due to relatively large capacitances to the ground. Such an event will likely result in arcing ground, leading to healthy phase voltage increment from phase voltage to line voltage. By using Ohm's law, the current passing through capacitance to ground can be written as:

$$I_C = \frac{3V_{pa}}{X_C} = -3j\omega CV_{pa} \quad (2.4.1)$$

By using the same analogy, the current through an arc suppression coil in transformer neutral can be written as:

$$I_L = \frac{V_{pa}}{X_L} = \frac{V_{pa}}{j\omega L} \quad (2.4.2)$$

The currents in equations 2.4.1 and 2.4.2 have opposite directions, meaning that if the arc suppression coil is equal to the system capacitance, the resulting ground current in transformer neutral can be eliminated. Consequently, by tuning the arc suppression coil to be equal to the capacitance to the ground, the arc suppression coil extinguishes the arcing ground. The correct size of the arc suppression coil for eliminating the fault current can be found by solving the equation  $|I_L| = |I_C|$ :

$$\frac{V_{pa}}{\omega L} = 3\omega CV_{pa} \quad (2.4.3)$$

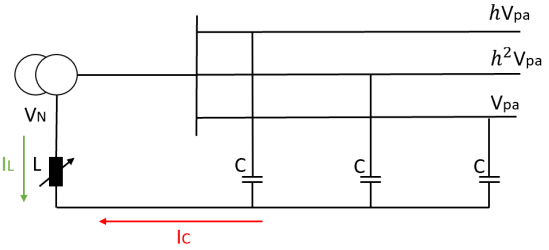


Figure 2.6: Power system grounded with arc suppression coil

Resulting in inductance that is equal to system capacitance:

$$L = \frac{1}{3\omega^2 C} \quad (2.4.4)$$

In reality, the arc suppression coil,  $L$ , in the equation 2.4.4, is not of a fixed value but can be varied by a regulator. In the event of changing network topology due to deliberate or non-deliberate disconnection of lines, the arc suppression coil regulator will run through the system resonance curve such that the correct value of  $L$  can be found. To ensure that the ground fault protection practice is reliable, the zero-sequence voltage threshold value should at all times be above the resonance voltage point, such that when the arc suppression coil is running through the resonance curve, a false ground fault indication can be avoided.

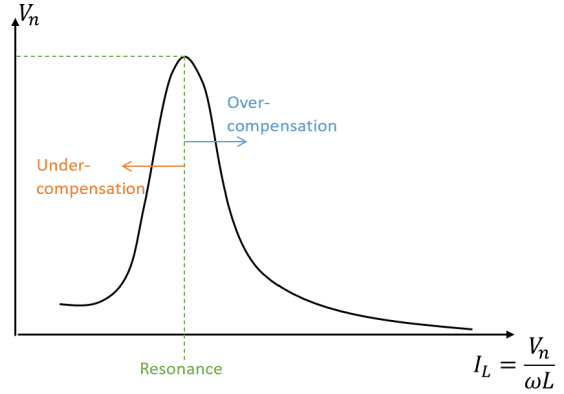


Figure 2.7: The shape of the system resonance curve demonstrates neutral voltage as a function of arc suppression coil current

Norwegian regulation on electrical supply systems (FEF) [10] specifies that the touch voltage in an electrical supply system has to be according to equation 2.4.5.

$$V_{EPT} \leq 4V_{TP} \quad (2.4.5)$$

Meaning that the allowed touch voltage has to be four times smaller than the theoretical earth potential rise:

$$V_{TP} = \frac{V_{EPT}}{4} \quad (2.4.6)$$

Where  $V_{EPT}$  is the theoretical earth potential rise, and  $V_{TP}$  is the touch voltage. Figure 2.8 demonstrates the touch voltage as a function of the current duration and shows that depending on the touch voltage, the ground fault protection in arc suppression coil grounded systems does not have to disconnect a potential ground fault immediately. This enables the arc suppression coil to extinguish the ground arcing and enables short-duration ground faults to disappear without interrupting the electrical supply.

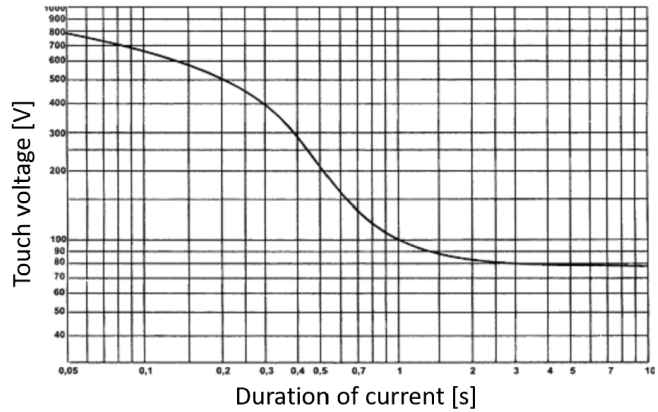


Figure 2.8: Touch voltage as a function of current duration [10]

---

## 2.5 Ground Fault Protection Practice

This subsection presents the practice and functionality of four different ground fault protection function principles that are of large relevance in this master thesis - Wattmetric, Wischer, Zero Sequence Energy, and Admittance. For the Wattmetric protection function, two principles are presented - ground fault detection using Wattmetric power and ground fault detection using zero-sequence vectors and corresponding angles. Wischer and Zero Sequence Energy fall under the same category, where both practices are utilized in Transient based ground fault protection. The Zero Sequence Energy method is used in more modern Transient based protection functions, whereas the Wischer principle is an excellent example of polarity differences when a ground fault occurs. Lastly, the principle of the Admittance-based protection function is presented, where the calculation of relevant parameters, as well as detection and operational characteristics, is presented.

The information and theory presented in this subsection are acquired from the preparation work for this thesis[5].

### 2.5.1 Wattmetric Based Protection Function

The Wattmetric protection function has been around for years in compensated networks. This is because the function is simple, secure, and dependable for low resistance ground faults. The function can detect a ground fault in either the forward direction or backward direction by utilizing phasors presented in equations 2.5.1 and 2.5.2 respectively [11].

$$I_0 = -V_0\left[\frac{1}{R_{0h}} + \frac{1}{3R_P} + j(\omega C_{0h} - \frac{1}{3\omega L_N})\right] \quad (2.5.1)$$

$$I_0 = V_0\left(\frac{1}{R_{0f}} + j\omega C_{0f}\right) \quad (2.5.2)$$

Where  $V_0$  is neutral voltage,  $R_{0h}$  and  $C_{0h}$ , are healthy feeder zero-sequence resistance and capacitance, respectively.  $R_P$  and  $L_N$  are the resistance of the parallel resistor and arc suppression coil inductance, respectively.  $C_{0f}$  and  $R_{0f}$  represent zero-sequence capacitance and leakage resistance of the faulty feeder.

By utilizing the equations presented above, the Wattmetric power can be calculated using real components of both the zero-sequence voltage and zero sequence current:

$$W = \Re(V_0 I_0^*) = V_0 I_0 \cos\phi \quad (2.5.3)$$

The sign of the active component of  $I_0$  is always positive for reverse faults and negative for forward faults. The resulting power calculated by using equation 2.5.3 can then be compared to threshold values, i.e,  $W < -\epsilon$  indicates a forward fault, and  $W > \epsilon$  indicates a backward fault. Due to active component of  $I_0$  being very small during a fault, the threshold value,  $\epsilon$ , should be very small as well[11].

Wattmetric function based on phasors measures the angle between zero sequence current and zero-sequence voltage. During a fault, zero sequence current in a healthy feeder can be written as shown in equation 2.5.4. The equation shows that the angle of zero sequence current in a healthy feeder,  $I_{0h}$  is close to  $90^\circ$  and the phasor itself is located in the first quadrant.

$$3I_{0H} = I_{Ah} + I_{Bh} + I_{Ch} = V_N(3G_h + j3\omega C_h) \quad (2.5.4)$$

The zero sequence current of a faulty feeder is demonstrated in equation 2.2.18, but is repeated here for the porpoise of clarity:

$$\begin{aligned}
3I_{0f} &= I_{Af} + I_{Bf} + I_{Cf} = V_N(3G_f + j3\omega C_f) + I_f \\
&= V_N(3G_f + j3\omega C_f - j3\omega C_t - \frac{1}{j\omega L} - 3G_t - \frac{1}{R_p})
\end{aligned} \tag{2.5.5}$$

As presented in equation 2.5.5, the angle of  $I_{0f}$  depends on the own contribution and compensation of the network. The last two elements, i.e  $3G_t - \frac{1}{R_p}$ , are the Wattmetric contribution, which decides the angle between the  $I_{0f}$  and  $V_N$ . The feeder is faulty if the phasor is located in the 2nd quadrant. REN[12] recommends an angle threshold of  $\pm 10^\circ$ , meaning that the angle between  $I_{0h}$  and  $V_N$  should be in the interval  $[-80^\circ, 80^\circ]$ , and between  $I_{0f}$  and  $V_N$  in the interval  $[100^\circ, 260^\circ]$ .

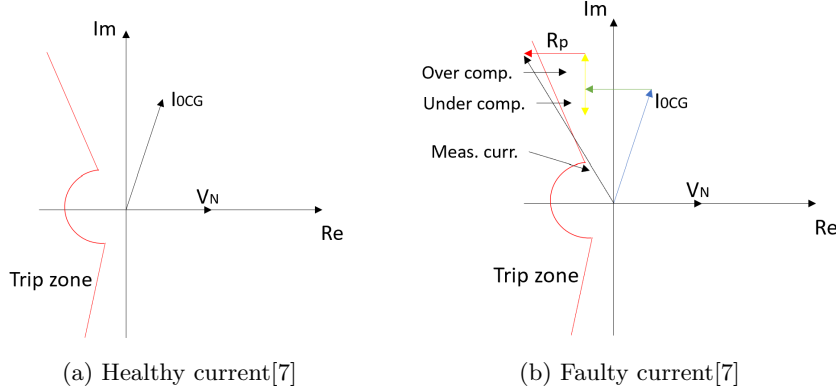


Figure 2.9: (a) Healthy current, equation 2.5.4, (b) Faulty current, equation 2.5.5

## 2.5.2 Wischer Principle

The Wischer principle is based on measuring the zero sequence current and voltage from the moment an earth fault occurs to the end of the first signal increase. The direction of the fault is established by measuring the charging transient flow in the zero-sequence network. One way of measuring the charging transient flow is to filter components below 100 Hz. When components below 100 Hz are filtered, the polarity of the transient can be established by comparing instantaneous values to a threshold value. Because transients will always decrease with time, the polarity has to be established within the first increase of the signal. If the first increase of the signal is missed, then the logic determining the direction will fail. When the polarity of the zero-sequence voltage and current is known, the direction can be established by comparing these two polarities[13]. The possible outcomes are presented in table 2.2.

Table 2.2: Wischer-principle direction determination by comparing polarity of zero-sequence voltage and current

$I_0$	$V_0$	<b>Direction</b>
Pos	Neg	Forward
Neg	Pos	Forward
Pos	Pos	Backward
Neg	Neg	Backward
Pos/Neg	-	Unknown

The polarity difference in currents, and the window to determine the polarity and direction, are illustrated in figure 2.10.

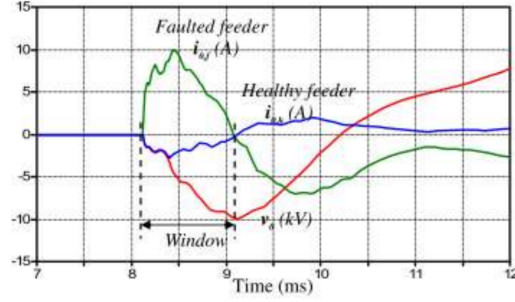


Figure 2.10: Illustration of polarity difference of currents in two feeders[7]

### 2.5.3 Zero Sequence Energy Method

Similar to the Wischer principle, the polarity of zero sequence current and voltage can be used to determine the direction of the ground fault using the zero sequence energy method. This is done by first measuring the quantities mentioned above and computing the zero sequence active power by using equation 2.5.6[13].

$$P_0(t) = \frac{1}{T} \int_0^T U_0(\tau) I_0(\tau) d\tau \quad (2.5.6)$$

Zero sequences active power is used to calculate the zero-sequence energy, as presented in equation 2.5.7.

$$E_0 = E_0(t-1) + \int_0^T P_0(t) dt \quad (2.5.7)$$

The calculated energy in equation 2.5.7 is compared to a threshold value,  $\epsilon$ . Due to  $V_0$  and  $I_0$  having opposite polarities during a fault, a fault is in forward direction if  $E_0 < -\epsilon$ , and backward otherwise. In cases where  $-\epsilon < E_0 < \epsilon$ , the active power and energy can be calculated for 2 additional times, meaning that the maximum amount of times the power can be measured is three[13]. Energy in faulty and healthy feeders is illustrated in figure 2.11.

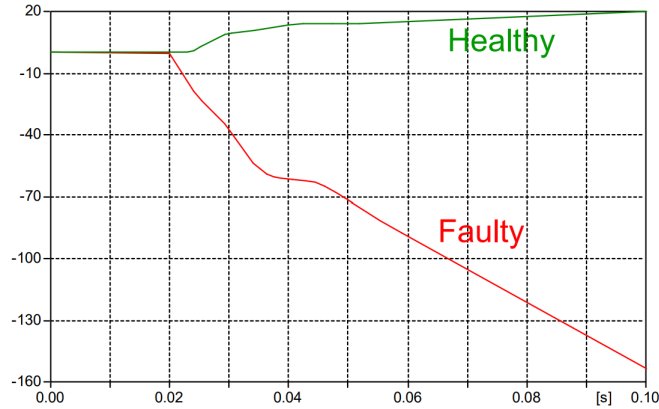


Figure 2.11: Illustration of energy in the faulty and healthy feeder[7]

### 2.5.4 Admittance Based Protection Function

Like many other functions, the admittance-based protection function is based on measurements of the fundamental component of residual voltage and current. Still, instead of these values being



the operational quantities, the protection function calculates zero-sequence admittance,  $Y_0$ , as demonstrated in equation 2.5.8.

$$Y_0 = \frac{I_0 \angle \theta}{V_0 \angle \theta} = G_0 + jB_0 \quad (2.5.8)$$

As seen in equation 2.5.8, the neutral admittance is composed of two values,  $G_0$  and  $B_0$ , representing conductance and susceptance respectively. The measured  $Y_0$  is directly related to known system parameters such as resistances, capacitances, and inductances. The advantage of this protection function is that the  $Y_0$  remains constant when fault resistance,  $R_f$ , changes because  $I_0$  and  $V_0$  will decrease with increasing  $R_f$ [14].

In case of a fault, the neutral admittance,  $Y_0$ , will be equal to the total neutral admittance of the background network,  $Y_{tot}$ . The conductance of  $Y_0$  will always be positive, whereas susceptance,  $B_0$ , depends on the tuning of the arc suppression coil. In addition, the protection function is set to operate with an additional resistive current component,  $I_R$ , i.e., the current through the parallel resistor of the coil. The increase in  $I_R$  can be measured in the conductance component of  $Y_0$ . The protection function operates when the inside fault admittance is measured and outside fault admittance is not[14]. An outside fault will have a neutral admittance equal to the admittance of a protected feeder, but with a negative sign. In addition, this neutral admittance will mainly be composed of a reactive component and a small resistive component due to leakage losses of the feeder. When a fault is inside a faulty feeder, the parallel resistor is connected in parallel to the arc suppression coil, increasing the real part of neutral conductance[15].

Taking the information presented above into consideration, the admittance of outside fault,  $Y_{outside}$ , can be written as:

$$Y_{outside} = -Y_{PF} \quad (2.5.9)$$

And inside fault, in a compensated network:

$$Y_{inside} = Y_B + Y_{grounding} \quad (2.5.10)$$

Where  $Y_{PF}$  is the total phase-to-earth admittance in the protected feeder,  $Y_B$ , is total background admittance, and  $Y_{grounding}$  is the admittance of the grounding arrangement, meaning arc suppression coil and parallel resistor. Figure below illustrates outside fault and inside fault, both with and without a parallel resistor connected to the arc suppression coil.

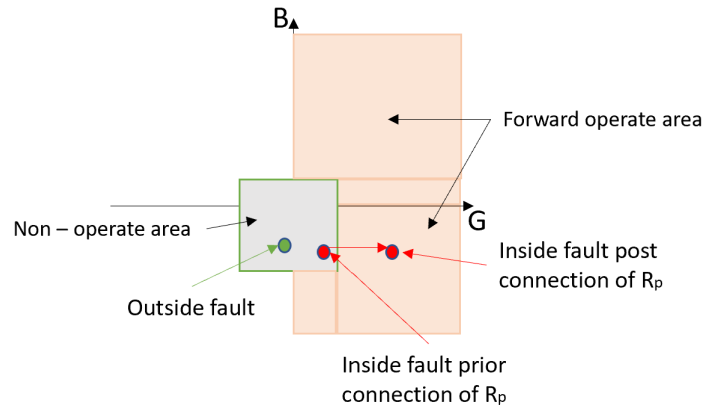


Figure 2.12: Illustration of the outside fault and the inside fault with and without a parallel resistor [16]

The information and theory presented above are acquired from preparation work for this thesis[5].

### 3 Siemens SIPROTEC 7UM85 Ground Fault Protection Functionality

Analysis and testing of ground fault protection functions in this master thesis are performed with Siemens SIPROTEC 7UM85 relay. This subsection will cover the relevant functions, settings, and working principles of Siemens SIPROTEC 7UM85. The ground fault protection functions that this section covers are listed below:

- Wattmetric based ground fault protection.
- Transient-based ground fault protection.
- Admittance-based ground fault protection with  $G_0$  or  $B_0$  measurement.

The contents of this subsection are based on preparation work for this thesis[5] and the Siemens SIPROTEC 7UM85 relay manual[17].

#### 3.1 Wattmetric Based Ground Fault Protection

The Wattmetric protection function in Siemens SIPROTEC 7UM85 is called Directional 3I0 Stage with  $\cos\phi$  or  $\sin\phi$  Measurement and is the most used protection function against ground faults. This function can either measure the zero-sequence voltage at the broken delta winding of a voltage transformer or perform a calculation of zero-sequence voltage by the summation method. Same yields the calculation of zero sequence current. Both measurements of zero sequence quantities process the sampled values and filter out the fundamental component numerically, isolating it and using it for fault detection and disconnection.

When measured/calculated values for zero sequence current and voltage exceed their threshold values, the ground fault detection, which frequently is referred to as pickup, is initiated. In cases where there may be unwanted oscillations, the direction determination can be delayed if desired. In addition, the function's operation functionality can also be delayed, providing the arc suppression coil with the opportunity to extinguish the fault without the need for immediate disconnection of the system.

The function uses characteristics as illustrated in figure 3.1. For systems grounded by arc suppression coil, Siemens recommends using the  $\cos\phi$  measuring method without  $\phi$ -correction. As shown in the figure 3.1, the zero-sequence current vector has to exceed a specified value,  $Min.polar.3I0 >$  for dir. det, for direction determination. In cases where the measured/calculated value of zero sequence current is smaller than the value of  $Min.polar3I0 >$  parameter, the direction determination will fail.

The most important settings for this ground fault protection function that can be altered in DIGSI, are covered below.

- Operate & ft. rec. blocked [Yes / No]: This setting is used to specify whether the operate functionality should be blocked. If [No] is chosen, the protection function will disconnect the fault in case of fault detection.
- Directional mode [Forward / Reverse]: Specifies which direction the ground fault function is looking.
- Dir. measuring method [ $\cos\phi$  /  $\sin\phi$ ]: Specifies the measuring method.  $\cos\phi$  is recommended for systems grounded through an arc suppression coil.

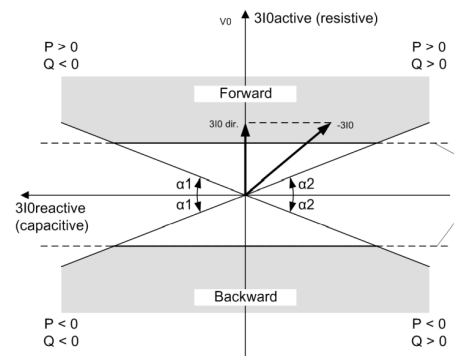


Figure 3.1: The characteristics for direction determination and operate functionality in Siemens 7UM85

- 
- Min. polar.  $3I_0 >$ : The Wattmetric contribution of fault current is specified with this parameter. It is recommended that this threshold value is half of the measured Wattmetric ground fault contribution
  - $V_0 >$  and  $3I_0 >$ : With these parameters, the threshold values for zero-sequence voltage and current are specified. A potential ground fault is detected if the measured zero-sequence voltage exceeds the specified threshold value  $V_0 >$ . The protection function will operate/disconnect the fault if measured values for zero-sequence voltage and zero sequence current exceed their specified threshold values.

### 3.2 Transient Based Ground Fault Protection

The ground fault in arc-suppression coil grounded systems can often extinguish within milliseconds of ignition. This function determines the ground-fault direction by utilizing the energy-integration method. This results in high sensitivity and stability against undesirable electric oscillations in the zero-sequence network. This function is also able to detect permanent ground faults because these start with a transient charging process in healthy phases.

This function will first measure the voltage in the system and convert it to zero-sequence voltage ( $V_0$ ). The instantaneous values of this voltage are then measured at a frequency of 8 kHz. The sampled  $V_0$  values are compared to a threshold such that time of a fault can be determined. Further, the sampling of both  $V_0$  and  $3I_0$  at a frequency of 8 kHz is used to determine the basis for the direction of the fault. When a ground fault is registered, the active energy of the zero-sequence system is calculated across approximately one cycle frequency. The sign of active energy in the zero-sequence network determines the direction of the fault - if the sign is negative, a forward fault is present and backward otherwise. In addition, operational zero-sequence currents can occur in closed loops, which are present during ground faults, and can contribute to false direction results. As a consequence, the Transient protection function eliminates operational zero-sequence currents.

The pickup for both occurrence of the fault and direction of the fault can be controlled by determining threshold values for voltage and current in zero sequence networks. This is also known as sensitivity. If the fundamental component of zero-sequence voltage exceeds its threshold value within 100 ms, and the RMS value of zero sequence current exceeds its threshold value, the ground fault direction will be reported. This way, high impedance ground faults are also reported in which the zero-sequence system values rise slowly, and for this reason, the occurrence of a ground fault is detected noticeably earlier than the exceeding of the predetermined threshold values.

Due to transmission grids being in somewhat constant change, the Transient ground fault protection function is protected against switching operations in the system. The change in the fundamental component of zero-sequence voltage is negligible during switching operations; therefore, the threshold setting for zero-sequence voltage suppresses the effects of a changing system. In events where the change of the transmission system causes long-lasting and high values of zero-sequence voltage, the protection function will compare the positive sequence current before and after the transient period, which is introduced by changes in the system. This way, the Transient protection function can distinguish between ground fault and switching operations.

The most important settings for this ground fault protection function that can be altered in DIGSI are covered below.

- Operate functionality [Yes / No]: Specifies whether the protection function should operate/disconnect ground faults.
- Directional mode: [Forward / Reverse]: Specifies the direction of ground fault protection.
- $V_0 >$  and  $3I_0 >$ : The threshold values for zero-sequence voltage and current must be exceeded for the function to detect and disconnect ground faults.
- Dropout delay: Specifies when the function should reset after fault extinction. For example, if the dropout delay is set to 10 ms, it will take 10 ms for the protection function to reset its pickup-timer after fault extinction.

### 3.3 Admittance Based Ground Fault Protection With $G_0$ or $B_0$ Measurement

This function measures the zero-sequence voltage by first measuring the neutral voltage and converting it to zero-sequence voltage. If the neutral voltage is not available, the zero-sequence voltage is measured by measuring phase to ground voltages of the line. When measuring  $3I_0$ , the function usually evaluates the sensitively measured ground current via a core balance current transformer. For larger secondary ground currents, the function switches to  $3I_0$  calculated from the phase currents. Methods for both zero-sequence voltage and current process the sampled values and filter out the fundamental component numerically, isolating it. The measured values mentioned above are used to calculate  $Y_0$ , which is used as a condition to recognize ground fault.

The characteristics for direction determination in the Admittance-based protection function are shown in figure 3.2. Siemens recommends using conductance as a direction measuring method in systems grounded with arc suppression coil. For fault direction determination, Siemens recommends the use of equations 3.3.1 and 3.3.2 for the tuning of the  $G_0$  parameter.

$$G_0 > k_{s1} \frac{I_{0,active}}{\sqrt{3}V_{sys}} + \frac{I_{0,min}}{V_0} > \quad (3.3.1)$$

Where  $k_{s1}$  is safety margin that should be set to  $k_s = 1.2$  for cable networks and  $k_s = 2$  for overhead lines.  $I_{0,active}$  is the Wattmetric residual current of the protected feeder,  $I_{0,min}$  is the lowest ground current in a healthy case, and  $V_0$  is the threshold value for zero-sequence voltage.

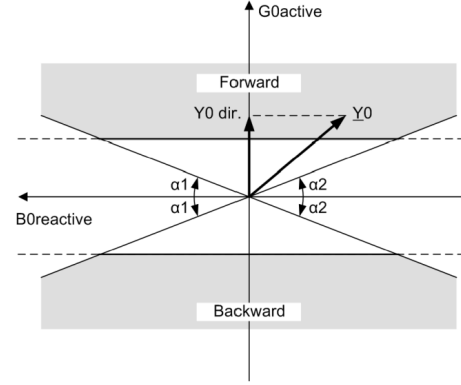


Figure 3.2: The characteristics for direction determination and operate functionality for Admittance based protection function in Siemens 7UM85

$$G_0 < \frac{1}{k_{s2}} \frac{I_{Rp}}{\sqrt{3}V_{sys}} \quad (3.3.2)$$

Where  $k_{s2}$  is a safety margin, and should be set to  $k_{s2} = 1.5$  and  $I_{Rp}$  is the current of the parallel resistor.

The most important settings for this ground fault protection function that can be altered in DIGSI are covered below.

- Operate functionality [Yes / No]: Specifies whether the protection function should operate/disconnect ground faults.
- Directional mode: [Forward / Reverse]: Specifies the direction of ground fault protection.
- Dir. measuring method [G0 / B0]: Specifies whether conductance or susceptance is used for direction determination. Measurement of G0 is recommended in arc suppression coil grounded systems.
- $V_0 >$  and  $3I_0 >$ : The threshold values for zero-sequence voltage and current must be exceeded for the function to detect and disconnect ground faults.
- $G_0 >$ : Specifies the threshold value that has to be exceeded for the protection function to register ground fault direction

The information presented in sections 3.1 - 3.3 is based on preparation work for this thesis [5] and the Siemens SIPROTEC 7UM85 relay manual[17].

## 4 Methodology

This section will present the approach to investigating the various ground fault protection functions used in this thesis. This is done in six subsections. The first subsection presents the design of the electrical distribution network in Simulink. The second subsection explains how permanent ground fault was applied and how intermittent ground fault was designed. The third subsection describes how COMTRADE files associated with Simulink were generated. The fourth subsection addresses the COMTRADE files and other information from the Norwegian electrical network company. The fifth subsection introduces how relay configuration software was used to configure the relay correctly. Lastly, the sixth subsection illustrates how the in-laboratory connections were made between the power source and the relay.

### 4.1 Modeling Using Matlab and Simulink

The model established in Simulink was a 22 kV, two feeder, radial network with arc suppression coil grounding in parallel with an external resistor. The external resistor was in continuous connection to the system. Due to the introductory phase of the investigation, the built power system was nearly perfect, meaning constant electrical load on both feeders and no disturbances to the zero-sequence system.

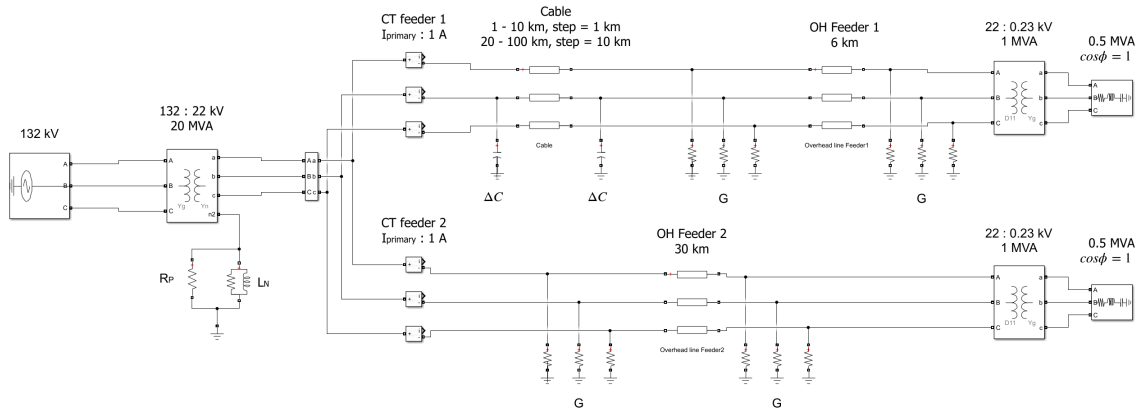


Figure 4.1: Simplified model of the established power system in Simulink

The model established in Simulink is presented in the figure 4.1, and shows that feeder two consists solely of an overhead line with a constant length of 30 km, whereas feeder one is mixed. In Simulink models, feeder 1, i.e. mixed feeder, was the protected feeder to which the faults were applied. The model presented in the figure 4.1 was used to perform two kinds of experiments:

1. Small system, where the protected feeder length is dominated by cable, whereas the background feeder was a pure overhead line of constant length.
2. Larger system, where the length of cable used in the protected feeder is increased greatly.

In the small Simulink system, the cable of the protected feeder varied between 1 and 10 km, with a step of 1 km. Being relatively small, this model was used to investigate how ground fault protection function parameters and threshold values affect performance in detecting and disconnecting ground faults. In the more extensive system, the cable length of the protected feeder varied between 20 and 100 km, with a step of 10 km. With increasing cable, the capacitance to the ground rises significantly due to cables being much more capacitive than overhead lines. Large capacitances to the ground affect the angle between the zero-sequence current and voltage. Consequently, long cable lengths were used to investigate how long a single cable can get before the ground fault protection functions encounter ground fault detection and disconnection difficulties.

---

The cable and overhead line parameters were obtained using the appropriate voltage levels from the SINTEF planning book. The cable and overhead line parameters were also used to calculate the appropriate asymmetry, which was added to phase B, and conductance to the ground. The asymmetry was set to 2% of total system capacitance to ground, whereas conductance to the ground was 6% of total overhead line capacitance.

The power system, in this case, was run in the resonance point, meaning that the inductance in a neutral point of the main transformer was equal to the capacitance in the system, resulting in parameter  $s$  in equation 2.2.13 being equal to 0. Due to the system being tested with 19 different cable lengths, an equal amount of different arc suppression coil sizes had to be found. This was done by following the steps described below:

1. Equation 2.2.13 was solved for  $s = 0$ .
2. An offset array was established, where the calculated inductance in the previous step was multiplied by numbers in the interval  $[0.5, 2]$ , with a step of 0.01, resulting in 151 values for the arc suppression coil.
3. The simulation containing the established power system was run with each value of the arc suppression coil found in the previous step.
4. Matlab-script was used to extract the maximum value of neutral voltage for each value of the arc suppression coil.
5. Relation  $I_L = \frac{V_n}{\omega L}$  was used to plot the neutral voltage as a function of arc suppression coil current.

The grounding of the main transformer in figure 4.1 shows that two resistors were used in parallel with the arc suppression coil. The first resistor was used to simulate the losses in the coil and was set to a high resistance value of  $50 \text{ k}\Omega$ . The second resistor,  $R_p$ , was used as a physical, parallel resistor for assisting protection functions in detecting ground faults. The size of this resistor was set to 125 kW, as REN recommends[12]. The resistive value was calculated by using the equation 4.1.1

$$R_p = \frac{\left(\frac{V_{sys}}{\sqrt{3}}\right)^2}{P_{resistor}} = \frac{V_{sys}^2}{3P_{resistor}} \quad (4.1.1)$$

Where  $V_{sys}$  is the network line-line voltage, and  $P_{resistor}$  is the size of the parallel resistor.

## 4.2 Application of Ground Fault

To apply a permanent ground fault, Three-Phase electrical fault block in Simulink was used to apply a single phase to ground fault on the end of feeder 1. During experiments on a small system, ground fault resistances were varied between  $0 \text{ }\Omega$  and  $4.5 \text{ k}\Omega$  with a step of  $500 \text{ }\Omega$ , and  $5 \text{ k}\Omega$  to  $14 \text{ k}\Omega$  with a step of  $1000 \text{ }\Omega$ . During experiments on the large system, i.e., cable lengths of 20 - 100 km, the fault resistances used were in the interval  $[0 \text{ }\Omega, 4.5 \text{ k}\Omega]$ . Table 4.1 presents the on and off times for ground faults of different fault resistance. Throughout the investigation of the Simulink model, the Fault on and Fault off times was kept the same, such that a direct comparison between ground fault protection function performance could be made.

Table 4.1: Permanent ground fault on and off times, based on the value of fault resistance. Same on and off times apply to  $5 \text{ k}\Omega \leq R_f \leq 14 \text{ k}\Omega$

$R_f [\text{k}\Omega]$	<b>0</b>	<b>0.5</b>	<b>1</b>	<b>1.5</b>	<b>2</b>	<b>2.5</b>	<b>3</b>	<b>3.5</b>	<b>4</b>	<b>4.5</b>
<b>Fault on [s]</b>	0.5	2.5	4.5	6.5	8.5	10.5	12.5	14.5	16.5	18.5
<b>Fault off [s]</b>	1	3	5	7	9	11	13	15	17	19

Application of intermittent ground faults was based on cable insulation breakdown and was therefore designed with section 2.3 as reference. Figure 4.2 demonstrates zero-sequence voltage during low impedance intermittent ground fault.

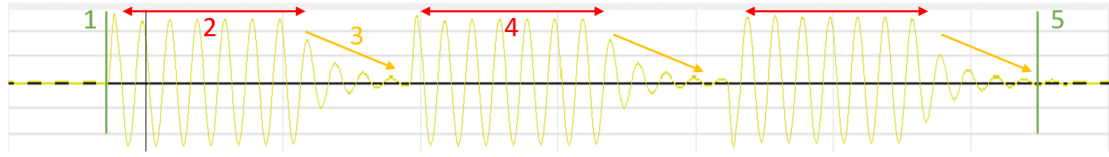


Figure 4.2: Zero sequence voltage during an intermittent ground fault

As demonstrated in figure 4.2, the intermittent ground fault follows the cycle of the intermittent ground fault shown in figure 2.5. The figure 4.2 highlights five different events:

- Event 1: Steady-state operation of power system
- Event 2: Ignition of ground fault
- Event 3: Power system stabilizes, zero-sequence voltage returns to its steady-state value, at the same time as phase voltages restore their nominal values
- Event 4: As the zero-sequence voltage has reached its steady-state value, cable insulation is unable to carry full phase voltage, re-igniting the fault
- Event 5: Intermittent ground fault is cleared by ground fault protection functions. The system returns to steady-state.

### 4.3 Generation of COMTRADE-files

For the generation of files that could be tested on real-life relays, IEEE Standard Common Format for Transient Data Exchange, 1999 (COMTRADE) was used. The Simulink results were sent to the Matlab workspace, and from there, using the 1999 COMTRADE format, a script was written to convert Simulink results to configuration (cfg) and data (DAT) files. Configuration files were the ones that were tested, whereas data files contained the specific information about the program that was used to create files.

As mentioned in the previous subsection, 20 different fault resistances for cable lengths 1 km - 10 km, and 10 different fault resistances for cable lengths 20 km - 100 km were tested, resulting in 290 individual COMTRADE files for single-phase to ground faults. To allow the in-laboratory work to be as efficient as possible, two COMTRADE files were established for each cable length - the first file containing results for a given cable length and fault resistances of 0  $\Omega$  to 4.5 k $\Omega$  with a step of 500  $\Omega$ , and a second file containing fault resistances of 5 k $\Omega$  to 14 k $\Omega$  with a step of 1000  $\Omega$ . The length of each COMTRADE file was set to 20 seconds due to the relay not allowing longer recordings. The steps explaining how the COMTRADE files were made are shown below, whereas the script itself is demonstrated in appendix D.

1. Time values for simulation start and end, fault on and off were defined. In addition, values for initial fault resistance, and fault resistance increment were defined.
2. Two array structures were defined - one temporary array for storing results for a single fault and one permanent which porpoise was to store all results.
3. Simulation was run 10 times. After each simulation, time values for simulation start and end, and fault on and off, were increased by 2 seconds. In addition, fault resistance was increased by 500  $\Omega$  or 1000  $\Omega$  for each run, depending on the information provided above.
4. During the first run, results were assigned to the permanent array.

5. During runs 2-10, the result for each fault was first stored in a temporary array. Then, the permanent array was expanded by a number matching the size of the temporary array. Lastly, the contents of the temporary array were assigned to the expanded slots of the permanent array.
6. Lastly, the permanent array containing results for all 10 fault resistances was passed to COMTRADE-script.

By reducing the number of COMTRADE files required for each cable length from 20 to 2, the efficiency in the laboratory was increased, as well as the possibility of error was minimized.

## 4.4 Processing Data From Norwegian Distribution Network

A single electrical grid company provided COMTRADE files, relay settings, and information regarding the protected feeder in Norway. Due to the sensitive information provided, the company's name and location will remain undisclosed. The given name for the company in this thesis is company A.

### 4.4.1 Company A

COMTRADE files provided by Company A were from a single, mixed feeder which was cable-dominated. The total length of the protected feeder was 23.237 km, of which 22.437 km was cable. The relevant information for the protection purposes for both low impedance and high impedance ground faults is demonstrated in figure 4.3.

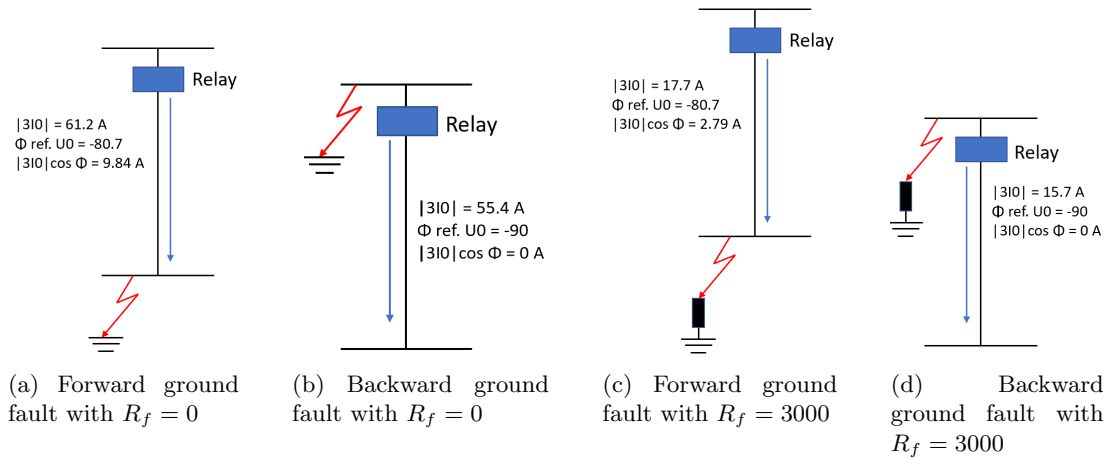


Figure 4.3: Company A: Zero sequence current and wattmetric current during low impedance and high impedance ground faults on cable dominated feeder

In addition, the ratios for instrument transformers that were used in experiments on the above-presented system, are shown in table 4.2

Table 4.2: Instrument transformer ratios that were used in experiments containing COMTRADE-files provided by Company A

$V_p$ [kV]	$V_s$ [kV]	$I_p$ [A]	$I_s$ [A]	$I_{p,0}$ [A]	$I_{s,0}$ [A]
22	0.11	300	5	100	1

The information regarding the system parameters in steady-state for the entire power system is shown in table 4.3.



Table 4.3: Company A: System parameters

System parameters	
$V_s$ [kV]	22
<b>Grounding</b>	Arc Suppression Coil
$I_0$ [A]	130
$I_0$ Distributed coils [A]	-30
<b>Sum <math>I_0</math> [A]</b>	100
Grounding parameters	
$I_L$ [A]	105
<b>Over. comp [A]</b>	5
$R_P$ [kW]/[ $\Omega$ ]	125/1290.7
$R_P$ connection delay	Always connected

The zero sequence current shown in table 4.3 includes the contribution from all cables and overhead lines. As seen from the table, distributed coils are used to reduce the capacitive network current by 30 A, resulting in a total zero sequence current of 100 A.

## 4.5 Configuration of Siemens 7UM85 and Protection Functions

Configuration of Siemens SIPROTEC 7UM85 was done using Siemens software DIGSI. Configuration of the relay for Simulink models and files received from the Norwegian electrical grid company was done somewhat differently. This is due to different CT and VT ratios, COMTRADE-files being of different lengths, and the real-life distribution grid having instrument transformers for zero sequence currents and voltages.

### 4.5.1 Configuration of DIGSI

When configuring Siemens 7UM85, a single line diagram was established in DIGSI that represented the protected line. The cable and overhead line were neglected due to no importance. As shown in figure 4.4, a busbar, circuit breaker, and instrument transformers were included. When the currents and voltages measured by instrument transformers exceed the values of operational parameters of protection functions, a signal is sent to the circuit breaker, disconnecting the downstream circuit.

As shown in the figure 4.4, a specific ratio for both current and voltage transformer in the single line diagram has to be specified. The values measured by the instrument transformers are sent to measuring points in the relay. Consequently, it is necessary that the instrument transformer ratio values match the measuring point ratio values, as demonstrated in figure 4.5.

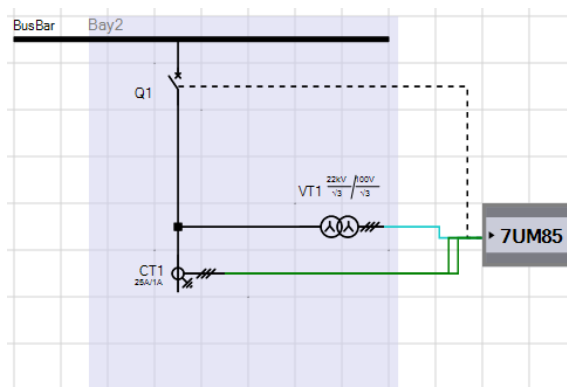


Figure 4.4: DIGSI: Single line diagram

Rated primary current:	25.0	A
Rated secondary current:	1 A	
Current range:	100 x IR	
Internal CT type:	CT protection	
Neutr.point in dir.of.ref.obj:	yes	
Inverted phases:	none	

(a) Current transformer ratio matching the measuring point ratio

Rated primary voltage:	22.000	kV
Rated secondary voltage:	100	V
VT connection:	3 ph-to-gnd voltages	
Inverted phases:	none	
Tracking:	active	
Measuring-point ID:	3	
Internal VT type:	Voltage transformer	

(b) Voltage transformer ratio matching the measuring point ratio

Figure 4.5: Demonstration of instrument transformer measuring point ratio corresponding to instrument transformer ratio in single line diagram

The Siemens SIPROTEC 7UM85 did not allow COMTRADE files with lengths of over 20 seconds. In addition, there was no easy or obvious way to introduce automatic re-closing of the circuit breaker after the initial trip. A logic was implemented to bypass this restriction, which is shown in the figure 4.6. As seen from the figure, a CFC block provided a high output when any of the ground fault functions registered operate/trip signal. This signal was reset by pressing the "Quit" button on the relay when the trip indication was visible. The output of the block was the external trip function, which was added in addition to the ground fault protection functions.

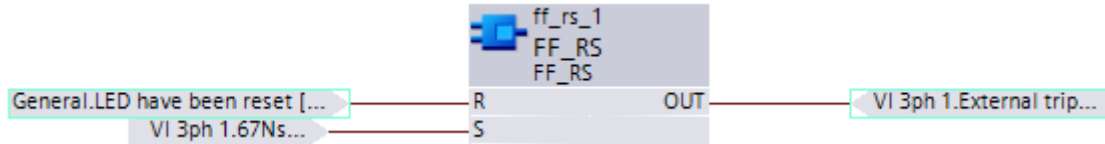


Figure 4.6: DIGSI: CFC block logic which enables multiple faults in a single COMTRADE-file

Examining the results of protection function performance was of much importance for conducting analysis. Therefore, information recorded by the fault recorder was set up, such that malfunctions could be investigated. The basics of the fault recorder settings are shown in figure 4.7. Fault recording was changed to "With pickup & AR" such that the fault recordings would record the fault, including both short and long interruptions. The maximum recording time was changed to the maximum allowed value, i.e., 20 seconds. In addition, the resulting magnitudes of currents and voltages were set to be scaled to primary values. In addition to basic fault recorder values, the ground fault protection detection and operation functionality was routed to the fault recorder, such that both detection and disconnection of faults could be investigated, as demonstrated in figure 4.8.

81.791.2761.130	Fault recording:	with pickup & AR cyc.
81.791.2761.131	Storage:	always
81.791.2761.111	Maximum record time:	20.00 s
81.791.2761.112	Pre-trigger time:	0.50 s
81.791.2761.113	Post-trigger time:	0.50 s
81.791.2761.116	Manual record time:	20.00 s
81.791.2761.140	Sampling frequency:	8 kHz
81.791.2761.141	Sampl. freq. IEC 61850 rec.:	8 kHz
81.791.2761.151	COMTRADE revision year:	COMTRADE 1999
81.791.2761.128	Scaling COMTRADE:	Primary values
81.791.2761.129	Cal.zero.seq.cur.channel:	3I0
81.791.2761.132	Cal.zero seq.volt.channel:	3V0

Figure 4.7: DIGSI: Configuration of the values that were written to the fault recorder for post-processing

Information				Source	Destination
				Func CFC	Binar LEDs Recorder
Signals	Fav	Number	Type		Fault recorder
(All)	(All)	(All)	(All)	*	*
VI 3ph 1		821			
General		821.9451			
Group indicat.		821.4501			
Reset LED Group		821.7381			
Process monitor		821.1131			
Operational values		821.761			
Fund./sym.comp.		821.771			
67Ns Dir.sens GFP1		821.1861			*
Group indicat.		821.1861.4...			
General		821.1861.2...			
3I0>cos/sing1		821.1861.1...			*
>block stage		821.1861.1...	SFS		
>block delay & op.		821.1861.1...	SFS		
Mode (controllable)		821.1861.1...	ENC		
Inactive		821.1861.1...	SFS		
Behavior		821.1861.1...	ENS		
Health		821.1861.1...	ENS		
Ground fault		821.1861.1...	ACD		
Pickup		821.1861.1...	ACD		*
general			SFS		
forward			SFS		X
backward			SFS		X
unknown			SFS		
Operate delay exp.		821.1861.1...	ACT		
Operate		821.1861.1...	ACT		*
general			SFS		X

Figure 4.8: Example of information routing for Wattmetric protection function. The signals for ground fault detection in forward and backward directions, as well as signal for operate are sent to the fault recorder by setting a mark, 'X', in the corresponding row and column

Due to files from company A containing both phase and zero sequence currents and voltages, the measuring points shown in figures 4.9 and 4.10 had to be changed such that direct zero-sequence quantities could be measured.

		1B			
		1B1-1B2	1B3-1B4	1B5-1B6	1B7-1B8
Measuring point	Connection type	V 1.1	V 1.2	V 1.3	V 1.4
(All)	(All)	(All)	(All)	(All)	(All)
Meas.point V-3ph 1	3 ph-to-gnd volt. + VN	V A	V B	V C	VN

Figure 4.9: DIGSI: Assignment of phase voltages and zero-sequence voltage

		1A1-1A2	1A3-1A4	1A5-1A6	1A7-1A8
Measuring point	Connection type	I P 1A1	I P 1A2	I P 1A3	I M 1A4
(All)	(All)	(All)	(All)	(All)	(All)
Meas.point I-3ph 1	3-phase + IN-separate	I A	I B	I C	IN

Figure 4.10: DIGSI: Assignment of phase currents and zero sequence current

As it is shown in figures 4.9 and 4.10, the three first ports of the relay were assigned to phase quantities, meaning phases A, B, and C for voltage and current. The fourth port for both voltage and current was assigned to zero sequence currents and voltages.

---

## 4.5.2 Configuration of Protection Functions for Simulink Model

Three ground fault protection functions were used - Wattmetric, Transient, and Admittance. Due to operate/trip conditions for all three of the protection functions being based on the same values, these values were calculated the same way. The threshold value for zero sequence current in the small Simulink model was chosen to be the worst case for each cable length, meaning at the highest expected fault resistance.

Table 4.4: Small Simulink model:  $I_0$  Threshold  
for  $R_f = 4500$

Cable length [km]	$I_0 > [\text{mA}]$
<b>1</b>	82
<b>2</b>	87
<b>3</b>	95
<b>4</b>	103
<b>5</b>	116
<b>6</b>	128
<b>7</b>	141
<b>8</b>	155
<b>9</b>	169
<b>10</b>	185

Table 4.5: Small Simulink model:  $I_0$  Threshold  
for  $R_f = 14000$

Cable length [km]	$I_0 > [\text{mA}]$
<b>1</b>	30
<b>5</b>	45
<b>10</b>	75

The setting of the zero-sequence voltage value was determining factor for fault detection. In cases where the threshold value for this parameter was set too high, the protection function would not see ground fault and therefore not operate/trip. Due to the small Simulink model being an introductory case of investigation, multiple values for this parameter were tested, such that protection function performance using different sensitivity could be established. It is crucial to remember that the zero-sequence voltage threshold value was never set to be below the operational value.

Table 4.6: Small Simulink model: Zero sequence voltage threshold for fault detection

Case	$V_0 > [\text{V}]$
$0 \leq R_f \leq 4500$	15
$0 \leq R_f \leq 4500$	5
$5000 \leq R_f \leq 14000$	5
$5000 \leq R_f \leq 14000$	3

Having tested the variety of settings in ground fault protection functions in the small Simulink model, the protection functions for the large Simulink model were configured so that the amplitude of zero sequence current and voltage vectors would not be a limiting factor for ground fault protection performance. None of the threshold values were set below the operational zero-sequence values.

Table 4.7: Large Simulink model: zero-sequence threshold values for cable lengths 20 km - 100 km

Cable length [km]	$V_0 >$ threshold [V]	$3I_0 >$ Threshold [mA]
<b>20-60</b>	10	290
<b>70</b>	9	290
<b>80</b>	8	290
<b>90</b>	7	290
<b>100</b>	6	290

### 4.5.3 Configuration of Protection Functions for Company A

Due to COMTRADE files received from company A were recordings from an actual power system, there was made a reasonable assumption that these files contained more realistic values for asymmetry, conductance, and disturbances to both the physical power system and the zero-sequence network. In addition, due to Company A using the Wattmetric protection function, it was desired to use the exact protection function settings for all of the tested functions, such that a direct comparison of ground fault protection performance could be made. The parameters that were used for zero sequence current and voltage are shown in table 4.8.

Table 4.8: Company A: Ground fault relay settings acquired from relay plan

	Primary	Secondary
$3I_0 > \text{dir. [A]}$	0.15	0.001
$\alpha_1$ reduction [Degrees]	1	-
$\alpha_2$ reduction [Degrees]	1	-
$3I_0 > [\text{A}]$	2.4	0.016
$V_0 > [\text{V}]$	3000	15
Dir. det. delay [s]	0.1	-
Operate delay [s]	1.9	-

As seen in table 4.8, the Wattmetric component of fault current has to exceed 1 mA referred to the secondary side for the direction determination to be initialized. Furthermore, for the protection function to become operational, meaning initiating the trip signal, both zero sequence current and voltage, referred to the secondary side, must exceed 16 mA and 15 V, respectively.

### 4.6 Connection Between Power Source and Relay

Physical connections made in the laboratory were between the relay and OMICRON, which was used as a power source. There were two different connections for currents and voltages throughout the laboratory work - one connection group without the measurement of zero sequence current and voltage, and one connection including direct measurement of zero-sequence. The connection of currents and voltages without zero-sequence is shown in figure 4.11

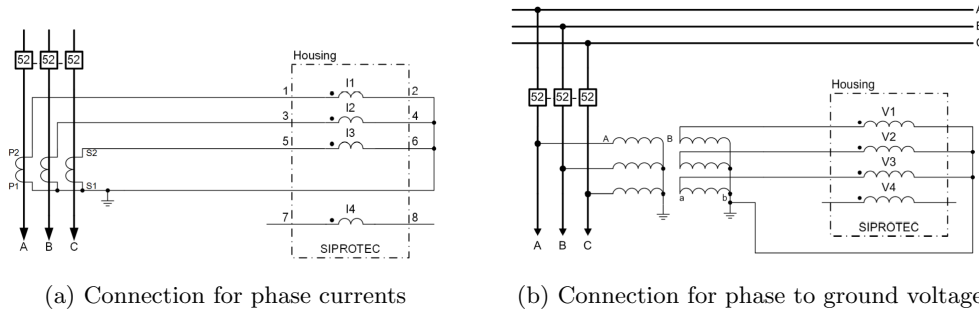
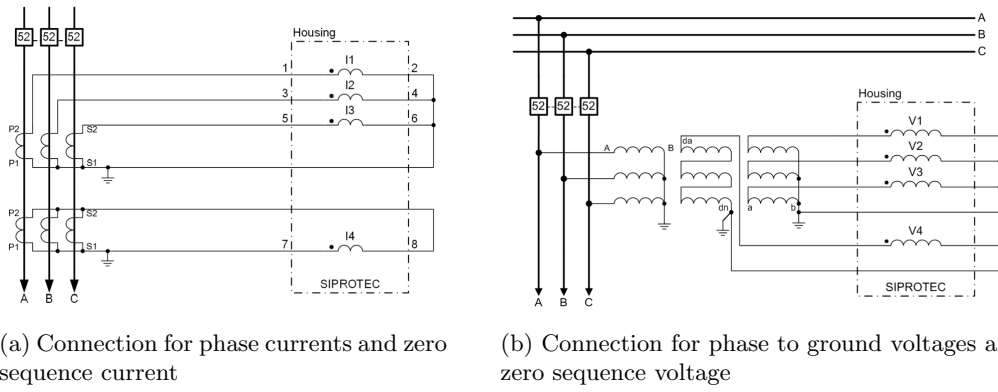


Figure 4.11: Connection for currents and voltages between OMICRON and Siemens 7UM85 [17]

As seen from figure 4.11, three ports for current and voltage were utilized, one port for each phase. By neglecting the connection of zero sequence, the relay itself performed the calculation of these quantities. The connection presented above was utilized when testing the system established in Simulink. The connection of voltages and currents when testing COMTRADE files from power company A is shown in figure 4.12



(a) Connection for phase currents and zero sequence current

(b) Connection for phase to ground voltages and zero sequence voltage

Figure 4.12: Connection for phase currents and voltages, including zero sequence measurements [17]

The measurement for zero sequence current and voltage in figure 4.12 was assigned to ports I4 and V4. The assignment of these ports was used due to COMTRADE files from company A containing measured zero-sequence quantities. It is important to notice that the phase and zero sequence quantities have separate grounding.

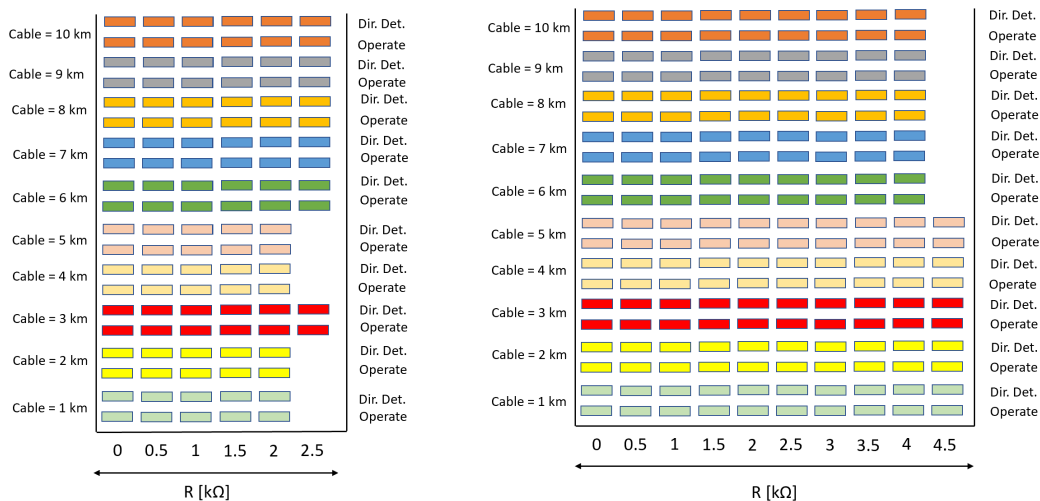
## 5 Ground Fault Protection Function Performance

This section presents the results of Wattmetric, Admittance, and Transient-based ground fault protection functions. The first subsection addresses the results regarding the small Simulink model and illustrates how the change in function settings sensitivity affects the performance of specified ground fault protection functions. The second and third subsection address results regarding the large Simulink model and illustrates how increasing cable length affects the performance of ground fault protection functions during both permanent and intermittent ground faults. The settings for different protection functions in relay performance testing that was done regarding Simulink were kept the same for each protection function, such that the performance of each protection function are directly comparable. The fourth subsection addresses the results of a real-life power system operated by Company A. The results regarding protection function performance presented in this section were obtained from the relay fault recorder and are illustrated in compressed figures for increased readability and understanding. The different colors displayed in the figures in this section are included to distinguish between different cable lengths and protection functions.

### 5.1 Ground Fault Protection Performance due to Parameter Sensitivity

Figure 5.1 demonstrates the performance of Wattmetric and Admittance protection functions with increasing fault resistance and cable length. With setting  $V_0 > 15$ , the functions are able to detect and disconnect faults with a fault resistances of up to  $2.5 [k\Omega]$ . When cable length is less than 50% of the total faulty feeder length, the functions struggle to detect and disconnect faults with fault resistances of  $2.5 [k\Omega]$ . When cable length is increased beyond 50% of the total faulty feeder length, the function becomes reliable for fault resistances of up to  $2.5 [k\Omega]$ .

Decreasing the  $V_0 >$  setting by 10 V to  $V_0 > 5$  drastically increases the protection function reliability and performance. As seen in figure 5.1 (b), by maintaining the threshold value for zero-sequence current and only decreasing the threshold for zero-sequence voltage, the function can detect and disconnect faults with fault resistance of up to  $4.5 [k\Omega]$ . With cable lengths of 50% of the total faulty feeder length or above, the function fails to detect the fault and thereby fails to disconnect.

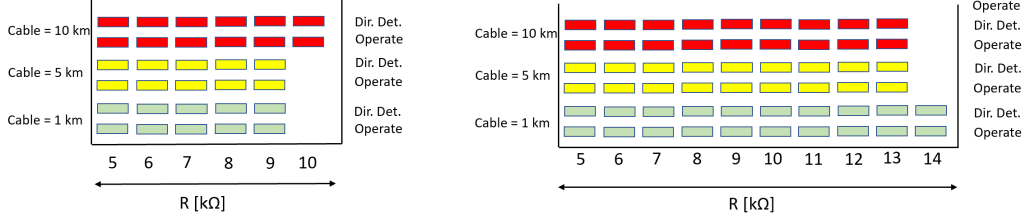


(a) Wattmetric and Admittance protection function performance,  $V_0 > 15V$ ,  $3I_0 >$  according to table 4.4.  $3I_0 \text{ dir} > 30mA$ ,  $G_0 > 0.1mS$ . No ground fault detection past  $R_f = 2.5k\Omega$

(b) Wattmetric and Admittance protection function performance,  $V_0 > 5V$ ,  $3I_0 >$  according to table 4.4.  $3I_0 \text{ dir} > 30mA$ ,  $G_0 > 0.1mS$ .

Figure 5.1: Wattmetric and Admittance function performance using different threshold values for zero sequence voltage

Figure 5.2 demonstrates the Wattmetric and Admittance based protection function performance with extreme fault resistances of  $R_f \geq 5[k\Omega]$ . Figure 5.2 (a) demonstrates that by keeping the zero sequence threshold value at 5 V and decreasing the threshold value for zero-sequence current, the functions can detect and disconnect faults of up to 10  $[k\Omega]$ . By further decreasing the threshold for zero-sequence voltage to 3 V, the functions can detect and disconnect faults with fault resistance of up to 14  $[k\Omega]$  for short cable lengths and up to 13  $[k\Omega]$  for longer cable lengths.

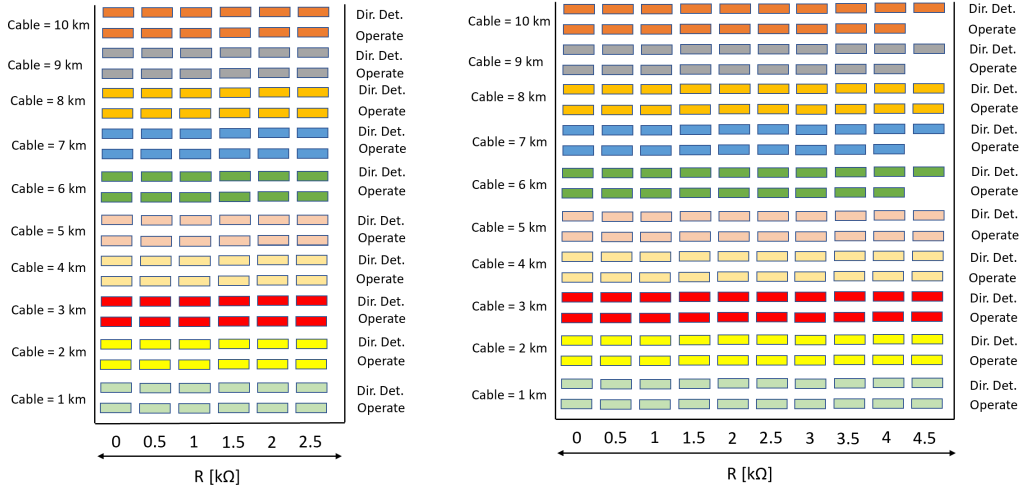


(a) Wattmetric and Admittance protection function performance,  $V_0 > 5V$ ,  $3I_0 >$  according to table 4.5.  $3I_0$ . dir  $> 30mA$ ,  $G_0 > 0.1mS$ . No ground fault detection past  $R_f = 10k\Omega$

(b) Wattmetric and Admittance protection function performance,  $V_0 > 3V$ ,  $3I_0 >$  according to table 4.5.  $3I_0$ . dir  $> 30mA$ ,  $G_0 > 0.1mS$ .

Figure 5.2: Wattmetric and Admittance protection function performance using different threshold values for zero sequence voltage

Figure 5.3 demonstrates the performance of the Transient protection function. By using 15 V for the zero-sequence voltage threshold, the protection function can detect and disconnect faults with fault resistances of up to 2.5  $[k\Omega]$ . Fault resistances beyond 2.5  $[k\Omega]$  lead to the zero-sequence voltage that is lower than the specified threshold value. This is illustrated in figure 5.3 (b), where the zero-sequence voltage threshold is decreased to 5 V. By lowering the threshold voltage by 10 V, the protection function can detect and disconnect faults with fault resistances of up to 4.5  $[k\Omega]$ . When cable length exceeds 50% of the total faulty feeder length, the Transient function does not disconnect the fault but does pick it up. This indicates that the zero-sequence current calculated by the relay was smaller than the calculated value in table 4.4.



(a) Transient protection function performance,  $V_0 > 15V$ ,  $3I_0 >$  according to table 4.4. No ground fault detection past  $R_f = 2.5k\Omega$

(b) Transient protection function performance,  $V_0 > 5V$ ,  $3I_0 >$  according to table 4.4

Figure 5.3: Transient protection function performance using different threshold values for zero sequence voltage



Figure 5.4 demonstrates Transient protection function performance with extreme fault resistances of  $R_f \geq 5[k\Omega]$ . By keeping the recommended threshold value for zero-sequence voltage (5 V) for detection of high resistive faults, the protection function detects and disconnects faults with fault resistances of up to 9  $[k\Omega]$ , as demonstrated in figure 5.4. By decreasing the zero-sequence threshold value to 3 V, detection and disconnection of faults with fault resistance of up to 10  $[k\Omega]$  are achieved.

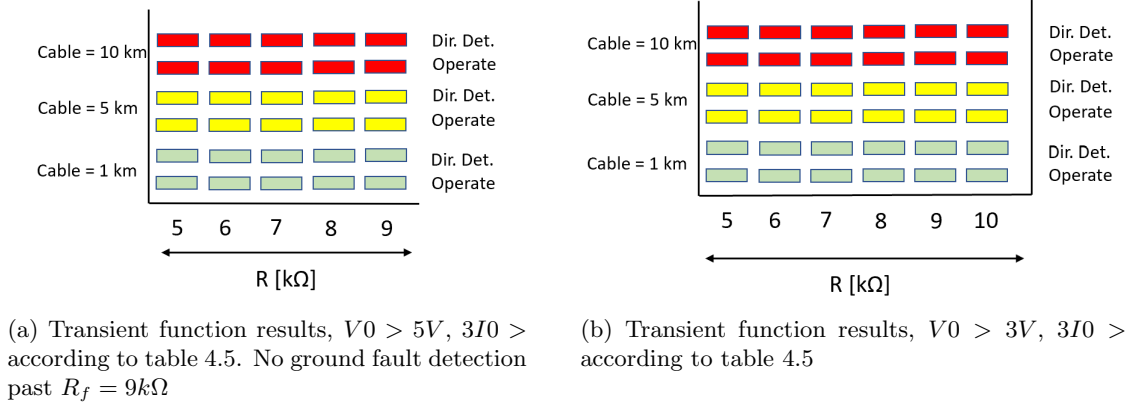


Figure 5.4: Transient function results using different threshold values for zero sequence voltage

It is worth mentioning that both Wattmetric and Admittance protection functions are highly dependent on the size of the parallel resistor in transformer neutral grounding. The results presented above were generated using the REN recommended parallel resistor power of 125 kW. Due to the relatively small Simulink model, using such a large resistor is beneficial for both Wattmetric and Admittance protection functions. Figure 5.5 demonstrates the performance of all three protection functions for a single cable length of 10 km, using a sensitive zero-sequence voltage threshold of 5 V, and parallel resistor power of 250 kW, which in  $\Omega$ , equals exactly half of REN recommended value:

$$R_p = \frac{22000^2}{3 * 250000} = 645.33\Omega$$

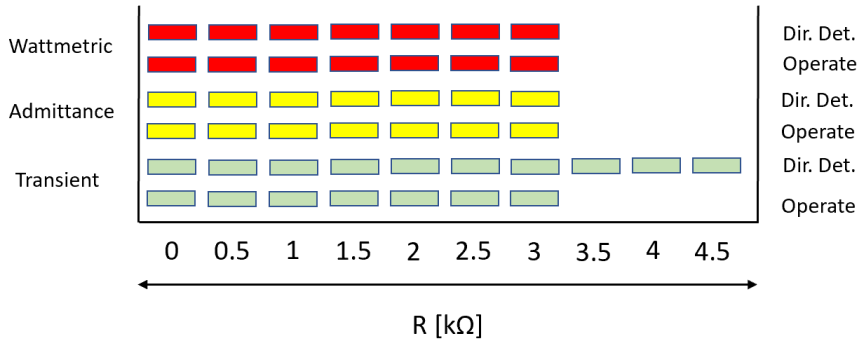


Figure 5.5: Performance of Wattmetric, Admittance, and Transient protection functions when the resistance of the parallel resistor is decreased.  $V_0 > 5V$ ,  $3I_0 >$  according to table 4.4.  $3I_0 > 30mA$ ,  $G_0 > 0.1mS$ .

As demonstrated in figure 5.5, by reducing the resistance of the parallel resistor by half, and keeping the same settings for detection and trip/operate as in figures 5.1 and 5.3, the performance of both Wattmetric and Admittance protection functions is reduced. Both Wattmetric and Admittance functions still detect and disconnect faults with fault resistances of up to 3  $[k\Omega]$ , which is the Norwegian requirement. Still, both functions fail to detect faults with higher fault resistances.

However, the fault detection of the Transient function is unaffected by the change in parallel resistor size, and the function is still able to detect every fault. Due to the reduction of parallel resistor resistance, the resulting, measured zero-sequence current during a fault was reduced, which is why the Transient function is unable to disconnect the fault.

## 5.2 Ground Fault Protection Performance due to Increasing Cable Length

Figure 5.6 demonstrates the Wattmetric protection function performance as cable length increases from 20 km - to 100 km. As shown in figure 5.6, the protection function has excellent performance for cable lengths 20 km - 50 km and can detect and disconnect ground faults with fault resistance up to 4500 [ $k\Omega$ ]. As cable length is further increased by 10 km, to a total length of 60 km, the large capacitance of the cable compromises the Wattmetric protection performance, resulting in malfunction at fault resistance of 4500 [ $k\Omega$ ]. When the cable is increased to 70 km, the Wattmetric protection function can still detect and disconnect ground fault resistance of 3 [ $k\Omega$ ], which is required by Norwegian regulations but fails to detect fault resistances beyond. For cable lengths beyond 70 km, the Wattmetric protection function can detect and disconnect faults with fault resistance of up to 2.5 [ $k\Omega$ ], depending on cable length, meaning that a single cable with a total length of above 70 km, does not comply with Norwegian requirement of ground fault disconnection of fault resistances of up to 3 [ $k\Omega$ ].

Figure 5.7 demonstrates the performance of Admittance-based ground fault protection as cable length increases from 20 km to 100 km. As shown, both cable length and fault resistance do not affect the performance of Admittance-based ground fault protection, except for fault resistance of 4.5 [ $k\Omega$ ] when the cable length is equal to 100 km. Both Wattmetric and Admittance based ground fault protection functions are highly dependent on the parallel resistor,  $R_p$ , as illustrated in figure 5.5, however, due to the Admittance based protection function using conductance,  $G_0$ , of the zero-sequence admittance,  $Y_0$ , as one of the ground fault detection criterion, the effect of large capacitances in the system has a much smaller effect on the performance of Admittance based protection function compared to Wattmetric protection function.

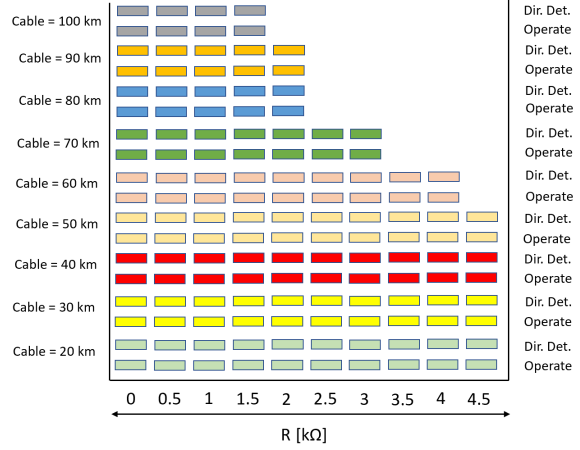


Figure 5.6: Wattmetric protection function performance as cable reaches extreme length.  $V_0 >$  and  $3I_0 >$  settings according to table 4.7.  $3I_0$  dir  $>$  30mA.

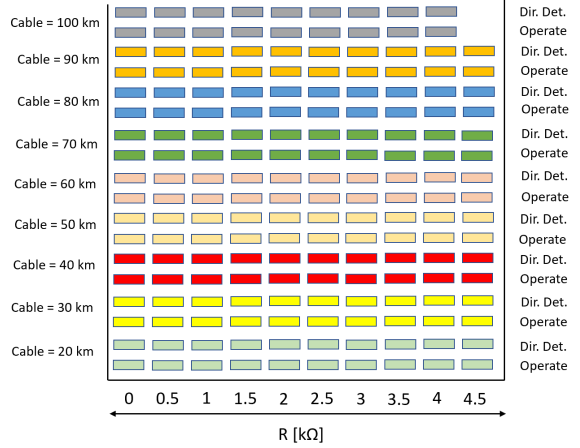


Figure 5.7: Admittance protection function performance as cable reaches extreme length.  $V_0 >$  and  $3I_0 >$  settings according to table 4.7,  $G_0 >$  threshold value of 0.1 mS

Figure 5.8 demonstrates Transient-based ground fault protection performance when cable increases from 20 km to 100 km. As the cable length increases beyond 40 km, the Transient based protection function becomes unreliable for fault resistances above 2 [ $k\Omega$ ]. The Transient based protection function was also tested with a sensitive  $V0 >$  setting of 5V, which did not impact the performance presented in figure 5.8. This result indicates that the design related to cable length in the electrical distribution grid significantly impacts the performance of the Transient-based ground fault protection function. In this case, the cable was modeled as a single cable of a specific length, resulting in a series connection of zero sequence resistance. Large zero-sequence resistance will have an impact on damping of zero sequence current and voltage, resulting in decreasing performance of the Transient ground fault protection function, as demonstrated in figure 5.8. The cable lengths of 20 km - 100 km were distributed on two parallel cables to investigate further the effect of series connection of zero sequence resistance. The Transient-based protection function's performance, where the power is distributed on two parallel cables, is demonstrated in figure 5.9.

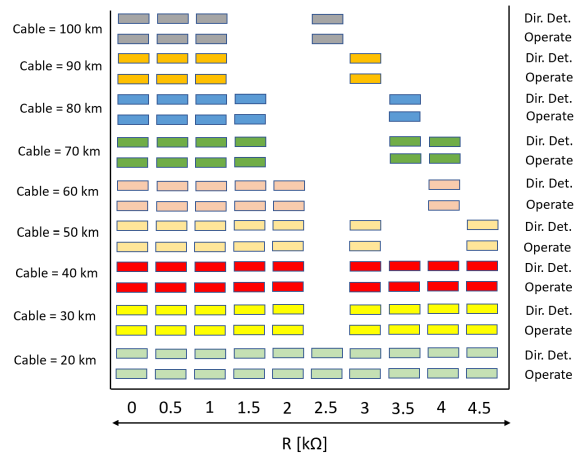


Figure 5.8: Transient protection function performance as cable reaches extreme length.  $V0 >$  and  $3I0 >$  settings according to table 4.7

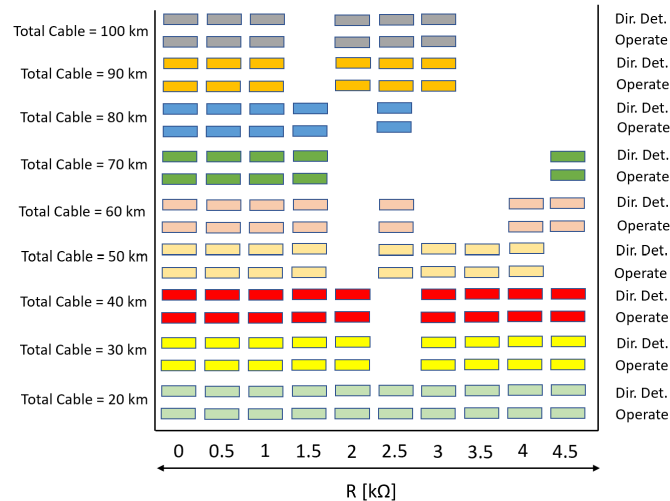


Figure 5.9: Transient-based ground fault protection function performance when two parallel cables of equal length are used.  $V0 >$  and  $3I0 >$  settings according to table 4.7

As demonstrated in figure 5.9, Transient based protection function performance improves as the electrical power across the conductor is distributed on two parallel cables. By choosing two long, parallel cables to carry the load current, the Transient based ground fault protection function can be reliable for a total cable length of 50 km, or 25 km/cable.

The ground fault protection function performance using the same zero-sequence threshold values in figures 5.6-5.8 is summarized in table 5.1

Table 5.1: Summary of ground fault protection function performance as a function of increasing cable length

Cable length [km]	20	30	40	50	60	70	80	90	100
<b>Wattmetric based ground fault protection</b>									
No. of ground faults picked up [%]	100	100	100	100	90	70	50	50	40
<b>Admittance based ground fault protection</b>									
No. of ground faults picked up [%]	100	100	100	100	100	100	100	100	90
<b>Transient based ground fault protection</b>									
No. of ground faults picked up [%]	100	90	90	70	60	60	50	40	40

### 5.3 Ground Fault Protection Performance During Intermittent Ground Fault

Figure 5.10 demonstrates the performance of Wattmetric (a), Admittance (b), and Transient (c) based ground fault protection functions during an intermittent ground fault. Figure 5.10 demonstrates that the difference between Wattmetric and Admittance-based protection functions is minimal during an intermittent ground fault, where both protection functions are able to disconnect intermittent ground fault for cable lengths of up to 50 km. During an intermittent ground fault, it was found that Transient based ground fault protection has the best performance, disconnecting low impedance,  $R_f = 0$ , ground fault for cable lengths 20 km - 100 km.

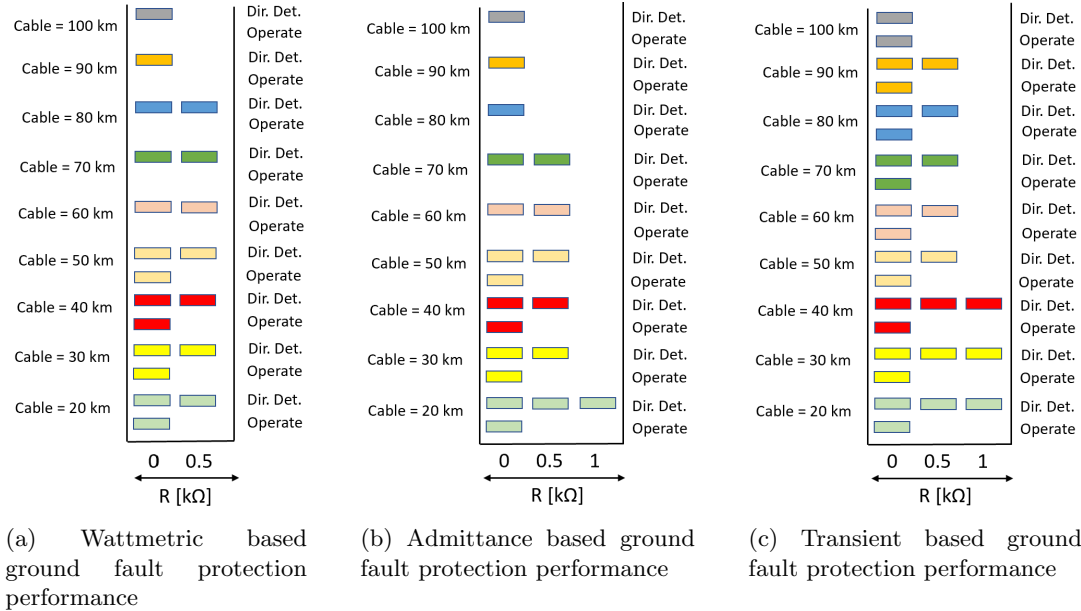


Figure 5.10: Ground fault protection function performance during intermittent ground fault. Zero sequence voltage and current threshold values according to table 4.7.  $G_0 >$  threshold for Admittance function set to 0.1 mS,  $3I_0$ .  $dir >$  for Wattmetric function set to 30 mA

Figure 5.11 demonstrates the Transient-based ground fault protection performance when a sensitive zero-sequence voltage value of 5 V is utilized.

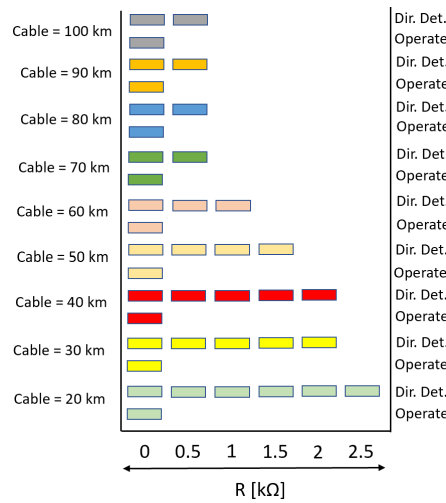


Figure 5.11: Transient based ground fault protection performance during intermittent ground fault with a sensitive  $V_0$  threshold of 5 V

By increasing the sensitivity of zero-sequence voltage, the fault detection performance significantly increased for cable lengths 20 km - 50 km. A comparison of figures 5.10 (c) and 5.11, demonstrates that by utilizing sensitive  $V_0$  of 5 V, ground fault pickup percentage for cable lengths 20 km - 40 km increases from 30% to nearly 60%, and for cable lengths 50 km - 60 km by 10% and 20%, respectively. The performance improvement is summarized in table 5.2

Table 5.2: Difference between Transient based ground fault protection performance when a sensitive threshold for  $V_0$  is used

Cable length [km]	20	30	40	50	60	70	80	90	100
<b>Zero sequence threshold values according to table 4.7</b>									
No. of ground faults picked up [%]	30	30	30	20	20	20	20	20	10
<b>Sensitive zero sequence voltage of 5 V</b>									
No. of ground faults picked up [%]	60	50	50	40	30	20	20	20	20

## 5.4 Ground Fault Protection Performance in Norwegian Distribution Grid

Figure 5.12 demonstrates the ground fault protection performance for 26 different COMTRADE files belonging to company A. As demonstrated, there was a large performance difference between all of the protection functions when using the settings according to table 4.8. The threshold for conductance,  $G_0$ , for the Admittance protection function in the first experiment was set to 0.54 mS. Both the Wattmetric and Transient protection functions struggle to detect more than 50% of the ground faults, whereas the Admittance function can detect more than 90% of the ground faults presented in figure 5.12. COMTRADE-file IDs 11, 12 and 15 are detected by all protection functions but only disconnected by the Wattmetric protection function.

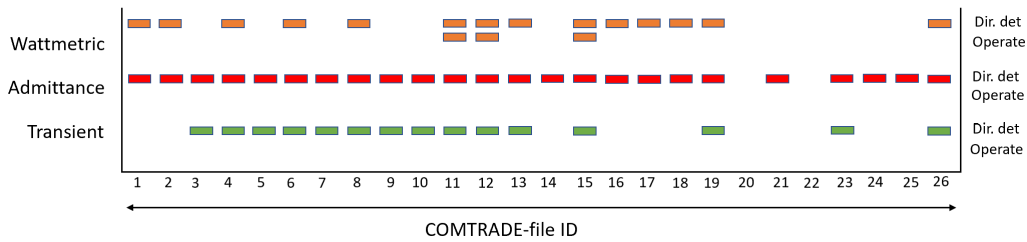


Figure 5.12: Company A: Ground fault protection function performance in company A power system. Threshold values for zero-sequence according to table 4.8. Conductance,  $G_0$ , threshold set to 0.54 mS

By utilizing the Siemens recommended zero-sequence voltage setting of 5 V for detection of high resistive ground faults, the performance of the Transient protection function increased considerably, as demonstrated in figure 5.13. By adjusting the zero-sequence voltage threshold from 15 V to 5 V, the fault detection performance increased from 57.69% to 73.1%. In addition, by increasing the sensitivity of the zero-sequence voltage threshold to 5 V, ground faults in COMTRADE-file IDs 11, 12, 15, and 26 are disconnected by the Transient protection function. The sensitivity for conductance,  $G_0$ , for the Admittance protection function increased by lowering the  $G_0$  threshold value to 0.1 mS. As demonstrated in figure 5.13, increased  $G_0$  sensitivity had no impact on fault detection performance but allowed the protection function to disconnect file IDs 11, 12, 15, and 26.

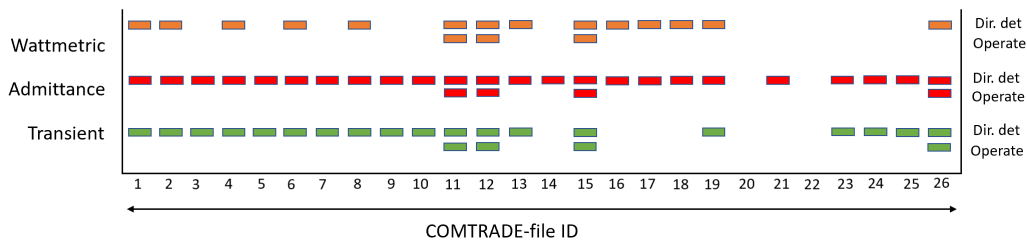


Figure 5.13: Company A: Ground fault protection function performance in company A power system. Wattmetric and Admittance protection function threshold values for zero-sequence according to table 4.8, Transient function zero sequence voltage threshold reduced to 5 V. Threshold for  $G_0$  set to 0.1 mS

The protection function performance presented in figure 5.14 show no difference between the protection functions when the Transient protection function is configured for high resistive ground faults. All 12 of the ground faults are picked up by the protection functions, and all of the functions can disconnect the same faults. This indicates that these 12 files were much more stable than the 26 files presented in figures 5.12 and 5.13. If the zero-sequence voltage threshold for the Transient function is set to 15 V, neither COMTRADE-file ID 28 nor 29 are disconnected.

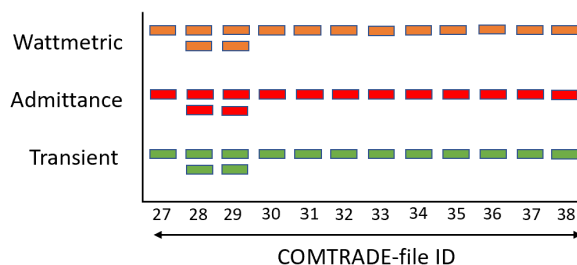


Figure 5.14: Company A: Ground fault protection function performance in company A power system. Wattmetric and Admittance function zero-sequence threshold values according to table 4.8, Transient function zero sequence voltage threshold reduced to 5 V.  $G_0$  for Admittance function set to 0.54 mS

---

Table 5.3 is based upon the ground fault protection performance presented in figures 5.13 and 5.14, and presents the overall performance of ground fault protection functions for company A. The Wattmetric protection function has the worst ground fault detection percentage, whereas the Admittance-based protection function detects close to 100% of the tested faults. The performance of the Transient protection function can be seen to be much better than the performance of the Wattmetric function, and slightly worse than the Admittance function.

Table 5.3: Overall ground fault protection function performance for company A

<b>Protection function</b>	<b>Total number of files</b>	<b>No. of faults detected</b>	<b>% of faults detected</b>
<b>Watmetric</b>	38	26	68.42
<b>Admittance</b>	38	36	94.73
<b>Transient</b>	38	31	81.57

---

## 6 Analysis of Ground Fault Protection Performance

This section presents the analysis of ground fault protection performance presented in section 5. The first subsection of this section analyses the protection function performance related to small Simulink model and presents the main reasons for protection function malfunction. The second subsection presents the analysis of the large Simulink model, where the effects of increasing cable length and capacitance on ground fault protection performance are analyzed. Lastly, the third subsection presents the analysis of ground fault protection performance in the electrical distribution network operated by Company A.

### 6.1 Effect of Varying Settings Sensitivity

Due to the Simulink model being a perfect system with a constant electrical load on both feeders and no disturbances to the zero sequence network, the main limiting factor to ground fault protection performance was the sensitivity of the function settings. As mentioned in section 4, in testing the COMTRADE files related to Simulink, the quantities of the zero-sequence system were calculated by the relay, which was another limiting factor for protection function performance.

The data presented in the table 6.1 is based upon figure 5.1 (b) and presents the zero sequence values for instances where neither Wattmetric nor Admittance protection functions could detect and disconnect the ground fault. Throughout the experiments shown in figure 5.1 (b), all the measured zero-sequence voltage values were above the specified threshold value. The limiting factor in this particular case was the zero-sequence current that the Siemens 7UM85 measured. Comparing columns 4 and 5 shows a difference between threshold values and measured values, which is why the Wattmetric and Admittance functions malfunctioning.

Table 6.1: Faulty measurement of zero sequence current leading to protection functions not being able to operate/trip

Cable length	$R_f$	$V0 >$ threshold [V]	$3I0 >$ threshold [mA]	<b>3I0 measured</b> by relay [mA]
<b>6 km</b>	4500	5	128	126
<b>7 km</b>	4500	5	141	134
<b>8 km</b>	4500	5	155	143
<b>9 km</b>	4500	5	169	153
<b>10 km</b>	4500	5	185	172

Another example of inaccurate measurement is demonstrated in figure 5.1 (a), where the Wattmetric protection function cannot detect and operate/trip for cable lengths 1 km - 2 km and 4 km - 5 km. Table 6.2 demonstrates that the measured zero-sequence voltage was 0.1 V - 0.3 V below the specified threshold value, leading to the protection function being unable to see the fault and therefore unable to operate/trip.

Table 6.2: Faulty measurement of zero-sequence voltage leading to protection functions not being able to operate/trip

Cable length	$R_f$	$V0 >$ threshold [V]	$3I0 >$ threshold [mA]	<b>3I0 measured</b> by relay [mA]	<b>V0 measured</b> by relay [V]
<b>1 km</b>	2500	15	128	126	14.9
<b>2 km</b>	2500	15	141	134	14.7
<b>4 km</b>	2500	15	155	143	14.9
<b>5 km</b>	2500	15	169	153	14.9



## 6.2 Effect of Increasing Cable Length

In section Theoretical Background, equations were presented that show that increasing capacitance to ground, while conductance remains the same, affects the angle between zero sequence current,  $3I_0$ , and zero-sequence voltage,  $3V_0$ . Figure 6.1 illustrates the effect of increasing cable length, meaning increasing capacitance to ground, with reference to Wattmetric-based ground fault protection performance presented in figure 5.6.

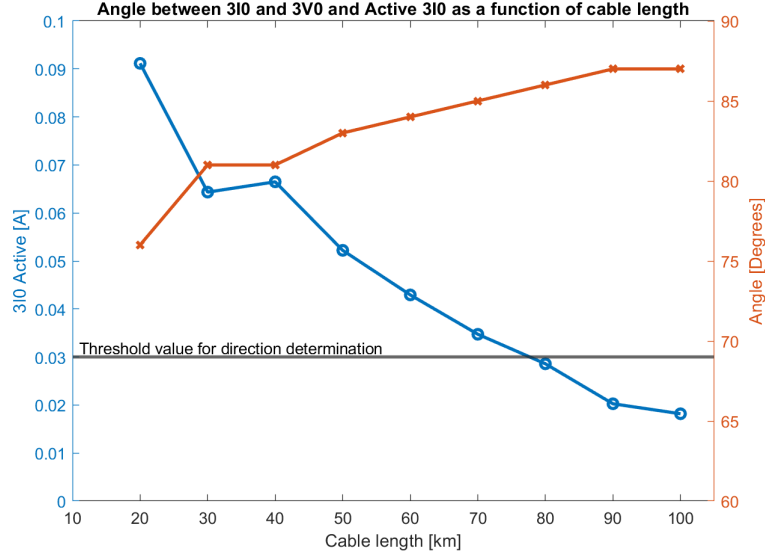


Figure 6.1: The angle between  $3I_0$  and  $3V_0$  (red) and active  $3I_0$  (blue) as a function of cable length

Figure 6.1 illustrates the angle difference between  $3I_0$  and  $3V_0$  and the active component of  $3I_0$  for each cable length when the fault resistance is  $R_f = 3k\Omega$ . Fault resistance  $R_f = 3k\Omega$  was chosen because it is required by Norwegian regulations to disconnect all faults up to  $R_f = 3k\Omega$ . Figure 6.1 shows that when cable length increases, increasing the capacitance to ground, the angle between  $3I_0$  and  $3V_0$  also increases. With increasing angle between  $3I_0$  and  $3V_0$ , the active component of  $3I_0$  decreases, as demonstrated below:

$$I_0 \angle \phi = I_0 (\cos \phi + j \sin \phi)$$

In figure 5.6, it was demonstrated that with a single cable length of 70 km, the Wattmetric-based ground fault protection function was able to detect and disconnect ground faults up to the required fault resistance of  $3 k\Omega$ , but not beyond. Table 6.3 presents the zero sequence current and voltage values that were measured by the relay for cable length 70 km as well as calculated active component of  $3I_0$ , for fault resistances 2-3  $k\Omega$ .

Table 6.3: Cable = 70 km: Measured zero sequence current and voltage during high impedance ground faults detected and disconnected by Wattmetric based protection function

$R_f [\Omega]$	<b>2000</b>	<b>2500</b>	<b>3000</b>
$3I_0 \angle \theta$ [mA]	469.5 $\angle -99$	429.6 $\angle -102$	398.4 $\angle -104$
$3V_0 \angle \theta$ [V]	38.7 $\angle 166$	35.7 $\angle 164$	33 $\angle 161$
$3I_0 \cos \phi$ [A]	0.0409	0.0300	0.0347

Figure 6.2 demonstrates the graphical representation of  $3I0$  and  $3I0\cos\phi$  vectors in Wattmetric characteristic presented in figure 3.1, and shows that both  $3I0\cos\phi$  for direction determination and  $3I0$  are inside the forward zone, resulting in direction determination and disconnection of faults.

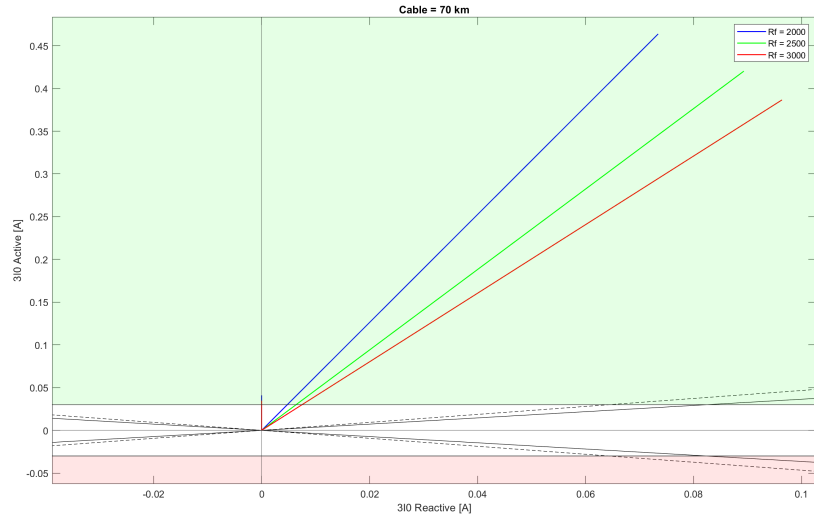


Figure 6.2: Vector for direction determination,  $3I0\cos\phi$ , as well as vector for operate,  $3I0$ , inside forward zone of Wattmetric characteristic for Cable = 70 km,  $R_f = [2000, 3000]\Omega$

Similarly, the same vectors can be calculated and graphically displayed for fault resistances  $R_f = [3.5 - 4.5]k\Omega$ , when the Wattmetric-based ground fault protection function could not detect or disconnect the faults.

Table 6.4: Cable = 70 km: Measured zero sequence current and voltage during high impedance ground faults not detected nor disconnected by Wattmetric based protection function

$R_f[\Omega]$	<b>3500</b>	<b>4000</b>	<b>4500</b>
$3I0\angle\theta$ [mA]	$360.6\angle -106$	$357\angle -110$	$354\angle -113$
$3V0\angle\theta$ [V]	$30\angle 160$	$31.2\angle 156$	$30\angle 153$
$3I0\cos\phi$ [A]	0.0252	0.0258	0.0247

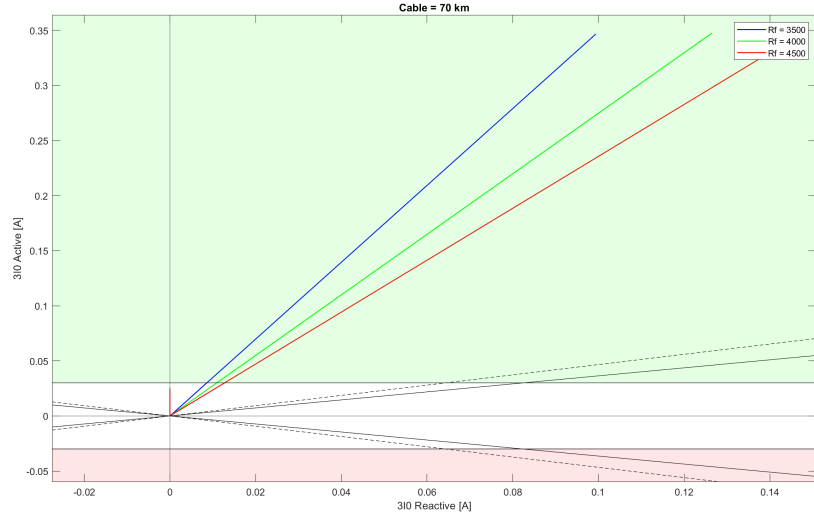


Figure 6.3: Vector for direction determination,  $3I_0\cos\phi$ , inside undefined zone, resulting in Wattmetric based protection function not detecting the fault, and therefore unable to disconnect

Figure 6.4 is based upon figure 5.7, and demonstrates measured conductance,  $G_0$ , for each cable length when the fault resistance is  $R_f = 3k\Omega$ . As demonstrated, the measured conductance is above the set  $G_0 >$  threshold value by a large margin, resulting in an excellent performance by the Admittance-based ground fault protection function. The dashed line,  $G_{0_{max}} >$ , demonstrates that the threshold value for conductance could have been set to a six times larger value, and yet, excellent performance could have been achieved for fault resistance  $0 \leq R_f \leq 3k\Omega$ .

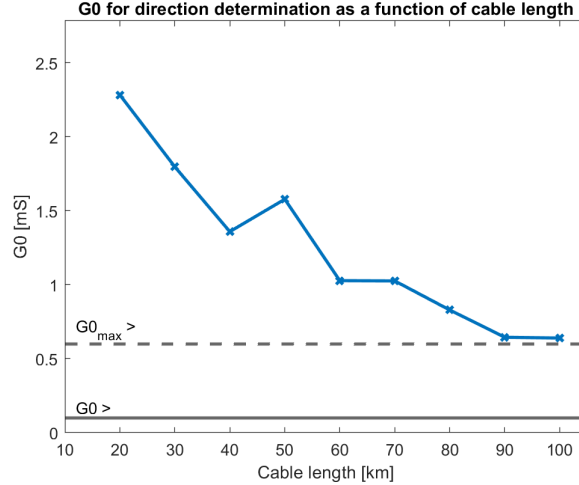


Figure 6.4: Measured conductance,  $G_0$ , as a function of cable length for fault resistance  $R_f = 3k\Omega$

In figure 5.8, it was demonstrated that Transient based ground fault protection function becomes unreliable as both cable length and fault resistance increase. Figure 6.5 demonstrates waveform of zero sequence current when low impedance fault is applied. The zero sequence current waveform of the fault-affected feeder is solely composed of the fundamental frequency due to the long cable and significant zero-sequence resistance. Furthermore, the first period of  $3I_0$  in a healthy feeder is highly affected by transients.

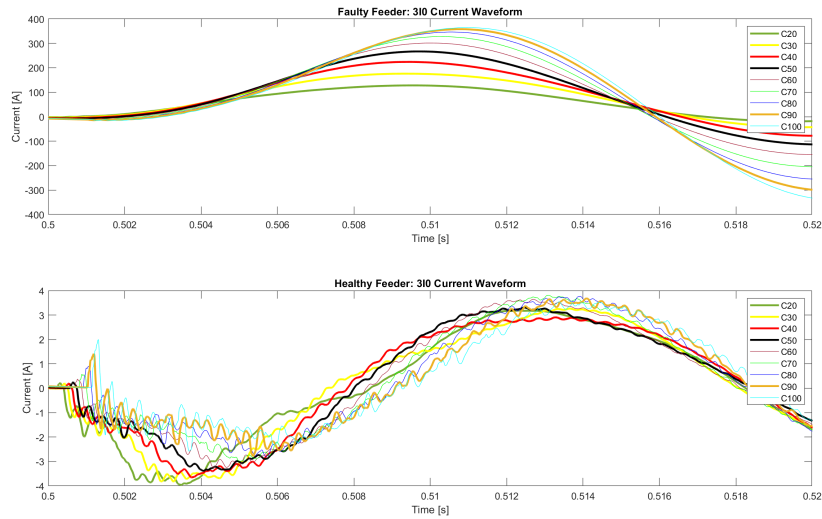


Figure 6.5: The waveform of zero sequence current for both faulty and healthy feeders for each cable length when low impedance ground fault ( $1 \Omega$ ) is applied. A thick line indicates fault detection and disconnection

By performing Fast Fourier Transform of the signal presented in figure 6.5, the zero-sequence current is split into higher frequencies at which ground fault direction is determined. As demonstrated in figure 6.6, the transient activity in fault-affected feeder dies out quickly. Furthermore, transients in both healthy and fault-affected feeders get closer to 50 Hz as the cable length increases. The techniques Siemens has implemented for signal filtering and calculation of zero sequence energy for direction determination are unknown. Still, a reasonable assumption can be made that the fundamental component is removed from the signal when looking at transient frequencies. Due to transient getting closer to the fundamental frequency as the cable increases, some of the higher frequencies may be removed due to 50 Hz removal.

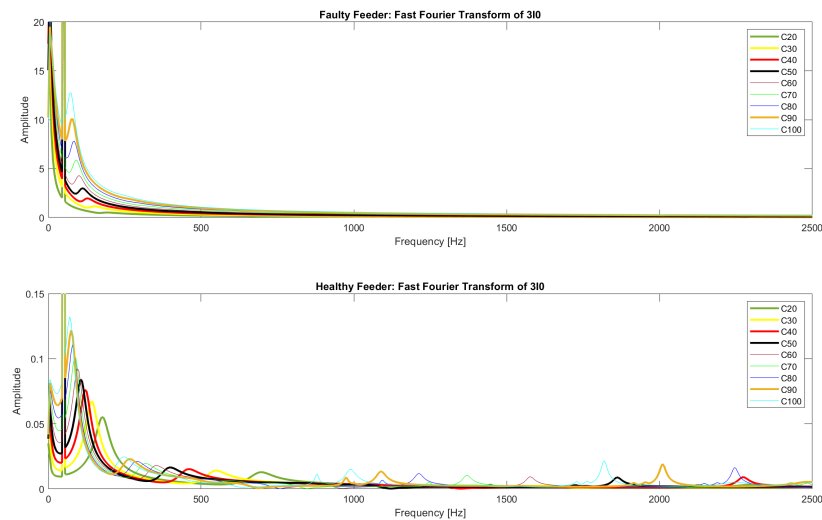


Figure 6.6: FFT of zero sequence current for both faulty and healthy feeder for each cable length when low impedance ground fault ( $1 \Omega$ ) is applied. A thick line indicates fault detection and disconnection

Figure 6.7 demonstrates zero-sequence current waveform when a ground fault with a high impedance of  $R_f = 3k\Omega$  is applied.

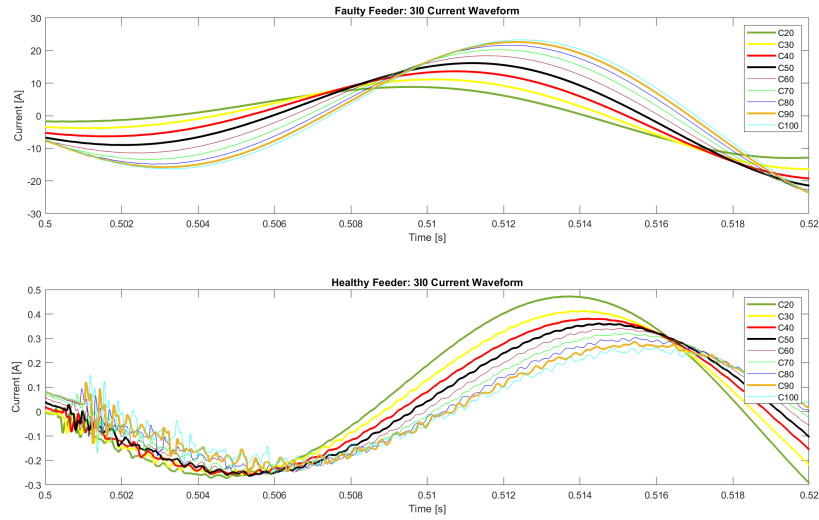


Figure 6.7: The waveform of zero sequence current for both faulty and healthy feeder for each cable length when high impedance ground fault ( $3 k\Omega$ ) is applied. A thick line indicates fault detection and disconnection

A comparison of zero sequence current waveforms during low impedance ground fault in figure 6.5, and high impedance ground fault in figure 6.7, demonstrate that during a ground fault with high impedance, the duration and amplitude of transients are significantly reduced. The reduction of transient magnitude is also illustrated in figure 6.8, where Fast Fourier Transform is performed on the zero-sequence current presented in figure 6.7. The scaling of the y-axis in the figure 6.8 was changed to logarithmic to clearly demonstrate the harmonic contributions to the zero-sequence current waveform.

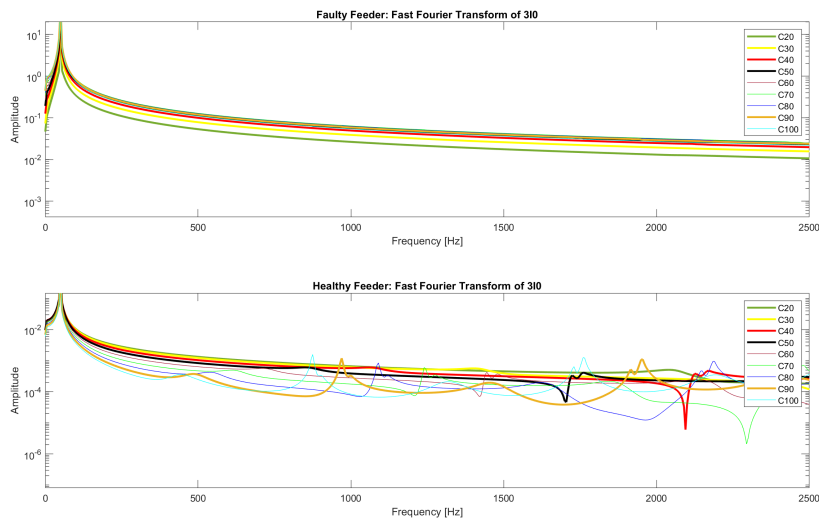


Figure 6.8: FFT of zero sequence current for both faulty and healthy feeder for each cable length when high impedance ground fault ( $3 k\Omega$ ) is applied. A thick line indicates fault detection and disconnection

Figures 6.5 - 6.8 demonstrate that a large fault impedance reduces the transient amplitude, whereas increasing cable length leads to transients moving closer to the fundamental frequency. A combination of these results, result in poor Transient based ground fault protection performance. Due to direction determination in Transient based ground fault protection function is done by measuring zero-sequence energy, as demonstrated in equation 2.5.7, the time for integration start is of much importance for correct direction determination. Furthermore, increased zero-sequence resistance due to cable length, in combination with larger fault resistances, will have an effect on both zero-sequence energy and the damping of signals. As a consequence, the start of integration and direction determination might start at a not-optimal time, resulting in a false direction indication.

### 6.3 Ground Fault Protection Function Performance in Norwegian Distribution Grid

Table 6.5 is based upon figures 5.12 and 5.13, in which the Transient protection function was tested with two different zero-sequence voltage threshold values and demonstrates that by using the same threshold value as for Wattmetric and Admittance protection functions, the performance of the Transient function is reduced. As shown in table 6.5, by using company A's standard threshold for zero-sequence voltage, the measured zero-sequence voltage is below the specified threshold value, resulting in the fault not being detected and therefore not disconnected. By utilizing the Siemens recommended threshold for high resistive faults, the measured zero-sequence voltage is well above the threshold value, resulting in the detection of the ground fault.

Table 6.5: Company A: Transient protection function malfunction due to zero sequence voltage threshold being too high

File ID	V0 > threshold [V]	3I0 > threshold [mA]	V0 during first period of transient [V]	3I0 during first period of transient [mA]
2	15	16	14.93	126
2	5	16	14.93	126

In figure 5.13, it was demonstrated that even by using a sensitive threshold for the zero-sequence voltage for the Transient protection function, neither Wattmetric nor Transient protection functions could detect the ground fault in file ID 14. Figure 6.9 presents the zero-sequence voltage and current waveforms when the ground fault in file ID 14 is initiated. A possible reason for the Transient protection function malfunction, in this case, is that the duration of the first transient zero-sequence voltage and current, which was 4 ms, is too short for the protection function to detect. Another possible reason might be that the zero-sequence energy calculation is started at a not optimal time, forcing the Transient protection function to report false ground fault indication.

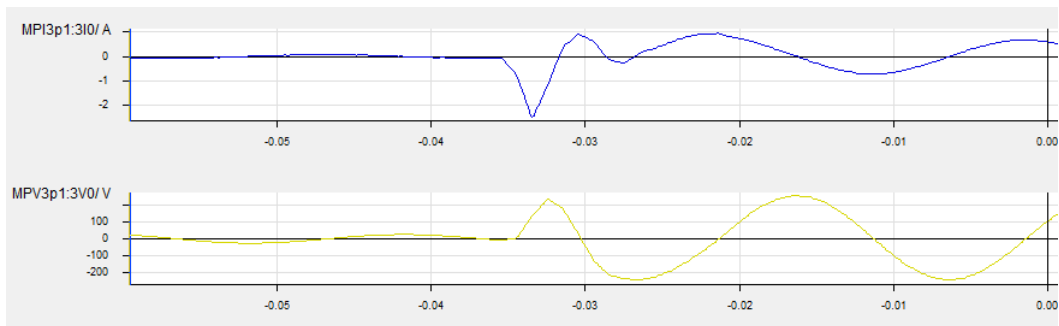


Figure 6.9: Company A, file ID 14: Duration of zero sequence disturbance being too short for Transient protection function to detect, resulting in malfunction of the function

The malfunction of the Wattmetric protection function during a ground fault in file ID 14, was found to be due to the angle between  $3I_0$  and  $V_n$ . Figure 6.10 presents the currents present in the system during the ground fault. Magnitudes of both zero sequence current and voltage are above the specified threshold values, but due to the angle between  $3I_0$  and  $V_n$ , the Wattmetric ground fault protection function struggles to identify the ground fault.

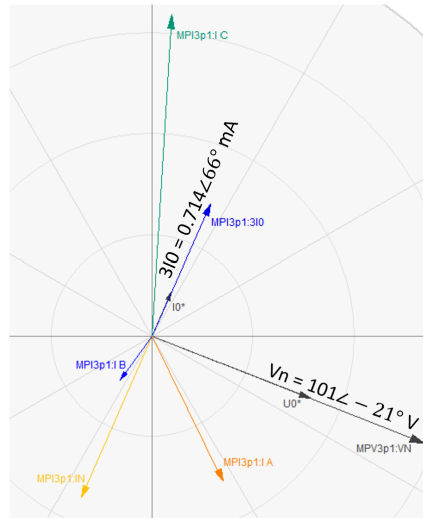


Figure 6.10: Company A, file ID 14: Currents that are present during ground fault in file ID 14

Even though the Admittance protection function could detect the fault, it is not optimal due to large variations in zero sequence current and voltage. Figure 6.11 demonstrates that during the ground fault in file ID 14, the Admittance protection function picks up the ground fault four times.

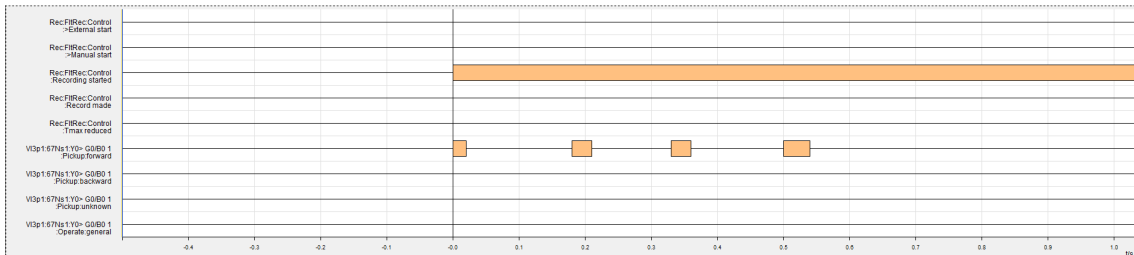


Figure 6.11: Company A, file ID 14: Admittance function pick up of the same ground fault multiple times

Table 6.6 presents the zero sequence conductance throughout the ground fault presented in figure 6.11. As can be seen from table 6.6, the Admittance function is highly sensitive to variations of zero sequence current and voltage, resulting in discontinuous ground fault detection.

Table 6.6: Company A, file ID 14: Admittance protection function multiple pickup of ground fault

Pickup nr.	$G_0 >$ threshold [mS]	$G_0$ measured by relay [mS]	Dropout nr.	$G_0$ measured by relay [mS]
1	0.1	1.3	1	0.05
2	0.1	1.76	2	0.05
3	0.1	1.53	3	0.005
4	0.1	1.77	4	-

In figure 5.13, it was presented that Wattmetric and Admittance function detected ground fault in file ID 16, but not by Transient protection function. The zero sequence current waveform during the ground fault is shown in figure 6.12, and demonstrates that the ground fault has a short duration, but does not cease to exist. The transient duration shown in the figure 6.12 is too short for the Transient function to detect.

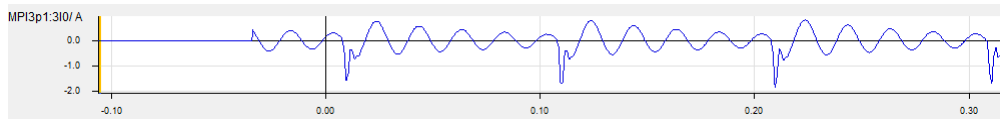


Figure 6.12: Company A, file ID 16: Intermittent ground fault with periods too short for Transient protection function to detect

In addition, file ID 16 demonstrates how single phase to ground faults can lead to immense damage. As seen in figure 6.12, after the fault ignites, the system tries to stabilize, as seen from the decreasing zero-sequence current. Once the system gets close to a stable case, the fault re-ignites. Such phenomena might be explained by damaged cable insulation. When the system tries to restore the voltage after ground fault ignition, the cable insulation cannot endure the nominal voltage of the system, resulting in the re-ignition of the fault. If the Transient protection function would be used, the ground fault would not be picked up, and constant re-ignition of the fault would appear. Due to the increased voltage of the healthy phases during a single phase to ground fault, this event might lead to a two-phase to ground fault, if any weak power electronic devices are coupled to the healthy phases.

Admittance function sensitivity was tested with two different values, as presented in figures 5.12 and 5.13. In figure 5.12, the Admittance protection function was able to detect the ground fault in file ID 12, but not disconnect. This was due to the upper limit sensitivity of the zero sequence admittance used. The limits of sensitivity can be written in a single equation, by combining equations 3.3.1 and 3.3.2:

$$k_{s1} \frac{I_{0,active}}{\sqrt{3}V_{sys}} + \frac{I_{0,min}}{V0} < G0 < \frac{1}{k_{s2}} \frac{I_{Rp}}{\sqrt{3}V_{sys}}$$

By utilizing the upper limit of zero sequence conductance, it was found that small variations in the zero-sequence network can lead to the protection function discontinuously detecting the fault, as demonstrated in figure 6.13.  $G0$  setting of 0.54 mS leads to the protection function to lose pickup multiple times throughout the ground fault. Each time the pickup is reset, the operate delay is reset, resulting in the function not being able to disconnect the fault, as presented in figure 5.12. By reducing the zero sequence conductance threshold value to a lower limit, i.e 0.1 mS, the disruption of pickup indication was removed, and disconnection of the fault was achieved, as demonstrated in figure 5.13. The effects varying  $G0 >$  sensitivity are shown in appendix B.

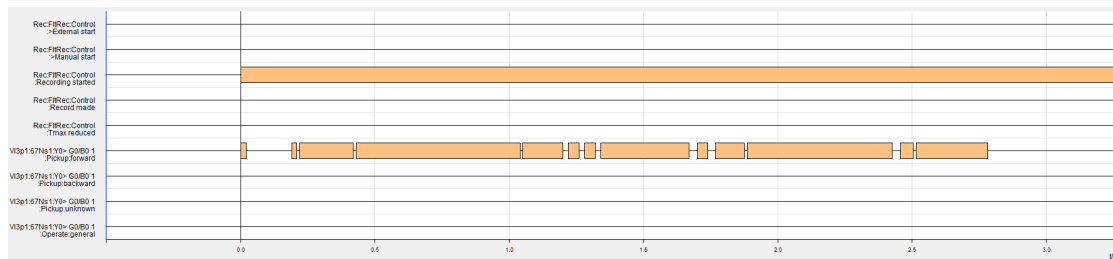


Figure 6.13: Company A, file ID 12: Demonstration of how variations in zero sequence network affect the pickup of Admittance function when low zero sequence conductance sensitivity is used



---

## 7 Discussion

### 7.1 Design of Simulink Model

During the entire analysis and testing of ground fault functions performance based on the simulated distribution system, the size of the arc suppression coil was such that the system was in resonance. This kind of configuration is not realistic, and ideally, the system should be operated in the over-compensation area of the resonance curve illustrated in figure 2.7. In reality, if a ground fault is detected, the faulty line will be disconnected, resulting in the arc suppression coil changing its degree of compensation to fit the adjusted size of the system. In investigations performed in the Simulink model, no loss of system components was planned, and therefore, it was made a conscious decision to operate the system at the resonance point.

The size of the parallel resistor,  $R_p$ , in the small Simulink model was set to a value of 125 kW, based on REN recommendations[12]. Given that the longest lengths of feeders 1 and 2 in the small Simulink model were set to 16 km and 30 km, respectively, the parallel resistor of 125 kW was extremely oversized with respect to system size. Due to Wattmetric and Admittance based ground fault protection functions being highly dependant on the resistive current in transformer neutral, such over-sizing provided the mentioned protection functions a large advantage over Transient based ground fault protection function, as illustrated in figures 5.1 - 5.4. To illustrate Wattmetric and Admittance-based ground fault protection function's dependability on the size of the parallel resistor, the resistive size of  $R_p$  was also halved, where the observed effect can be explained by figure 2.9.

The cable in the fault-affected feeder in the large Simulink model was modeled as a single cable of lengths ranging from 20 km to 100 km. The idea behind using a single cable of such lengths was to create a rural cable network, where cable-dominated feeders can become relatively long, resulting in large uncompensated capacitive currents. Such networks can be described as narrow and long, which fits the description of the Simulink model presented in figure 4.1. Even though a single cable of such lengths can be considered extreme and unusual, it was made a decision to keep increasing cable length, and, therefore total capacitance of the feeder, such that ground fault protection function performance and limits could be investigated. In addition, ground fault protection performance in a system with parallel cables, demonstrated in figure 5.9, was included, since such network topology is more common practice in actual, physical distribution systems.

In both small and large Simulink models, a small load of 0.5 MW, with power factor  $\cos\phi = 1$  was applied, as presented in figure 4.1. As the cable length increased to extreme lengths, the capacitive current in the mixed feeder became dominant. Consequently, the capacitive current in the mixed feeder, i.e feeder 1, increased greatly. The load was kept at 0.5 MW throughout the investigation, such that the only changing parameters in the system would be the length of the cable and fault resistance. To ensure that the current magnitude measured by current transformers was the same throughout the investigation, the turn ratio of the current transformer,  $\alpha$ , was always set to  $\alpha = \hat{I}_{primary} : 1$ .

A single line to ground fault was applied at the end of fault affected feeder, regardless of the feeder length. Increasing cable length, and therefore total feeder length, will have an effect on the time current uses from the station to the fault location, which may affect the results of certain ground fault protection functions. The fault location was not varied since this has little effect, and the objective of this thesis is to study the influence of cable lengths and fault resistance on ground fault protection functions. An intermittent single line to ground fault due to cable insulation breakage was also investigated. Even though intermittent ground faults are not known to contribute with large fault resistances, fault resistances in the range of 0  $\Omega$  - 4.5  $k\Omega$  were included to investigate the sensitivity and optimal area of use for the three ground fault protection functions.

---

## 7.2 Ground Fault Protection Function Configuration

Configuration of ground fault protection functions for small Simulink model was varied, as presented in section 4.5.2 - Configuration of Protection Functions for Simulink Model. This was done to demonstrate that the configuration of zero sequence current and voltage sensitivity have a large impact on what fault resistances can be detected and disconnected. The settings for each cable length were calculated for the worst-case scenario, meaning the highest fault resistance, such that settings in themselves would not be the limiting factor on protection performance. Zero sequence voltage threshold values of  $V_0 > 5V$  for Wattmetric and Admittance-based protection functions are largely unrealistic in a physical distribution system. Due to Siemens's recommendation of  $V_0 > 5$  for Transient based ground fault protection function for high resistive faults[17], the same threshold values were used on all protection functions, enabling a direct comparison between protection function performance linked to settings sensitivity.

In section 4.6 - Connection Between Power Source and Relay, connections between the relay and power source were demonstrated. For both the small and large Simulink models, zero sequence quantities were not directly calculated and applied to the relay. The summation was instead made by the relay, which reduced the accuracy as demonstrated in figures 5.1 - 5.3, as well as tables 6.1 and 6.2. Due to the current source being an ideal simulation, not utilizing the zero sequence connection ports was less of a problem than in reality. In addition, by not utilizing the connection ports for zero sequence current and voltage, restrictions on setting sensitivity linked to direction determination were imposed by configuration software DIGSI. Consequently, the configuration of settings related to direction determination,  $I_0.dir >$  and  $G_0 >$ , for Wattmetric and Admittance-based protection functions, respectively, were chosen to be as sensitive as DIGSI allowed. The largest sensitivity for Wattmetric based direction determination,  $I_0.dir >$  was set to 30 mA, whereas for Admittance based direction determination,  $G_0 > 0.1$  mS, referred to the secondary side. If connection ports for zero sequence current and voltage were utilized, both protection functions could have been configured more sensitive, increasing protection function performance. In theory, the direction determination parameter for both Wattmetric and Admittance-based protection functions could be configured to maximum sensitivity. The downside is that a false ground fault indication would become more than likely with too much sensitivity.

In section 4.5.3 - Configuration of Protection Functions for Company A, a table was presented where parameters such as  $I_0.dir >$ , for direction determination, as well as zero-sequence voltage and current threshold values,  $V_0 >$  and  $3I_0 >$ , respectively, were presented. These zero-sequence threshold values were obtained from Company A's relay plan, and it was desirable to test the exact same zero-sequence threshold values on all of the ground fault protection functions. By performing experiments on Admittance and Transient based protection functions with settings that are in use in the actual Norwegian distribution grid, it was desired to determine if a switch from Wattmetric based protection function to either Admittance based or Transient based protection functions was made, would the threshold values for operate/trip signals have to be altered. In addition, due to Company A not utilizing the Admittance-based ground fault protection function, the direction determination setting,  $G_0 >$ , was not specified. Consequently, the Siemens relay manual[17] was used to calculate both the smallest and largest value for  $G_0 >$ . When performing experiments on the Admittance-based protection function, both lower and upper limits of  $G_0 >$  were tested. The reasoning behind testing two different sensitivity values of  $G_0 >$  was that some degree of zero-sequence voltage and current variation in a physical distribution system was expected. In cases where various weather conditions could lead to large variations in the zero-sequence system, a large direction determination setting,  $G_0 >$ , could lead to the Admittance-based protection function "losing contact" with a potential ground fault, resetting the operation delay timer.

---

### 7.3 Ground Fault Protection Performance in Small Simulink Model

Wattmetric and Admittance-based ground fault protection function performance in the small Simulink model was identical, as presented in figures 5.1 and 5.2. The reason for this result is due to three factors:

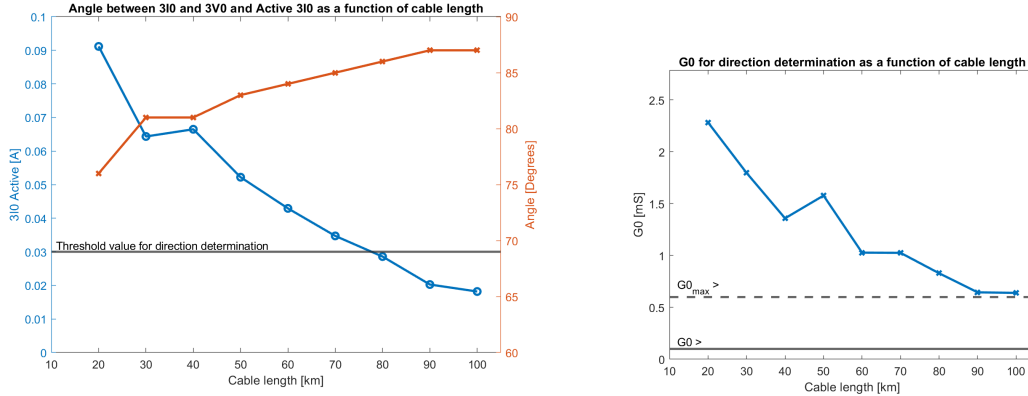
1. The system that experiments were performed on was very small. In combination with a small background network, a short length of faulty feeder does not contribute to a large enough relation between conductance and capacitance for the angles between zero sequence current and voltage to reach critical values. This is proven by equation 2.2.18, and illustrated in figure 2.9.
2. Both Wattmetric and Admittance-based protection functions were configured with maximum sensitivity. By using Wattmetric and Admittance-based ground fault protection characteristics illustrated in figures 3.1 and 2.12, respectively, one can see that the resistive current for direction determination must be small when maximum sensitivity is used.
3. Both Wattmetric and Admittance-based ground fault protection functions are highly dependant on the resistive current that flows through transformer neutral. This is proven by figure 3.1 for Wattmetric-based protection function, and by equation 2.5.8 as well as figures 2.12 and 3.2 for Admittance-based protection function.

A combination of factors and theory presented above resulted in equal protection performance for both Wattmetric and Admittance-based protection demonstrated in figures 5.1 and 5.2. When a parallel resistor of 125 kW was used, the resistive current through the transformer neutral was more than sufficient for both protection functions to work identically. This was further investigated in the protection performance presented in figure 5.5, where the resistive value of the parallel resistor was reduced to half the original value. Consequently, as presented in figure 5.5, the performance of both protection functions was reduced drastically, demonstrating that both of the functions are highly dependent on the resistive current. These results indicate that the performance would decrease correspondingly if the parallel resistor was further reduced. These results also indicate that no matter the size of the system, if the parallel resistor fails to connect during a ground fault, neither Wattmetric nor Admittance-based protection functions would be able to detect the potential ground fault, and would therefore not be able to disconnect it.

In the small Simulink model, Transient based protection function had a better performance for fault resistances  $0 \Omega - 4.5k\Omega$ , than both Wattmetric and Admittance-based protection functions. Due to all protection functions being tested with exactly the same zero-sequence threshold values, the difference between the performances in the small Simulink model is because of the measurement error mentioned in section 7.2 - Ground Fault Protection Function Configuration. This measurement error can also be seen by comparing figures 5.1 (a), where neither Wattmetric nor Admittance-based protection functions can disconnect fault resistance  $R_f = 4.5k\Omega$  and 5.1 (b), where the  $R_f = 4.5k\Omega$  is disconnected. The fact that the cable length of 3 km in figure 5.1 (a) disconnects the fault resistance of  $R_f = 4.5k\Omega$ , but not the two cable lengths below nor above, strengthens the possibility of measurement error. Lastly, figures 5.2 and 5.4 demonstrated that both Wattmetric and Admittance-based protection functions perform better than Transient-based protection functions for fault resistances  $R_f = 5k\Omega - 14k\Omega$ . The excellent performance of both Wattmetric and Admittance-based protection functions is largely due to factors presented at the start of this subsection. However, it is important to remember that configuration of both Wattmetric and Admittance-based protection functions with a zero-sequence voltage threshold of 5 V or 3 V is highly unrealistic in a physical distribution system. On the other hand, the Transient-based protection function seems to stop working at fault resistance of  $R_f = 10k\Omega$ . This indicates that when fault resistance reaches extreme values, the damping of transient current becomes so severe, that the Transient based protection function cannot detect the ground fault. This phenomenon is investigated more closely in the large Simulink model and is analyzed in figures 6.5 - 6.8.

## 7.4 Ground Fault Protection Performance in Large Simulink Model

In the large Simulink model, the effect of large capacitance was visible in Wattmetric-based protection performance, illustrated in figure 5.6. As figure 5.6 demonstrates, the Wattmetric protection function works exceptionally well for cable lengths up to 50 km, but as the cable length increases beyond the length of 50 km, the performance starts decreasing. The same principle of the increasing angle between 3I0 and 3V0 was observed in Admittance-based ground fault protection function, except that the Admittance-based protection function was configurable with a more sensitive direction determination setting,  $G0 >$ , resulting in much better performance. Figures 6.1 and 6.4 demonstrate how measured values linked to direction determination decrease as a function of cable length. These figures are repeated below for increased understanding and readability.



(a) Wattmetric based protection function: Angle between 3I0 and 3V0, as well as the active component of 3I0 as a function of cable length

(b) Admittance based protection function: G0 as a function of cable length

Figure 7.1: Comparison of direction determination parameters for Wattmetric and Admittance based ground fault protection functions, first presented in section 6

As demonstrated in figure 7.1 (a), for fault resistance of  $R_f = 3k\Omega$ , the Wattmetric-based protection function stopped detecting ground faults at a cable length of 80 km. Figure also demonstrates that in case the direction determination setting,  $3I0.dir >$  was to be decreased to below 20 mA, the Wattmetric-based protection function would have been able to detect and disconnect the fault. In figure 7.1 (b) on the other hand, zero sequence conductance,  $G0$ , is demonstrated as a function of cable length. Even though  $G0$  follows the same trend as  $3I0.dir >$ , the lowest value of  $G0$  that was measured for this model was still well above the set threshold value. In fact, the sensitivity of Admittance-based ground fault protection function could have been decreased from 0.1 mS to 0.6 mS, and it would still have been able to detect and disconnect all ground faults with fault resistance of  $R_f = 3k\Omega$  for all cable lengths. Even though the sensitivity of Admittance based protection function could have been decreased, as mentioned above, choosing sensitivity to be close to the upper limit, as indicated by the dashed line in figure 7.1 (b), one might face the risk that in the oscillating and varying zero-sequence system, the zero-sequence conductance might enter the "unidentified" zone of characteristics, forcing the operate delay timer to reset. Consequently, the probability of achieving a trip would decrease. This phenomenon is more closely investigated in the distribution system belonging to Company A and is in fact demonstrated in figure 6.13.

Transient-based ground fault protection performance due to increasing cable length and fault resistance, presented in figure 5.8 were quite surprising and unexpected. As presented in figures 6.5 - 6.8, an attempt was made to analyze these results. The mentioned figures demonstrate that during a low impedance fault, the zero-sequence current of a healthy feeder is largely affected by transient currents, as well as transient currents at higher frequencies were visible. When a high impedance fault of  $R_f = 3k\Omega$  was applied, it was demonstrated that transient amplitude decreases greatly, as well as transients at higher frequencies become hard to register. In these figures, the fundamental frequency of 50 Hz was not filtered out, which may affect the transient

---

amplitudes shown in figures 6.5 - 6.8. The difficulties in identifying the reason for such Transient based protection function performance were largely due to the Siemens manual not specifying how the direction determination, i.e zero-sequence energy is calculated, and what threshold value the zero sequence energy has to pass for direction identification. Conversations with Siemens revealed that direction determination is highly reliant on the time that Transient based function detects a ground fault, and the integration process is started. In addition, Siemens provided information that large fault resistances might lead to large damping in the system, resulting in the Transient based protection function starting the integration process at a not optimal time, leading to malfunction. Conversations with an electrical engineer representative from ABB revealed that in their experience with rural cable networks, such as those investigated in the large Simulink model, damping seems to be either uncertain or undefined, and can vary between systems. Based on the information provided above, a reasonable explanation for Transient based protection function performance presented in figure 5.8, is that damping due to large fault resistance and due to large zero-sequence resistance as a consequence of a single long cable, results in poor performance by the Transient based ground fault protection function. During the investigation of Transient based protection function performance, a closer look was taken into the zero-sequence resistance, where instead of using a single cable, two parallel cables were utilized. These results were presented in figure 5.9 and demonstrated that when the length of a single cable decreases, the Transient-based protection function's performance slightly increases. This might indicate that the Transient-based protection function might be more suitable for urban areas, where the electrical system is wide and short, meaning many feeders with shorter cable lengths.

The large Simulink model was also used to investigate intermittent ground faults. These results were not analyzed due to neither Wattmetric nor Admittance-based protection functions would be used for detection and disconnection of these kinds of faults in a realistic distribution system, but a selection of fault recordings are demonstrated in appendix C. Nevertheless, it has been demonstrated that for cable lengths of 50 km or below, both Wattmetric and Admittance-based protection functions can detect and disconnect ground faults in instances where fault resistance is zero. The disconnection of these faults was due to an idealized electrical system, as well as a very small operation delay setting. In reality, in arc suppression coil grounded systems, the operate delay would be much larger, resulting in neither Wattmetric nor Admittance based protection functions being able to disconnect the fault. Figures 5.10 and 5.11 demonstrated that the Transient based protection function is superior to Wattmetric and Admittance-based protection functions when intermittent ground faults are applied. These results were as expected, due to a sudden disturbance in a electrical grid, introduces transients, which the Transient based protection function is designed to detect. It was also demonstrated that when reducing the zero-sequence voltage threshold value to 5 V, referred to the secondary side, the Transient based ground fault protection function can detect close to twice as large fault resistance, compared to a zero-sequence voltage threshold value of 10 V. Consequently, if Transient based protection function was to be used for detection and disconnection of intermittent ground faults, the threshold value for zero-sequence voltage should be set to 5 V. This is of course dependant on the ratio of voltage transformer - in Simulink model, the secondary voltage of instrument transformer is 100 V, such that threshold value of 5 V is equal to 5% of 100 V. In instances where the secondary voltage of instrument transformer is larger, the zero-sequence voltage threshold value should still be 5%.

---

## 7.5 Ground fault Protection Performance in Real Distribution Grid

The most interesting ground fault protection function performance has been analyzed in section 6.3 - Ground Fault Protection Function Performance in Norwegian Distribution Grid, where most of the focus have been directed towards Admittance based and Transient based ground fault protection functions, such that their behaviour during realistic ground faults could be highlighted. The analysis of ground fault protection function performance in Company A's distribution grid was limited to some degree, due to limited information about the background network and the overall system.

It was demonstrated that Wattmetric, Admittance, and Transient based protection functions detected 68.42%, 94.73%, and 81.57% of ground faults, respectively, presented in section 5.4 - Ground Fault Protection Performance in Norwegian Distribution Grid. At most, four disconnections were registered. The reason for only four disconnections is that all of the ground fault protection functions were configured with the same operate delay as Company A uses in their ground fault protection scheme, meaning that the detection of ground faults had to last at least 1.9 seconds for the ground fault to be disconnected.

Comparison of figures 5.12 and 5.13 demonstrate that sensitivity of zero-sequence voltage threshold value for Transient based protection function, and sensitivity of  $G0 >$  parameter for Admittance based protection function is of much importance for optimal performance. In experiments where the threshold value for the zero-sequence voltage for the Transient based protection function was set to 15 V, no disconnections were registered, as well as fewer ground faults were detected. Transient based protection performance increased greatly when the threshold value was reduced to 5 V. Due to the ratio of the instrument transformer measuring voltage in Company A's distribution system being 22 kV : 0.11 kV, the correct configuration of the threshold value for zero-sequence voltage would have been 5.5 V, which is 5% of 0.11 kV. Nevertheless, it is reasonable to assume that the increased sensitivity of 0.5 V used in experiments did not result in a large difference in performance. Similarly, when using the upper limit of  $G0 >$ , the performance of the Admittance-based protection function was poor, in the sense of discontinuous ground fault detection, as demonstrated in figure 6.13. Reducing the  $G0 >$  value achieved both continuous fault detection and disconnection. Admittance-based protection function tested in this thesis has shown to be highly dependable on the sensitivity of the  $G0 >$  parameter. When experiments were performed on both simulated and realistic system containing solely permanent or intermittent ground faults, the performance of this function have shown to be excellent when sensitivity is high. This thesis, however, does not investigate how the Admittance-based protection function would react when exposed to a changing system, where the zero sequence admittance might change. By choosing too sensitive  $G0 >$  parameter, loss of lines or other components might force Admittance based protection function to indicate a false ground fault.

---

## 8 Conclusion

Analysis and testing of Wattmetric, Admittance, and Transient based ground fault protection function performance in this thesis have been performed using three different arc suppression coil grounded distribution systems. Systems that were analyzed were a small Simulink model where effects of protection function sensitivity have been investigated, large Simulink model where effects of increasing cable length, and therefore capacitance have been investigated, as well as ground fault protection recordings from an existing Norwegian distribution system.

Ground fault protection performance demonstrated in this thesis has shown that the difference between ground fault protection function performance in small simulated systems is close to non-existent. As the protected feeder increases in length, that is, cable length, it was found that after 50 km of cable, in a simulated distribution system, the traditional, i.e., Wattmetric-based protection function begins to encounter difficulties in detecting high impedance faults. The limit for cable length for the Wattmetric-based protection function in this thesis has been found to be 70 km after which the protection function is no longer able to detect or disconnect ground faults with fault resistances above  $3k\Omega$ . It was also demonstrated that when a single cable of large lengths is used to transfer electric power, the Transient based protection function is highly affected by damping due to large zero-sequence resistance, as well as high fault resistance, resulting in both poor and inconsistent performance. However, it has been demonstrated that reducing zero-sequence resistance by utilizing parallel cables improves the Transient-based ground fault protection performance. Using a simulated distribution system, it has been demonstrated that the Admittance-based protection function is superior to both Wattmetric and Transient-based protection functions due to its excellent performance for cable lengths 20 km - 100 km and fault resistances up to  $4.5k\Omega$ .

Analysis and testing of ground fault protection function performance in an existing Norwegian distribution system were performed on a single, cable-dominated feeder, where the total feeder length was 23.247 km, of which 22.437 km was cable. The performance of the Wattmetric-based ground fault protection function was shown to be sub-optimal, where 68.42% of all ground faults were detected. Furthermore, this thesis has demonstrated that Transient based protection function had above sub-optimal performance, where 81.57% of ground faults were detected. Admittance-based ground fault protection function detected 94.57% of all ground faults that were tested, demonstrating that Admittance-based ground fault protection function is superior to both Wattmetric and Transient-based protection functions.

By taking ground fault protection function performance from both simulated and real distribution systems into consideration, the Admittance-based ground fault protection function appears to be the optimal ground fault protection function for achieving optimal protection from single line to ground faults. However, it has been demonstrated that both Wattmetric and Transient based ground fault protection functions can detect an acceptable percentage of ground faults, such that if arc suppression coil grounded distribution systems are designed to meet the limits of chosen ground fault protection functions, satisfactory ground fault protection performance can be achieved by using either ground fault protection function. By taking the results from a real Norwegian distribution grid into consideration, if the Admittance based protection function is taken into use, the lower limit of  $G0 >$  setting, defined by equations 3.3.1 and 3.3.2, should be used, such that unintentional drop out of ground fault detection can be avoided, as illustrated in figure 6.13, as well as appendix B. In cases where the Transient based ground fault protection function is taken into use, the zero sequence voltage threshold value,  $V0 >$ , should be set to approximately 5% of secondary transformer voltage value,  $V0 > 0.05V_{T,s}$ , such that satisfactory ground fault protection performance can be achieved.

---

## 9 Recommendations for Further Work

Recommendations for further research that would further improve the understanding of the subject of this thesis, are listed below:

- Introduce current transformers with measuring error in simulations for investigation of how ground fault protection function performance is affected due to error in current angles.
- Introduce variable load in combination with small disturbances in a zero-sequence system to investigate how operational changes in the distribution system affect ground fault protection functions.
- Expand the simulated model and investigate how disconnection of transmission lines affects the zero sequence admittance that is used by the Admittance-based protection function.
- Cooperate with Norwegian electrical grid companies to investigate how realistic changes in network topology affect the Admittance-based ground fault protection functions.
- Perform analysis and testing of ground fault protection functions using relay provided by ABB. The latest relays from ABB are equipped with MFA - Multi-frequency Admittance function, which might be the future of ground fault protection schemes.
- In the case of ground fault detection and disconnection, the network topology will change. During this time, the arc suppression coil will go through a tuning process to adjust its size to the new network topology. If a ground fault strikes during this time, the system will be operated in a highly overcompensated degree. Implementation of arc suppression coil regulator to investigate how the mentioned scenario affects ground fault protection function performance would be of large relevance.
- Transient-based ground fault protection function has been shown to have inconsistent performance in long, cable-dominated feeders. Investigation of how damping, grounding, and zero sequence components affect the performance of Transient based ground fault protection function would be of great relevance.



---

## References

- [1] Inno Davidson. ‘Modelling and Analysis of a Multi-Bus Reticulation Network with Multiple Distributed Generation Injection (Part II – Electrical Fault Analysis)’. In: Sept. 2004.
- [2] Alexander Neufeld, Nils Schäkel and Lutz Hofmann. ‘Harmonic Resonance Analysis for Various Degrees of Cable Penetration in Transmission Grids’. In: *2018 53rd International Universities Power Engineering Conference (UPEC)*. 2018, pp. 1–5. DOI: 10.1109/UPEC.2018.8541878.
- [3] Christoph E Mueller, Silke I Keil and Christian Bauer. ‘Underground cables vs. overhead lines: quasi-experimental evidence for the effects on public perceptions and opposition’. In: ().
- [4] JE Trohjøll and IH Vognild. ‘Underground cables as an alternative to overhead lines. A comparison of economic and technical aspects of voltages over 22 kV’. In: (1994).
- [5] Pål Wagner. ‘Fault Handling in Resonance Grounding’. In: (2021).
- [6] Vijay Venu Vadlamudi. *Lecture on Unsymmetrical Faults*. University Lecture. 2020.
- [7] Hans Kristian Høidalen. *TET4215 Power system Protection and Control*. University Lecture. 2021.
- [8] Ari Wahlroos, Janne Altonen and Joe Xavier. ‘Can compensated networks be an alternate solution to reduce the risk of ground faults causing forest fires?’ In: *2021 74th Conference for Protective Relay Engineers (CPRE)*. IEEE. 2021, pp. 1–34.
- [9] H Kuusti et al. ‘Intermittent earth faults challenge conventional protection schemes’. In: *15th International Conference and Exhibition on Electricity Distribution (CIRED)*. Ranska: Nice. 1999.
- [10] *Forskrift om elektriske forsyningsanlegg : med veiledning*. nob. Lysaker, 2006.
- [11] Jeff Roberts, Hector J Altuve and Daqing Hou. ‘Review of ground fault protection methods for grounded ungrounded and compensated distribution systems’. In: *USA, SEL* (2001), pp. 1–40.
- [12] REN. ‘Retningslinjer for systemjording med spole for 12-22 kV nett’. In: *RENblad* 7505 (2020), pp. 1–31.
- [13] Matthieu Loos. ‘Single Phase to Ground Fault Detection and Location in Compensated Network’. PhD thesis. PhD thesis, Université Libre de Bruxelles, 2014.
- [14] Ari Wahlroos et al. ‘Easy admittance: The ultimate earth-fault protection function for compensated networks’. eng. In: *ABB review* 2 (2013). ISSN: 1013-3119.
- [15] Relion Protection. ‘Control 615 series Technical Manual’. In: *Document ID: 1MRS756887 Issued* (2018).
- [16] Ari Wahlroos, Janne Altonen and ABB Oy Distribution Automation-Finland. ‘Compensated networks and admittance based earth-fault protection’. In: *Kaunas University of Technology and Aalto University organized seminar on Methods and techniques for earth fault detection, indication and location, Espoo, Finland*. 2011.
- [17] SIEMENS Protection. ‘SIPROTEC 5 Generator Protection 7UM85’. In: *Document version: : C53000-G5040-C027-8.04 Issued* (2020).

---

## A Simulink Model Parameters

Table A.1: Simulink solver parameters

Parameter	Value
Simulation type	Discrete
Solver type	Fixed-step
Sampling time period	100000s
Sampling frequency	$1e^{-5}$
Solver	ode1be (Backward Euler)

Table A.2: Transmission line parameters in Simulink

	$R_1$ $\Omega/\text{km}$	$R_0$ $\Omega/\text{km}$	$L_1$ $\text{mH}/\text{km}$	$L_0$ $\text{mH}/\text{km}$	$C_1$ $\text{nF}/\text{km}$	$C_0$ $\text{nF}/\text{km}$
Overhead line, feeder 1	0.259	0.605	1.149	3.8069	10.126	5.374
Cable, feeder 1	0.320	0.320	0.636	0.636	200	200
Overhead line, feeder 2	0.259	0.605	1.149	3.8069	10.126	5.374

Table A.3: System parameters

Parameter	Value
System frequency	50 Hz
System grounding	Arc Suppression Coil
Parallel resistor in system neutral	125 kW / 1290.7 $\Omega$
$L_{ASC,C1}$	8.3756 H
$L_{ASC,C2}$	5.7428 H
$L_{ASC,C3}$	4.2019 H
$L_{ASC,C4}$	3.4802 H
$L_{ASC,C5}$	2.7969 H
$L_{ASC,C6}$	2.3962 H
$L_{ASC,C7}$	2.1054 H
$L_{ASC,C8}$	1.8739 H
$L_{ASC,C9}$	1.6851 H
$L_{ASC,C10}$	1.5283 H
$L_{ASC,C20}$	0.7970 H
$L_{ASC,C30}$	0.5360 H
$L_{ASC,C40}$	0.4038 H
$L_{ASC,C50}$	0.3226 H
$L_{ASC,C60}$	0.2677 H
$L_{ASC,C70}$	0.2281 H
$L_{ASC,C80}$	0.1981 H
$L_{ASC,C90}$	0.1747 H
$L_{ASC,C100}$	0.1559 H

Table A.4: High and low voltage transformers

	V [kV]	$R_1$ [pu]	$L_1$ [pu]	Connection group	$f_n$ [Hz]
High voltage transformer, 5MW					
Primary winding	132	$1e^{-6}$	0.1	$Y_g$	50
Secondary winding	22	$1e^{-6}$	0.0625	$Y_n$	50
Magnetization resistance, $R_m$ [pu]	500				
Magnetization inductance, $L_m$ [pu]	500				
Low voltage transformer, 2 MW					
Primary winding	22	$1e^{-6}$	0.1	D11	50
Secondary winding	0.23	$1e^{-6}$	0.0625	$Y_g$	50
Magnetization resistance, $R_m$ [pu]	500				
Magnetization inductance, $L_m$ [pu]	500				

## B Effects of Varying Sensitivity of $G_0 >$ Parameter for Admittance Based Ground Fault Protection Function

The figures presented below were obtained during experiments performed on Company A's COMTRADE files, and were downloaded from relay fault recorder. Figures B.1 - B.4 demonstrate the Admittance based ground fault protection performance for COMTRADE file IDs 11, 12, 16 and 26, respectively, using  $G_0 >$  sensitivity of 0.54 mS. Figures B.5 - B.8 demonstrate the Admittance based ground fault protection function performance for same COMTRADE file IDs, but with increased  $G_0 >$  sensitivity to 0.1 mS.

### B.1 Low $G_0 >$ sensitivity of 0.54 mS

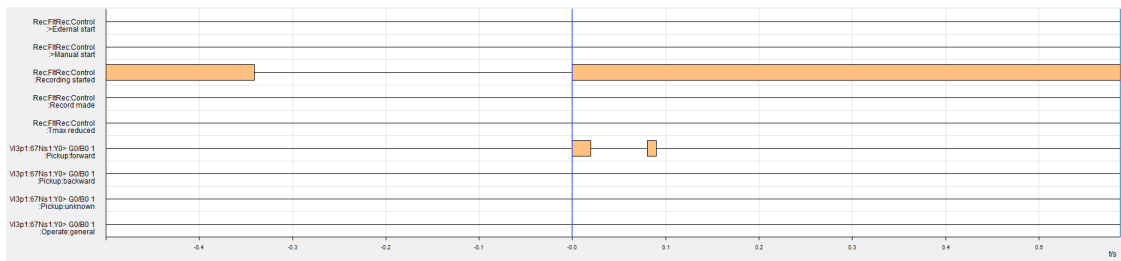


Figure B.1: Company A, File ID 11: Admittance based ground fault protection function for file ID 11, with  $G_0 >$  sensitivity of 0.54 mS

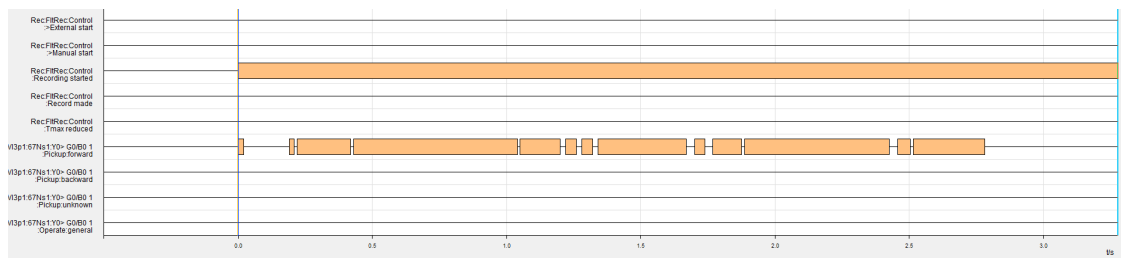


Figure B.2: Company A, File ID 12: Admittance based ground fault protection function for file ID 12, with  $G_0 >$  sensitivity of 0.54 mS

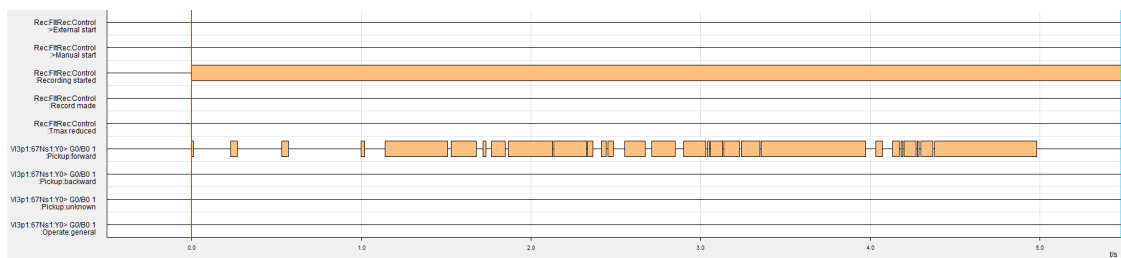


Figure B.3: Company A, File ID 16: Admittance based ground fault protection function for file ID 16, with  $G_0 >$  sensitivity of 0.54 mS

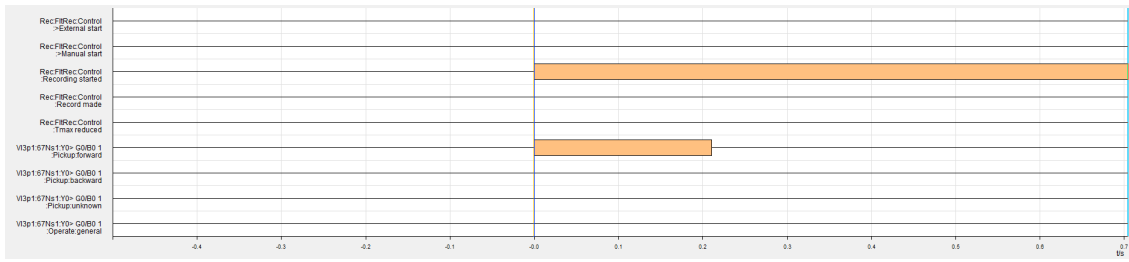


Figure B.4: Company A, File ID 26: Admittance based ground fault protection function for file ID 26, with  $G_0 >$  sensitivity of 0.54 mS

## B.2 High $G_0 >$ sensitivity of 0.1 mS

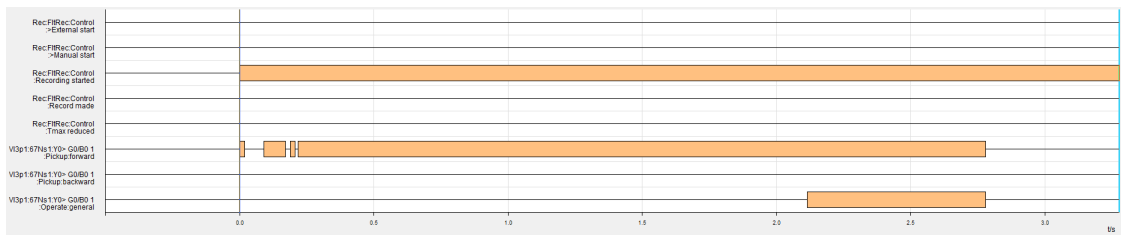


Figure B.5: Company A, File ID 11: Admittance based ground fault protection function for file ID 11, with  $G_0 >$  sensitivity of 0.1 mS

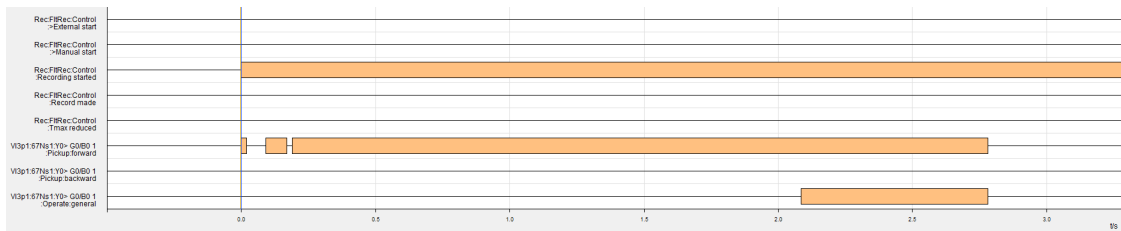


Figure B.6: Company A, File ID 12: Admittance based ground fault protection function for file ID 12, with  $G_0 >$  sensitivity of 0.1 mS

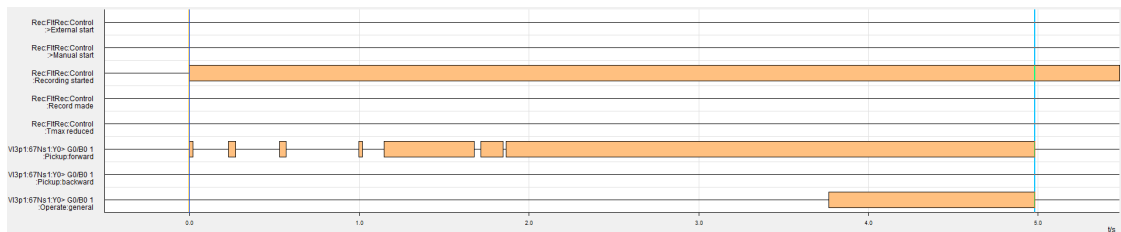


Figure B.7: Company A, File ID 16: Admittance based ground fault protection function for file ID 16, with  $G_0 >$  sensitivity of 0.1 mS

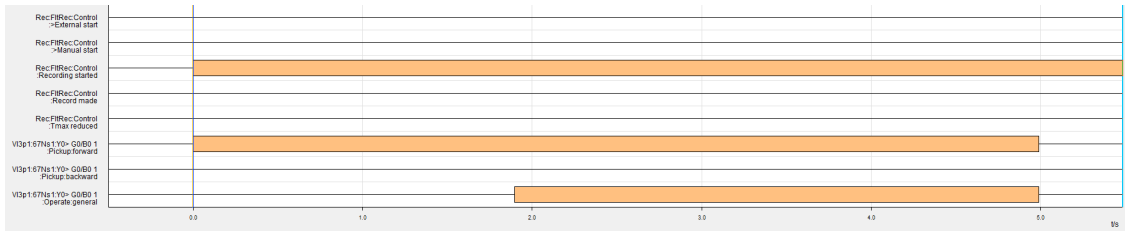


Figure B.8: Company A, File ID 26: Admittance based ground fault protection function for file ID 26, with  $G_0 >$  sensitivity of 0.1 mS

## C Demonstration of Ground Fault Protection Function Performance During Intermittent Ground Fault

Figures presented below demonstrate the Wattmetric, Admittance and Transient based ground fault protection performance during intermittent ground fault. Figures below demonstrate the performance of ground fault protection functions for cable lengths 20, 50 and 100 km. The performance of Transient based protection function is demonstrated using two different sensitivities of  $V0 >$  parameter. All of the figures presented in this appendix, demonstrate that the Transient based ground fault protection function, with both high and low sensitivity of  $V0 >$  parameter, is able to maintain a longer detection of intermittent ground faults compared to Wattmetric and Admittance based ground fault protection functions.

### C.1 Wattmetric Based Ground Fault Protection Performance During Intermittent Ground Fault

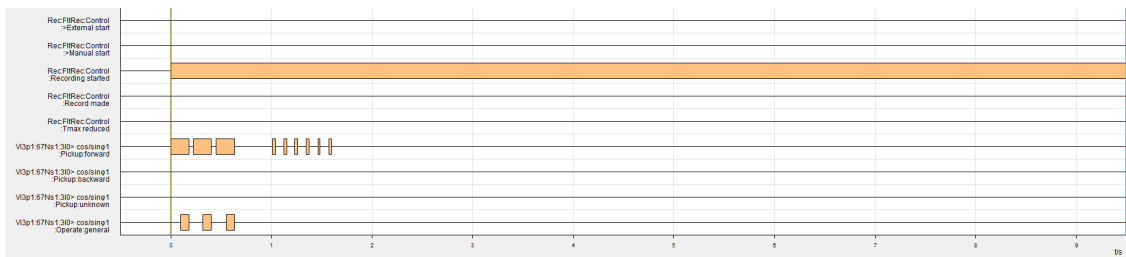


Figure C.1: Intermittent ground fault: Wattmetric based ground fault protection performance during intermittent ground fault at cable length of 20 km

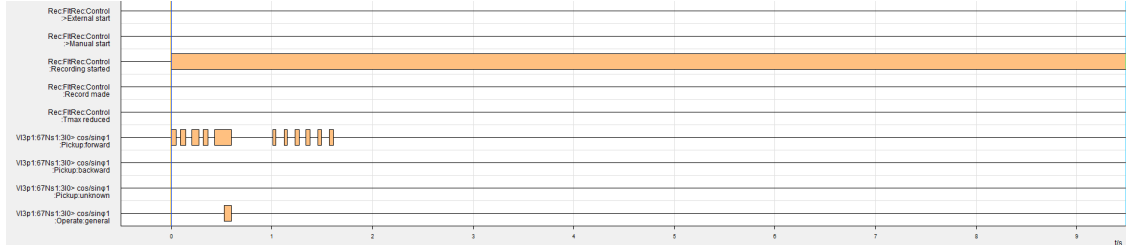


Figure C.2: Intermittent ground fault: Wattmetric based ground fault protection performance during intermittent ground fault at cable length of 50 km

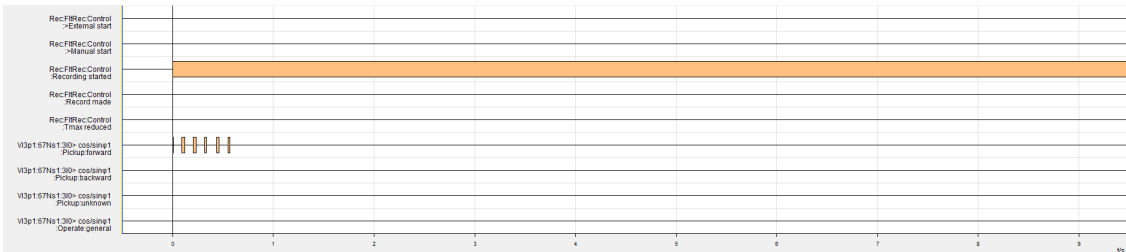


Figure C.3: Intermittent ground fault: Wattmetric based ground fault protection performance during intermittent ground fault at cable length of 100 km

## C.2 Admittance Based Ground Fault Protection Performance During Intermittent Ground Fault

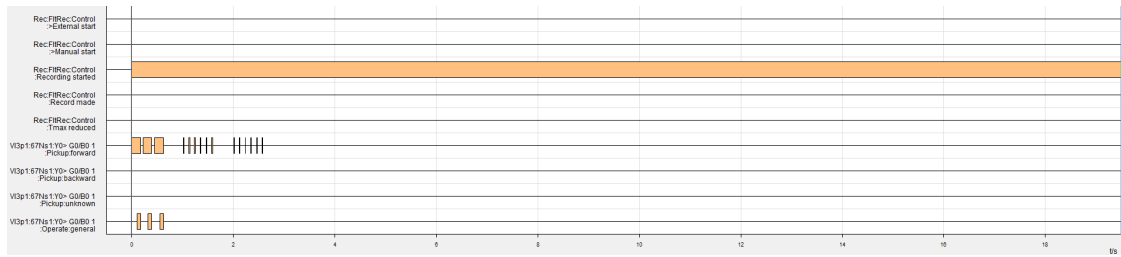


Figure C.4: Intermittent ground fault: Admittance based ground fault protection performance during intermittent ground fault at cable length of 20 km

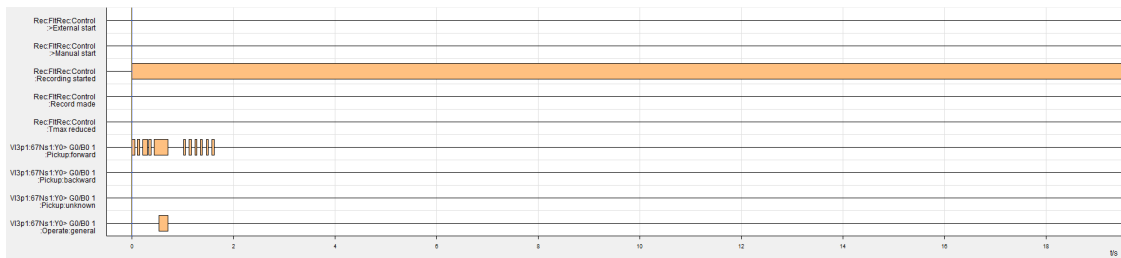


Figure C.5: Intermittent ground fault: Admittance based ground fault protection performance during intermittent ground fault at cable length of 50 km

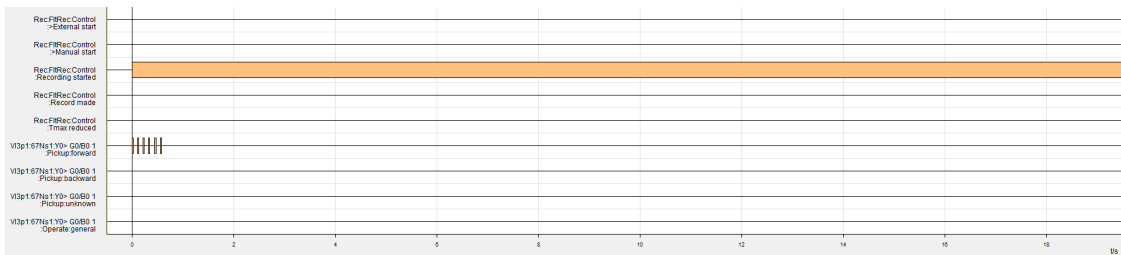


Figure C.6: Intermittent ground fault: Admittance based ground fault protection performance during intermittent ground fault at cable length of 100 km

## C.3 Transient Based Ground Fault Protection Performance During Intermittent Ground Fault

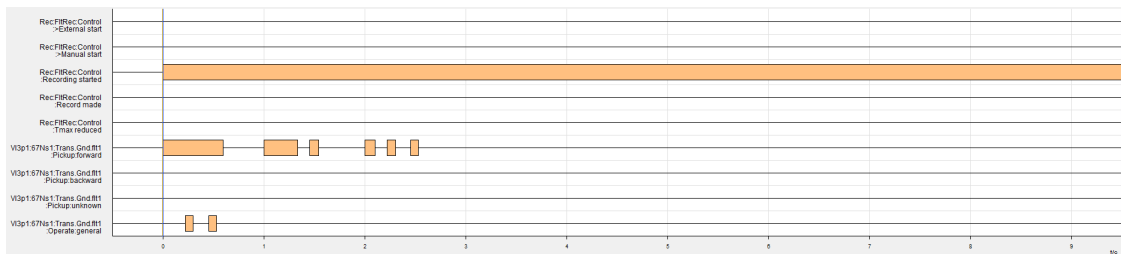


Figure C.7: Intermittent ground fault: Transient based ground fault protection performance during intermittent ground fault at cable length of 20 km, using low sensitivity for  $V_0 >$



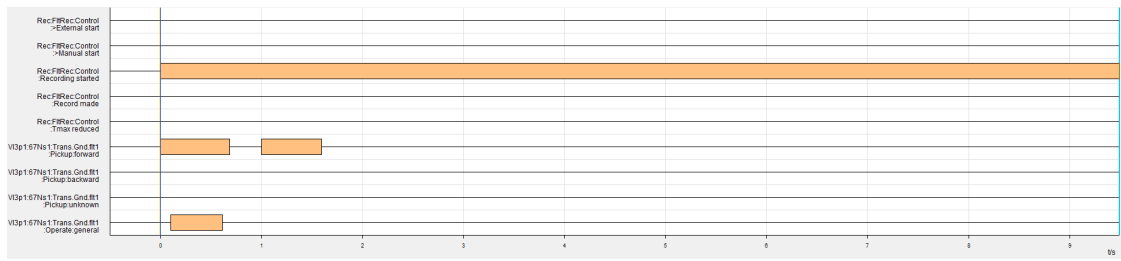


Figure C.8: Intermittent ground fault: Transient based ground fault protection performance during intermittent ground fault at cable length of 50 km, using low sensitivity for  $V0 >$

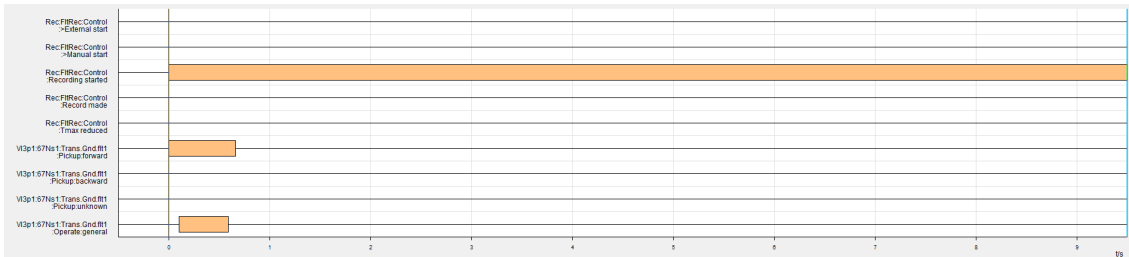


Figure C.9: Intermittent ground fault: Transient based ground fault protection performance during intermittent ground fault at cable length of 100 km, using low sensitivity for  $V0 >$

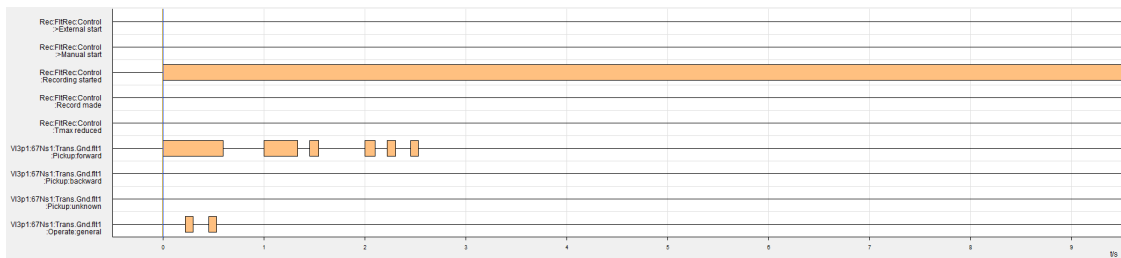


Figure C.10: Intermittent ground fault: Transient based ground fault protection performance during intermittent ground fault at cable length of 20 km, using high sensitivity for  $V0 >$

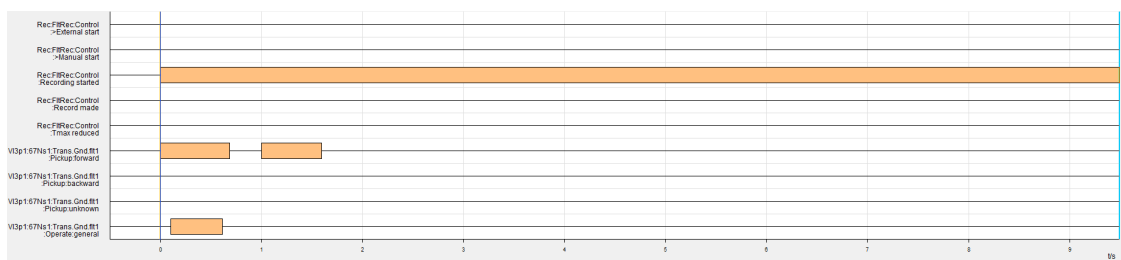


Figure C.11: Intermittent ground fault: Transient based ground fault protection performance during intermittent ground fault at cable length of 50 km, using high sensitivity for  $V0 >$

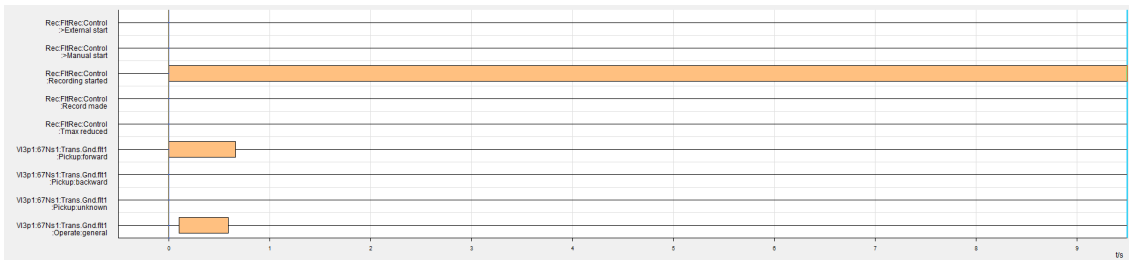


Figure C.12: Intermittent ground fault: Transient based ground fault protection performance during intermittent ground fault at cable length of 100 km, using high sensitivity for  $V_0 >$

---

## D COMTRADE script for simulations in Simulink

```
1 InitialRun = 1;
2 SimStart = 0;
3 SimEnd = 2;
4 SimulationTime = 2;
5 FaultIncrement = 500;
6 FaultAdjustment = 2;
7
8
9 Fault_on = 0.5;
10 Fault_off = 1;
11 R_f = 0.001;
12
13 out = sim('LARGE_MODEL');
14 SIGNAL = zeros(length(out.Voltages.signals.values), 13);
15 SIGNALS = zeros(length(out.Voltages.signals.values), 13);
16
17
18 for i = 1:10
19
20     out = sim('LARGE_MODEL');
21     SIGNALS(1:end,2) = round(out.Voltages.time*1e6);
22     SIGNALS(1:end,3:5) = round(out.Voltages.signals.values);
23     SIGNALS(1:end,6:13) = round(out.Currents.signals.values);
24
25     ColLen = length(out.Voltages.signals.values);
26
27     if InitialRun == 1
28         SIGNAL(1:end, 2) = round(out.Voltages.time*1e6);
29         SIGNAL(1:end,3:5) = round(out.Voltages.signals.values);
30         SIGNAL(1:end,6:13) = round(out.Currents.signals.values);
31
32     elseif InitialRun == 0
33         SIGNAL(ColLen * (i-1) + 1 : ColLen * i, 2) = SIGNALS(1:end, 2);
34         SIGNAL(ColLen * (i-1) + 1 : ColLen * i, 3:5) = SIGNALS(1:end,
35             3:5);
36         SIGNAL(ColLen * (i-1) + 1 : ColLen * i, 6:13) = SIGNALS(1:end
37             ,6:13);
38     end
39
40     SimStart = SimStart + SimulationTime;
41     SimEnd = SimStart + SimulationTime;
42     Fault_on = Fault_on + FaultAdjustment;
43     Fault_off = Fault_off + FaultAdjustment;
44     R_f = R_f + FaultIncrement;
45     InitialRun = 0;
46 end
47
48 SIGNAL(1:end,1) = linspace(1, length(SIGNAL), length(SIGNAL));
49
50 input = inputdlg('Provide a comtrade file name (i.e. Case1, Case2 or
51     CaseX)', 'New comtrade');
52 basename = cell2mat(input);
53 if isempty(basename); error('Why filename is empty'); return; end
54
55 dlmwrite(strcat(basename, '.dat'), SIGNAL, 'delimiter', ',', 'precision', 8,
56     'newline', 'pc');
```

---

```

53 fileID = fopen(strcat(basename, '.cfg'), 'w');
54 fprintf(fileID, 'Master Thesis – Analysis And Testing of Ground Fault
    Protection Performance in Compensated Distribution systems –
    Effects of Increasing Cable Length,, 1999\r\n');
55 fprintf(fileID, '11,11A,0D\r\n');
56 fprintf(fileID, '1,R1 Va-g,,,V,1,0,0,%i,%i,22000,100,P\r\n',min(SIGNAL
    (1:end,3)),max(SIGNAL(1:end,3)));
57 fprintf(fileID, '2,R1 Vb-g,,,V,1,0,0,%i,%i,22000,100,P\r\n',min(SIGNAL
    (1:end,4)),max(SIGNAL(1:end,4)));
58 fprintf(fileID, '3,R1 Vc-g,,,V,1,0,0,%i,%i,22000,100,P\r\n',min(SIGNAL
    (1:end,5)),max(SIGNAL(1:end,5)));
59 fprintf(fileID, '4,R1 I_A1,,,A,1,0,0,%i,%i,25,1,P\r\n',min(SIGNAL(1:end
    ,6)),max(SIGNAL(1:end,6)));
60 fprintf(fileID, '5,R1 I_B1,,,A,1,0,0,%i,%i,25,1,P\r\n',min(SIGNAL(1:end
    ,7)),max(SIGNAL(1:end,7)));
61 fprintf(fileID, '6,R1 I_C1,,,A,1,0,0,%i,%i,25,1,P\r\n',min(SIGNAL(1:end
    ,8)),max(SIGNAL(1:end,8)));
62 fprintf(fileID, '7,R1 I_A2,,,A,1,0,0,%i,%i,25,1,P\r\n',min(SIGNAL(1:end
    ,9)),max(SIGNAL(1:end,9)));
63 fprintf(fileID, '8,R1 I_B2,,,A,1,0,0,%i,%i,25,1,P\r\n',min(SIGNAL(1:end
    ,10)),max(SIGNAL(1:end,10)));
64 fprintf(fileID, '9,R1 I_C2,,,A,1,0,0,%i,%i,25,1,P\r\n',min(SIGNAL(1:end
    ,11)),max(SIGNAL(1:end,11)));
65 fprintf(fileID, '10,R1 I_01,,,A,1,0,0,%i,%i,25,1,P\r\n',min(SIGNAL(1:end
    ,12)),max(SIGNAL(1:end,12)));
66 fprintf(fileID, '11,R1 I_02,,,A,1,0,0,%i,%i,25,1,P\r\n',min(SIGNAL(1:end
    ,13)),max(SIGNAL(1:end,13)));
67 fprintf(fileID, '%i\r\n',50);
68 fprintf(fileID, '%i\r\n',1);
69 fprintf(fileID, '%i,%i\r\n',100000,10*length(out.Currents.signals.values
    ));
70 fprintf(fileID, '%s000\r\n',datestr(now, 'dd/mm/yyyy, HH:MM:SS.FFF'));
71 fprintf(fileID, '%s000\r\n',datestr(now, 'dd/mm/yyyy, HH:MM:SS.FFF'));
72 fprintf(fileID, 'ASCII\r\n');
73 fprintf(fileID, '%i\r\n',1);
74 fclose(fileID);

```

---

## E Siemens 7UM85 Wattmetric based protection function settings

Table E.1: Parameters, settings and default settings for Wattmetric based protection function

Parameter	Setting options	Default setting
$3I0 > \cos/\sin\phi1$ : Mode	Off ; On ; Test	Off
$3I0 > \cos/\sin\phi1$ : Operate & flr.rec. blocked	No ; Yes	No
$3I0 > \cos/\sin\phi1$ : Blk. by meas.-volt. failure	No ; Yes	Yes
$3I0 > \cos/\sin\phi1$ : Blk. by interm.gnd.ftt	No ; Yes	No
$3I0 > \cos/\sin\phi1$ : Blk. w. inrush curr. detect	No ; Yes	No
$3I0 > \cos/\sin\phi1$ : Blk. after fault extincion	No ; Yes	Yes
$3I0 > \cos/\sin\phi1$ : Directional mode	Forward ; Reverse	Forward
$3I0 > \cos/\sin\phi1$ : Dir. measuring method	$\cos\phi$ ; $\sin\phi$	$\cos\phi$
$3I0 > \cos/\sin\phi1$ : $\phi$ correction	$-45^\circ$ to $45^\circ$	$0^\circ$
$3I0 > \cos/\sin\phi1$ : Min. polar. $3I0 >$ for dir. det	0.030 to 35.000 A	0.030
$3I0 > \cos/\sin\phi1$ : a1 reduction dir. area	$1^\circ$ to $15^\circ$	$2^\circ$
$3I0 > \cos/\sin\phi1$ : a2 reduction dir. area	$1^\circ$ to $15^\circ$	$2^\circ$
$3I0 > \cos/\sin\phi1$ : $3I0 >$ threshold value	0.030 to 35.000 A	0.050
$3I0 > \cos/\sin\phi1$ : $V0 >$ threshold value	0.300 to 200.000 V	30.000 V
$3I0 > \cos/\sin\phi1$ : Dir. determination delay	0.00 to 60.00 s	0.10 s
$3I0 > \cos/\sin\phi1$ : Operate delay	0.00 to 60.00 s	2.00 s

---

## F Siemens 7UM85 Admittance based protection function settings

Table F.1: Parameters, setting options and default settings for admittance based with G0 or B0 7UM85

Parameter	Setting options	Default setting
Y0 >G0/B0 #:Mode	Off ; On ; Test	Off
Y0 >G0/B0 #:Operate & ft.rec. blocked	No ; Yes	No
Y0 >G0/B0 #:Blk. by meas.-volt. failure	No ; Yes	Yes
Y0 >G0/B0 #:Blk. by interm.gnd.ft.	No ; Yes	No
Y0 >G0/B0 #:Blk. w. inrush curr. detect.	No ; Yes	No
Y0 >G0/B0 #:Blk. after fault extinction	No ; Yes	Yes
Y0 >G0/B0 #:Directional mode	Forward ; Reverse	Forward
Y0 >G0/B0 #:Dir. maesuring mode	G0 ; B0	G0
Y0 >G0/B0 #: $\phi$ correction	$-45^\circ$ to $45^\circ$	0
Y0 >G0/B0 #:Polarized G0/B0 Threshold	0.10mS to 100.00mS	2.00mS
Y0 >G0/B0 #: $\alpha_1$ reduction dir. area	$-1^\circ$ to $15^\circ$	$-2^\circ$
Y0 >G0/B0 #: $\alpha_2$ reduction dir. area	$-1^\circ$ to $15^\circ$	$-2^\circ$
Y0 >G0/B0 #: 3I0>release threshold value	0.001A to 175.00A	0.15A
Y0 >G0/B0 #:V0>Threshold value	0.300V to 200.00V	30.000V
Y0 >G0/B0 #:Dir. determination delay	0.00s to 60.00s	0.10s
Y0 >G0/B0 #:Operate delay	0.00s to 60.00s	2.00s

---

## G Siemens 7UM85 Transient ground function settings

Table G.1: Parameters, setting options and default settings for transient ground fault function 7UM85

<b>Parameter</b>	<b>Setting options</b>	<b>Default setting</b>
Trans.Gnd.ftt:Mode	Off ; On ; Test	Off
Trans.Gnd.ftt.1:Operate & ft.rec. blocked	No ; Yes	No
Trans.Gnd.ftt.1:Blk by meas.-volt. failure	No ; Yes	Yes
Trans.Gnd.ftt.1:Blk. after fault extinction	No ; Yes	Yes
Trans.Gnd.ftt.1: Operate functionality	No ; Yes	No
Trans.Gnd.ftt.1:Directional mode	Forward ; Reverse	Forward
Trans.Gnd.ftt.1: V0 >Threshold value	0.300V to 200.000V	15.00V
Trans.Gnd.ftt.1: Maximum operational V0	0.300V to 200.00V	3.00V
Trans.Gnd.ftt.1: 3I0 >Threshold for pickup	0.000A to 175.000A	0.000A
Trans.Gnd.ftt.1: 3I0 >Threshold for operate	0.000A to 175.000A	0.000A
Trans.Gnd.ftt.1: Operate delay	0.00s to 60.00s	0.5s
Trans.Gnd.ftt.1: Dropout delay	0.00s to 60.00s	0.00s

